Distribution Agreement

In presenting this thesis or dissertation as a partial fulfillment of the requirements for an advanced degree from Emory University, I hereby grant to Emory University and its agents the non-exclusive license to archive, make accessible, and display my thesis or dissertation in whole or in part in all forms of media, now or hereafter known, including display on the world wide web. I understand that I may select some access restrictions as part of the online submission of this thesis or dissertation. I retain all ownership rights to the copyright of the thesis or dissertation. I also retain the right to use in future works (such as articles or books) all or part of this thesis or dissertation.

Signature: _____ _____

Alyssa M. Duffy Date

Mechanisms of efficacy and toxicity of immune checkpoint inhibitors in human cancer patients

By
Alyssa M. Duffy
Doctor of Philosophy

Graduate Division of Biological and Biomedical Sciences
Cancer Biology

_____
Kavita Dhodapkar, MD
Advisor

_____
Madhav Dhodapkar, MD
Committee Member

_____
Haydn Kissick, PhD
Committee Member

_____
Ignacio Sanz, MD
Committee Member

_____
Gregory Lesinski, PhD
Committee Member

Accepted:

_____
Kimberly Jacob Arriola, PhD, MPH
Dean of the James T. Laney School of Graduate Studies

_____
Date

Mechanisms of efficacy and toxicity of immune checkpoint inhibitors in human cancer patients

By

Alyssa M. Duffy
M.S., Drexel University College of Medicine, 2018
B.S., The Pennsylvania State University, 2016

Advisor: Kavita Dhodapkar, MD

An abstract of
A dissertation submitted to the Faculty of the
James T. Laney School of Graduate Studies of Emory University
in partial fulfillment of the requirements for the degree of
Doctor of Philosophy
in the Graduate Division of Biological and Biomedical Science
in Cancer Biology
2024

Abstract

Mechanisms of efficacy and toxicity of immune checkpoint inhibitors in human cancer patients

By Alyssa M. Duffy

Immune checkpoint inhibitors (ICIs) have revolutionized the landscape of cancer treatment, leading to impressive and durable results in patients with a wide range of tumor types. However, significant clinical challenges remain surrounding patient response rates and autoimmune toxicities. Herein, we investigate the underlying mechanisms of efficacy and toxicity in human cancer. We assessed changes in circulating immune cells among patients who received either anti-PD-1 or anti-PD-L1, finding distinct, nonoverlapping genomic signatures of each. In particular, anti-PD-L1 is characterized by changes in the myeloid compartment, with increased signatures associated with inflammation. Importantly, we find that PD-L1 blockade acts directly on DCs, resulting in enhanced maturation and expansion of antigen-specific T cells, suggesting a key role of anti-PD-L1 within the afferent arm of the cancer immunity cycle. Furthermore, we establish a novel role for T:B interactions in the development of immune-related adverse events (irAEs) following combination anti-CTLA-4 and anti-PD-1 (CCB) therapy. We show CCB leads to the enrichment of TPH-like cells, which support B cell activation and differentiation through IFNg and IL-21 signaling. Importantly, we highlight key cellular and molecular differences associated with the development of severe irAEs. First, we illustrate alterations in circulating CD11c+Tbet+CD21lo B cells in patients with severe irAEs following CCB, suggesting a pathogenic role. We also report that the expansion of Tregs suppresses T:B interactions, protecting patients from irAEs. Thus, the work presented here provides new insights into the cellular and molecular mechanisms of ICI efficacy and toxicity, furthering the understanding of ICIs and ultimately improving patient outcomes.

Mechanisms of efficacy and toxicity of immune checkpoint inhibitors in human cancer patients

By

Alyssa M. Duffy
M.S., Drexel University College of Medicine, 2018
B.S., The Pennsylvania State University, 2016

Advisor: Kavita Dhodapkar, MD

A dissertation submitted to the Faculty of the
James T. Laney School of Graduate Studies of Emory University
in partial fulfillment of the requirements for the degree of
Doctor of Philosophy
in the Graduate Division of Biological and Biomedical Science
in Cancer Biology
2024

Acknowledgements

Earning a PhD is no easy feat, and I could not have done it without the wonderful community of friends and family I am surrounded by. I must first thank my mentor, Dr. Kavita Dhodapkar. Thank you for your immense support and expertise throughout the past six years. I am truly grateful for your patience, your humor, and your encouragement, for guiding me when I wasn't sure which direction to take next, for your open-door policy and our many scientific chats, and for your contagious enthusiasm for science. Through your guidance, you have pushed me to become a great scientist and leader, and for that I owe you so many thanks. I would also like to thank my committee- Drs. Madhav Dhodapkar, Haydn Kissick, Ignacio Sanz, and Greg Lesinski. Thank you for your endless encouragement and your valuable feedback, all of which has contributed to my growth and confidence as a scientist. In particular, I want to acknowledge Dr. Madhav Dhodapkar, who acted as a "bonus mentor" much of the time. Thank you for all your scientific insights, enthusiasm, and support. To all- it has been an absolute pleasure learning from and working with every single one of you.

To all of the Dhodapkar lab members, both past and present, thank you for being there for me, for many wonderful collaborations and scientific discussions, for always lending a hand, and for the endless laughs. I would especially like to thank Sayalee Potdar and Dr. Samuel McCachren for your incredible friendship and support while we all completed our PhDs together. It has been remarkable to learn from and work with both of you. I cherish all our memories and inside jokes together and feel so lucky to have been on this journey alongside two wonderful, brilliant scientists. To the members of the Emory Cancer Biology program, especially my 2018 cohort, thank you for your friendship, support, and many laughs. I must also thank the Flow Cytometry Core, specifically Bob Karaffa, Kametha Fife, and Sommer Durham. I spent many, many hours at the sorting facility and I am so grateful for your expertise, your flexibility, your friendliness, and for being so willing to teach me the ins and outs of flow cytometry.

I am so grateful to have found such an incredible community here in Atlanta outside of Emory. To my ATL gorls, Torri, Daniella, and Iesha, thank you endlessly for your beautiful friendship, for always cheering me on, for providing me with a safe space to be myself, and for being inspirational, strong, independent women. To the other pillars of my Atlanta community, Robin, Mikaela and Taylor, thank you for your endless support, for your pep talks, and for your truly wonderful friendship. To all my friends from Penn State and from high school, who have been by my side through the many stages of life, especially Camille, Shavani, and Micah, thank you for countless years of beautiful friendship, for endless laughter, for always believing in me and cheering me on. Finally, I would like to thank our friends Jack and Jordan, who have been incredibly supportive throughout the past 6 years. Thank you for always showing an interest in my research, thank you for being my backboard as I talk things out, and thank you for constantly encouraging and motivating me.

There is no way to express enough gratitude or thanks to my family. To both my parents, thank you for always setting the example and for teaching me the value of hard work and determination. Thank you for instilling the love of science in me and for always supporting my dreams, whatever they may be. I would not be where I am today without all you have done for me or all you have taught me. To my mother, Roseanne, thank you for being my greatest role model, for always

lending an ear to listen, and for your endless love and support. To my father, James, thank you for your silly sense of humor, for all our scientific chats, and for your unwavering love and support. To my younger sister, Caitlin, the next Dr. Duffy, thank you for always cheering me on, for being so inspiring with your dedication and hard work, and for being the best not-so-little, little sister.

Finally, to my husband, Taylor Jackson, who has been by my side through all the ups and downs of this journey and well before this dream even existed. Thank you for unconditionally loving me, for always making me laugh, especially in the times I need it the most, for believing in me and being my biggest cheerleader, for being my rock, for always encouraging my growth and supporting my dreams, and for being the best partner in crime. I could not have done this without you by my side and I am so grateful for you. Thank you and I love you. And lastly, and arguably most importantly, thank you to our dog Turtle for the best cuddles and for being the best dog in the world.

Table of Contents

List of Figures

List of Tables

List of Abbreviations

ADCC	antibody dependent cellular cytotoxicity
AMM	asymptomatic multiple myeloma
APC	antigen presenting cell
BC	breast cancer
BCC	basal cell carcinoma
BCR	B cell receptor
BM	bone marrow
CAR-T	chimeric antigen receptor T cell
CCB	combination checkpoint blockade
CCR7	C-C chemokine receptor type 7
CD3	Cluster of Differentiation 3
CD4	Cluster of Differentiation 4
CD8	Cluster of Differentiation 8
CD11c	Cluster of Differentiation 11c
CD14	Cluster of Differentiation 14
CD16	Cluster of Differentiation 16
CD19	Cluster of Differentiation 19
CD21	Cluster of Differentiation 21
CD28	Cluster of Differentiation 28
CD25	Cluster of Differentiation 25
CD27	Cluster of Differentiation 27
CD38	Cluster of Differentiation 38

CD40	Cluster of Differentiation 40
CD40L	CD40 ligand
CD45RA	Cluster of Differentiation RA
CD45RO	Cluster of Differentiation RO
CD80	Cluster of Differentiation 80
CD83	Cluster of Differentiation 83
CD86	Cluster of Differentiation 86
CD127	Cluster of Differentiation 127
CD138	Cluster of Differentiation 138
CRC	colorectal cancer
cRPMI	complete Roswell Park Memorial Institute
cSCC	cutaneous squamous cell carcinoma
CTLA4	cytotoxic T-lymphocyte associated protein 4
CXCL1	chemokine C-X-C motif ligand 1
CXCL2	chemokine C-X-C motif ligand 2
CXCR3	C-X-C chemokine receptor type 3
CXCR5	C-X-C chemokine receptor type 5
cyTOF	cytometry by time of flight
DC	dendritic cell
DEG	differentially expressed gene
dMMR	mismatch repair deficient
ELISA	enzyme linked immunosorbent assay
EOT	end of therapy

ESCC	esophageal squamous cell carcinoma
FBS	fetal bovine serum
FDA	Food and Drug Administration
flowSOM	flow self-organizing map
Flu-MP	influenza-matrix peptide-specific
FOXP3	forkhead box P3
GI	gastrointestinal
GM-CSF	granulocyte-macrophage stimulating factor
GSEA	gene set enrichment analysis
HBEGF	heparin-binding EGF-like growth factor
HCC	hepatocellular carcinoma
hCD45	human Cluster of Differentiation 45
HD	healthy donor
HG-irAE	high-grade immune-related adverse event
HL	Hodgkin's lymphoma
HLA	human leukocyte antigen
HLA-DR	human leukocyte antigen-DR isotype
HNSCC	head and neck squamous cell carcinoma
IBD	inflammatory bowel disease
ICI	immune checkpoint inhibitor
ICOS	inducible T-cell costimulatory
IFN-a	interferon alpha
IFNg	interferon gamma

IgD	immunoglobulin D
IgG	immunoglobulin G
IgM	immunoglobulin M
IL-1	interleukin-1
IL-1B	interleukin-1 beta
IL-2	interleukin-2
IL-4	interleukin-4
IL-6	interleukin-6
IL-8	interleukin-8
IL-17	interleukin-17
IL-18	interleukin-18
IL-21	interleukin-21
IL21R	interleukin-21 receptor
IP-10	interferon gamma-induced protein 10
irAE	immune-related adverse event
Ki-67	antigen Kiel 67
KLRF1	killer cell lectin-like receptor G1
Lag-3	lymphocyte-activation gene 3
LPS	lipopolysaccharide
MC	metacluster
MCC	Merkel cell carcinoma
mCD45	mouse Cluster of Differentiation 45
MGUS	monoclonal gammopathy of unknown significance

MHC major histocompatibility complex

MISTRG6 M-CSF$^{h/h}$ IL-3/GM-CSF$^{h/h}$ SIRPa$^{h/h}$ TPO$^{h/h}$ RAG2$^{-/-}$ IL2Rg$^{-/-}$ IL6$^{h/h}$

MM multiple myeloma

Mo-DC monocyte-derived DC

MSI-H microsatellite instable high

NK natural killer

NLRP3 NOD-, LRR- and pyrin domain-containing protein 3

NSCLC non-small cell lung cancer

OX40 tumor necrosis factor receptor superfamily member 4

PBMCs peripheral blood mononuclear cells

PBS phosphate buffered saline

PD-1 programmed cell death protein 1

PD-L1 programmed death-ligand 1

PD-L2 programmed death-ligand 2

PMA phorbol-12-myristate-13-acetate

RA rheumatoid arthritis

RCC renal cell carcinoma

SCC squamous cell carcinoma

SCLC small cell lung cancer

SEB staphylococcal enterotoxin B

SLE systemic lupus erythematosus

SOX2 SRY-box transcription factor

Tbet T-box expressed in T cell

Tcm	central memory T cell
TCR	T cell receptor
Tem	effector memory T cell
TFH	T follicular helper cell
Th1	type 1 T helper cell
THBS	thrombospondin-1
TIGIT	T cell immunoreceptor with Ig and ITIM domains
TIL	tumor infiltrating lymphocyte
TIM3	T-cell immunoglobulin and mucin-domain containing-3
TMB	tumor mutational burden
TME	tumor microenvironment
TNBC	triple negative breast cancer
TNF-α	tumor necrosis factor 1
TPH	T peripheral helper cell
Tregs	T regulatory cells
TREM1	triggering receptor expressed on myeloid cells 1
TRM	tissue-resident memory T cells
t-SNE	t-distributed stochastic neighbor embedding
UC	urothelial carcinoma
UMAP	uniform manifold approximation and projection

Chapter 1: Introduction

1.1 Introduction to cancer and the immune system

Our understanding of the interactions between tumor cells and the tumor microenvironment has grown profoundly throughout the years. In particular, studying the relationship between tumors and the immune system has allowed for tremendous advancements in medicine through harnessing the body's own defense system to mount an anti-tumor response. Cancer immunotherapies have been studied in the clinical setting for decades, and today, they are used as frontline therapies for a number of different malignancies. Clinical data has shown impressive efficacy and durable results, revolutionizing the treatment of cancer and solidifying immunotherapy as a new pillar of cancer treatment[1].

At the most basic level, cancer can be characterized as "a robust and evolvable system that arises due to the accumulation of various genetic alterations and the loss of normal cellular regulatory processes"[2,3]. Several early studies in murine models showed that genomic mutations in tumor cells have the potential to lead to the formation of a repertoire of tumor-specific antigens that cause the immune system to recognize tumor cells as foreign and thereby ellicit an anti-tumor immune response[4-9]. This act of "immunosurveillance" demonstrated a clear role the immune system played in modulating and controlling tumor growth.

The immune surveillance theory was described over 60 years ago. It suggests the immune system monitors cells and tissues, detecting tumor specific antigens on newly developing cancer cells and eliminating them before they can cause harm[10,11]. The importance of the immune system in

regulating tumor development has been demonstrated through several murine studies and clinical observations. For example, studies have shown that genetically engineered mice deficient in CD8+ T cells, CD4+ Th1 cells, or NK cells have markedly increased tumor incidence, suggesting that both the innate and the adaptive immune system are important players in the surveillance and elimination of tumor cells[12,13]. Similarly, immunosupression in patients is often associated with increased risk of malignancy, with studies reporting anywhere from a 3- to 100-fold increase in risk[14,15]. Alternatively, in clinical settings, tumor infiltration by CD8+ T cells or NK cells is associated with more favorable outcomes in a number of tumor types including melanoma[16,17], once again reinforcing the importance of the immune system.

Although it is clear the immune system plays a critical role in keeping tumor formation in check, tumors still develop even in the presence of a functioning immune system. Updated theories describe this concept as immunoediting, whereby the selective pressure of the immune system leads to mutations in any remaining cancer cells, resulting in the persistance of variants that are able to evade immune detection and elimination[18]. Tumor cells can escape the immune system through many different mechanisms, from alterations on the cellular level to changes within the tumor microenvironment[18]. Some mechanisms include decrease in tumor immunogenicity[18,19], downregulation of molecules required for T cell activation, such as major histocompatability complex (MHC) molecules or the loss of antigen expression[20], expression of inhibitory checkpoint molecules[21-25], and the infiltration or increased abundance of immunosuppressive cell types such as T regulatory cells (Tregs)[26,27]. These mechanisms, either alone or in combination, provide a way for tumors to “hide” from the immune system, allowing them to persist and grow.

The manner in which the immune system targets and eliminantes tumor cells in a T cell-mediated fashion, or the anti-tumor response, has been termed the cancer immunity cycle. It was first described a decade ago as a series of stepwise events by which host immune cells may effectively target and kill cancer cells[3] (Figure 1.1). Importantly, this concept reinforced the idea that T cells do not respond or work alone, but rather do so within a network of other immune cells, in a series of highly regulated steps[28]. The first step of the cancer immunity cycle consists of the release of neoantigens as cancer cells die off. These neoantigens are captured by dendritic cells (DCs) to be processed (step 2) and presented on MHC I and MHC II to T cells in nearby secondary lymphoid organs (step 3). This process results in the priming and activation of T cells, leading to the expansion of effector T cells against the specified cancer antigens (step 3). These activated effector T cells then migrate to and infiltrate the tumor (step 4), eventually leading to targeting and killing cancer cells (step 5). As tumor cells are killed, more cancer antigens are released, leading to the start of the cycle again[28].

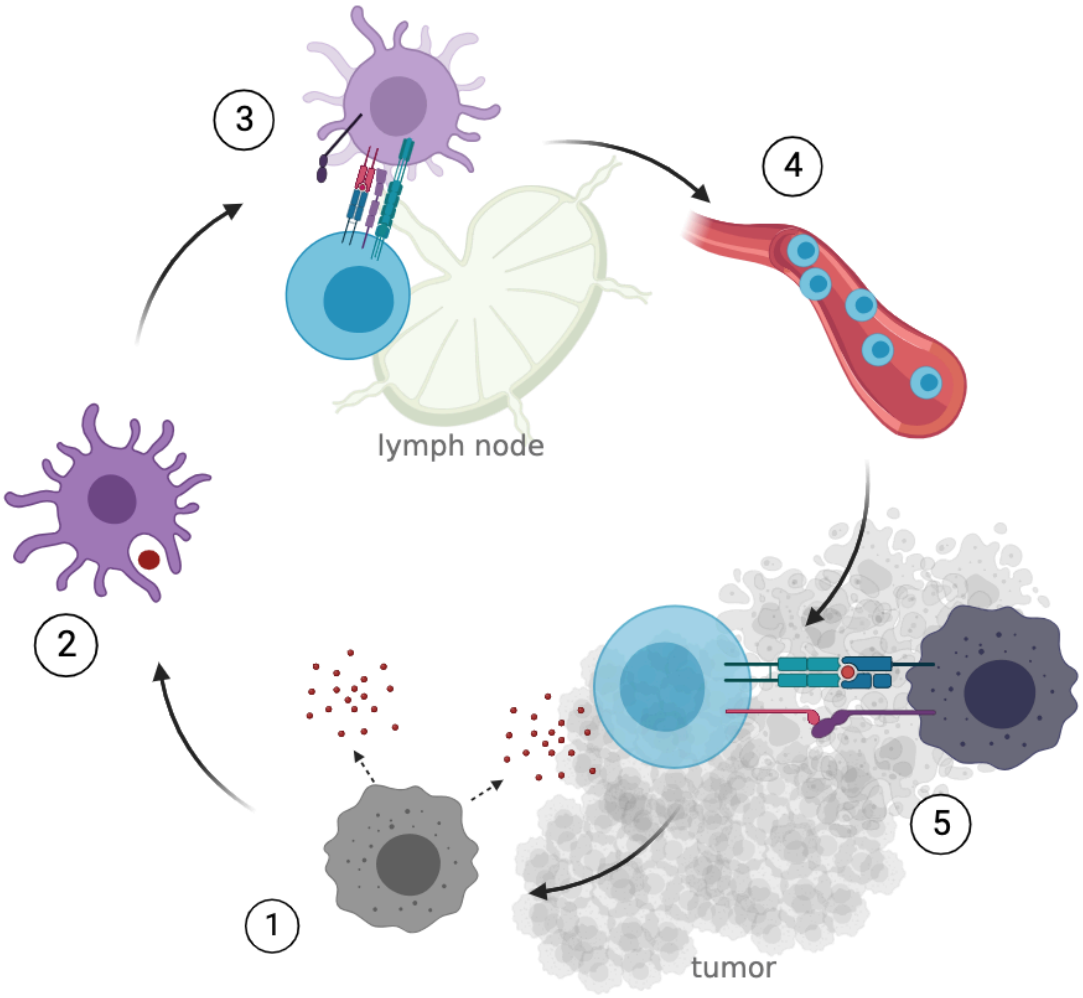

Figure 1.1: Cancer immunity cycle. A schematic of the cycle by which the immune system mounts an anti-tumor response. This response is initiated by the release of cancer specific antigens, which are presented by DCs to prime tumor specific T cells, resulting in the trafficking and activation of an effector anti-tumor T cells and the elimination of tumor cells.

Each step of the cancer immunity cycle is highly regulated by a number of stimulatory and inhibitory mechanisms, offering a wide variety of potential therapeutic targets. Scientists have worked over the years to better understand these regulatory mechanisms, and have discovered ways to maniplulate various steps in the cycle in order to overcome immunoediting and activate or introduce cancer-specific cytotoxic T cells. Several successful immunotherapies have been developed through these studies including monoclonal antibody-based therapies that bind one or two antigens to induce T cell-mediated tumor cell killing, chimeric antigen receptor (CAR) T cells to improve antigen recognition and direct killing of cancer cells, and checkpoint inhibitors to block inhibitory signals and enhance T cell priming, activation, and killing[28]. Clinical data demonstrate the impressive efficacy and durability of these immune based therapies in several tumor types[29-31]. However, these immunotherapies still face significant challenges such as overactivation of immune responses, unwanted damage of healthy cells and tissues, and altered function of immune cell populations. To improve patient care and the efficacy of these immunotherapies, these challenges must be addressed.

1.2 Targeting checkpoint molecules using monoclonal antibodies

The immune system maintains several strict regulatory mechanisms, which are crucial to ensure a proper response and prevent inappropriate activation of immune cells. In particular, T cell activation requires two major signals: 1) binding of the T cell receptor (TCR) with its cognate antigen presented on an MHC molecule and 2) binding of costimulatory molecules[32]. Additionally, the release of cytokines are important to instruct T cell differentiation and expansion[29]. Signal 2 is primarily mediated by CD28, a receptor located on T cells, and its ligands CD80 and CD86[29]. These molecules belong to a class of extracellular proteins termed checkpoint molecules, which

consist of both costimulatory and inhibitory molecules. Costimulatory molecules aid in the activation of T cells by amplifying the TCR signaling[32,33]. Besides CD28, some examples are OX40, CD40, and ICOS. Alternatively, there are several ways in which the immune system negatively regulates T cell activation in an effort to regulate T cell responses and prevent off-target damage and autoimmunity[32,33]. Some examples of inhibitory molecules include CTLA-4, PD-1, TIGIT, and Lag-3.

Inhibitory checkpoint molecules are not only critical for the prevention of autoimmunity, but also play a role in regulating T cell responses to chronic viral infections and tumor antigens[34]. Cytotoxic T-lymphocyte associate protein 4, or CTLA-4, was the first checkpoint molecule studied in the context of tumor immunity[35]. CTLA-4 is expressed exclusively on T cells and plays an important role in the early stages of T cell priming and activation[29]. Upon T cell activation, expression and trafficking of CTLA-4 to the cell membrane is increased, where it functions to attenuate the T cell immune response[32]. The importance of CTLA-4 in maintaining immune homeostasis was originally demonstrated by studies of Ctla4-knockout mice, which displayed systemic immune hyperactivation, severe autoimmune toxicity, and lethality[36,37]. Early preclinical studies conducted by Dr. James Allison fully confirmed CTLA-4 as an inhibitory checkpoint. His study demonstrated the opposing effects of CTLA-4 and CD28, illustrating how CTLA-4 outcompetes CD28 to bind CD80 (B7-1) and CD86 (B7-2), resulting in inhibition of T cell proliferation and IL-2 production[38]. Further studies in murine models showed that blocking CTLA-4 with an antibody led to a T cell-mediated anti-tumor immune response and tumor regression[35,39]. These effects were seen in mice that had partial immunogenic tumors but not in mice with poor immunogenic tumors, suggesting blocking CTLA-4 enhances the endogenous anti-tumor response[39]. Additional preclinical studies

further explored this anti-tumor mechanism and determined that CTLA-4 blockade increased the frequency of effector CD4+ and CD8+ T cells, while decreasing the levels of immunosuppresive Tregs[40]. These monumental studies conducted by Allison and colleagues laid the groundwork for the development of immune checkpoint inhibitors.

While initial preclinical studies were conducted using murine melanoma models, additional studies showed CTLA-4 blockade led to tumor regression in several other tumor models[39]. These findings demonstrated that this therapeutic intervention could be broadly applied across several different tumor types. The success of these preclinical studies led to the development of the first immune checkpoint inhibitor (ICI)- ipilimumab. Ipilimumab is a fully humanized monoclonal antibody that targets and blocks CTLA-4[32]. Clinical trials started in 2000, with initial studies conducted utilizing patients with advanced cancer who did not previously respond to other treatments[41]. Subsequent phase II and III trials demonstrated the impressive efficacy of ipilimumab, as it was the first therapy to improve overall survival in patients with metastatic melanoma[42,43]. What was the most interesting to investigators was that patients showed ongoing responses and survival, even after the completion of treatment. In particular, a group of patients with metastatic melanoma had durable responses and long term survival benefits that lasted up to 10 years[43]. After several successful clinical trials, ipilimumab was approved by the FDA for the treatment of advanced metastatic melanoma in 2011, paving the way for the development and approval of several additional ICIs to treat a wide variety of tumor types.

Another inhibitory signaling axis that has been studied extensively in cancer is programmed death ligand (PD-1) and its ligands PD-L1 and PD-L2. PD-1 is more broadly expressed than CTLA-4

and is primarily found on activated T cells, B cells, and NK cells[44-46]. On the other hand, PD-L1 can be found on several different types of cells including antigen presenting cells like dendritic cells or macrophages, other lymphoid cells, myeloid cells, and tumor cells[29]. In contrast to CTLA-4, PD-1 is responsible for regulating effector T cell activity and maintaining T cell tolerance in the periphery, with its expression induced upon T cell activation[47,48]. When bound to its ligands, PD-1 inhibits T cell activity via downstream phosphatases that abrogate TCR signaling[49]. Prolonged antigen exposure, as in the case with chronic viral infections or cancer, can lead to persistent PD-1 expression, resulting in T cell exhaustion. Exhaustion is defined as a state of dysfunction characterized by reduced effector function, lack of response to stimuli, and altered transcriptional and epigenetic states[50,51]. Studies in both mice and humans have found that T cell exhaustion is not necessarily a permanent state of dysfunction and can be partially reversed by blockade of the PD-1/PD-L1 signaling pathway[50].

High levels of PD-1 expression has been illustrated on tumor-infiltrating lymphocytes (TILs), including on exhausted T cells, in several different tumor types[23,52]. Additionally, several studies have shown human cancer cells upregulate and express high levels of PD-L1, particularly within melanoma, ovarian cancer, lung cancer, and colon cancer[53-55]. Based on the discovery of PD-1 expression on TILs and PD-L1 on tumor cells, it was hypothesized that this inhibitory sgnaling axis contributes to the development of tumors, and blocking it could provide therapeutic benefit. Indeed, preclinical studies found that induced expression of PD-L1 on the surface of mouse tumor cells led to T cell death and reduced anti-tumor T cell response[25,55]. Further studies determined that blocking this signaling axis, by targeting either PD-1 or PD-L1, enhances recruitment and activity of effector T cells, leading to tumor regression in several murine tumor models[25,56,57].

These preclinical studies clearly illustrated promising results of targeting PD-1/PD-L1, which led to the initiation of clinical trials for the first PD-1 targeting antibodies in the early 2000s and anti-PD-L1 antibodies shortly after. Early trials enrolled patients with melanoma, renal cell carcinoma (RCC), and non-small cell lung cancer (NSCLC). Outcomes from these trials mimicked the findings from preclinical studies, demonstrating drastic and durable tumor regression with the blockade of PD-1[58,59]. Notably, toxicities observed in these patient cohorts were less severe than those treated with anti-CTLA-4[59]. Successful trials led to the FDA back-to-back approval of the first anti-PD-1 antibodies, pembrolizumab and nivolumab, for the treatment of advanced melanoma in 2014. Following the initial trials for anti-PD-1 antibodies, a series of additional clinical trials were conducted to test the efficiacy of these therapies in a wide variety of tumor types. These trials, termed KEYNOTE for the study of pembrolizumab and CheckMate for nivolumab, showed consistent improved patient survival outcomes and subsequetly resulted in the expanded approval of these therapies for additional tumor types including NSCLC, RCC, Hodgkin's lymphoma, and head and neck squamous cell carcinoma (HNSCC), among many others[60].

In the 13 years since the first FDA approval of immune checkpoint inhibitors, there have been many advancements in the field with the development of new inhibitors, approval of ICIs to treat additional tumor types, combinations of ICIs with other therapies, expansion from second line to first line treatment, and the inclusion of both advanced and earlier stage cancers. Currently, there are nine FDA approved inhibitors (Table 1.1) that are utilized in a range of different tumor types[32].

Table 1.1: List of FDA approved antibodies and approved tumor types[32].

Target	Agent	Indications
CTLA4	Ipilimumab	Stage III or metastatic melanoma
PD1	Nivolumab	MSI-H or dMMR CRC, ESCC, HCC, HL, HNSCC, melanoma, NSCLC, RCC, UC, Hodgkin's lymphoma, gastric carcinoma
	Pembrolizumab	Melanoma, squamous and non-squamous NSCLC, HNSCC, HL, RCC, SCLC, SCC, cSCC, CRC, CSCC, TNBC, ESCC, MCC, HCC, UC, cervical cancer, endometrial carcinoma, gastric adenocarcinoma, mesothelioma, MSI-High/MMR-deficient/TMB-high cancers, large B cell lymphoma
	Cemiplimab	cSCC, NSCLC, BCC
	Dostarlimab-gxly	MMR-endometrial carcinoma
	Retifanlimab-dlwr	MCC
PD-L1	Atezolizumab	BC, HCC, metastatic melanoma, NSCLC, SCLC, UC
	Avelumab	MCC, RCC, UC
	Durvalumab	NSCLC, SCLC, biliary tract cancer

Both anti-CTLA-4 and anti-PD-1 therapies produce potent anti-tumor effects in similar manners, but the mechanisms by which they do so are very different[61,62]. As previously described, CTLA-4 and PD-1 are non-redundant inhibitory molecules found on T cells at different stages of activation, typically in different anatomical locations. Thus, anti-CTLA-4 primarily affects T cell expansion and trafficking while anti-PD-1 mostly enhances effector T cell function in the periphery[61]. Unfortunately, approximately only 20% of patients respond to monotherapy ICI[32]. To improve the number of patients who benefit from ICI, investigators have explored new therapeutic methods. Based on the different modes of action, it was hypothesized that the combination of anti-CTLA-4 and anti-PD-1 would elicit a broader anti-tumor T cell response and therefore result in higher overall response rates. Preclinical murine models confirmed this hypothesis, showing evidence of synergy with combination therapy[22]. Clinical trials were then initiated in 2010, originally administering concurrent ipilimumab and nivolumab in a cohort of patients with advanced melanoma, which resulted in deep tumor regression and higher response rates than monotherapy[63]. Success in clinical trials led to the FDA approval of combination ipilimumab and nivolumab to treat metastatic melanoma in 2015, the first approval for combined immunotherapies. Subsequent clinical trials were conducted in patients with a variety of solid tumr types, consistently demonstrating higher response rates and improved overall survival compared to single agent ICI[32]. This combination therapy is now approved for several additional tumor types including hepatocellular carcinoma, non-small cell lung cancer, and renal cell carcinoma, and is currently being evaluated as a therapeutic option for others such as breast cancer[32,64].

Although ICI therapy, whether alone or in combination, provides a substantial survival benefit to many patients, there is a pressing need for new therapeutic targets and therapy combinations to

treat patients who do not respond to traditional ICI. In particular, hematological tumors and several solid tumors such as glioblastoma, pancreatic cancer, and prostate cancer have been challenging to treat with ICI[32]. Several new checkpoint targets have been investigated in the past few years in an effort to overcome this hurdle. Some examples of inhibitory molecules of interest are lymphocyte activation gene 3 (LAG-3) and T cell immunoglobulin and immunoreceptor-tyrosine-based-inhibitory-motif (TIGIT). So far, these have proven to be promising targets, with many therapeutics currently in clinical trials[65,66]. Furthermore, new ICI combinations are also being investigated. There have been studies evaluating the efficacy of ICI with chemotherapy, radiation, targeted therapy, or other ICIs[32]. The discovery of new therapeutic targets and therapeutic combinations will continue to move the ICI field forward, boosting patient response and overcoming challenges of resistance.

1.3 Underlying mechanisms of ICI efficacy

Targeting inhibitory checkpoint molecules elicits strong anti-tumor responses by essentially removing the "brake" on T cells and allowing for the reinvigoration and activation of anti-tumor T cells. While this general mechanism of action holds true across the varying types of ICIs, the underlying cellular mechanisms are distinct.

Treatment with either anti-CTLA-4 or anti-PD-1 leads to the expansion of tumor-specific CD8+ T cells. Preclinical murine studies and clinical investigations utilizing melanoma tumor samples identified two intratumoral populations that appear to contribute to most of the anti-tumor response. These subsets include less exhausted non-terminally differentiated and fully exhausted terminally differentiated CD8+ T cells[61]. Notably, phenotypically exhausted PD-1hiTIM3+ CD8+

T cells demonstrate high levels of proliferation particularly following anti-PD-1 treatment, suggesting anti-PD-1 specifically targets this population[61]. Additionally, within circulating lymphocytes, PD-1 blockade is uniquely associated with increased expression of genes involved in cytolytic function, such as granzyme B, and regulation of T effector and natural killer function, like KLRF1[62]. Thus, it is well understood that anti-PD-1 directly modulates exhausted-like CD8+ T cells, enhancing their anti-tumor effector functions.

While PD-1 blockade primarily affects the CD8+ T cell compartment, CTLA-4 blockade seems to have a more pronounced impact on CD4+ T cells. Both anti-CTLA-4 and anti-PD-1 treatment lead to a shift in effector and regulatory T cell populations, with an overall relative decrease in Treg frequency[40,61]. However, the decrease in Tregs is much greater following CTLA-4 blockade[61]. Murine tumor models also show that targeting CTLA-4 results in the depletion of intratumoral Tregs[67,68]. This indicates one distinct mode of action of CTLA-4 blockade may be the reduction of immunosuppressive Tregs within the tumor microenvironment, allowing for the full activation of anti-tumor effector T cells. Additionally, CTLA-4 blockade is associated with the enrichment of activated CD4+ T cells, particularly among Tbet+ Th1-like CD4+ effector cells[61,69-71]. Interestingly, these expanded Th1-like CD4+ T cells are reported to also express PD-1 and ICOS and produce IFNg[61,70,71], although the exact function of these cells is not yet fully understood. Furthermore, in contrast to PD-1, anti-CTLA-4 induces the expression of several proliferation and cell cycle-associated genes in circulating T cells. In particular, there is a notable upregulation of Ki-67, a prominent proliferation marker, on a subset of transitional memory T cells[62]. Together, these data indicate that blockade of CTLA-4 or PD-1 are mechanistically different, with distinct, largely non-overlapping cellular and genomic signatures.

1.4 Immune Related Adverse Events Induced by ICI

Blockade of checkpoint inhibitors has resulted in impressive and durable tumor regression across several cancer types. However, these therapies are often associated with the development of immune related adverse events (irAEs)[72,73]. irAEs pose a great challenge as they often require patients to pause treatment or completely stop treatment altogether, limiting the optimal application of ICI[73]. These autoimmune toxicities are extremely diverse and have been reported to affect almost every organ system, with the most common being skin, GI tract, and liver[72,73]. Clinical data indicates that 70-80% of patients receiving ICI treatment develop irAEs, with high grade (grade 3-4) irAEs developing in 8% of patients receiving ipilimumab (anti-CTLA-4) and 19% of patients receiving nivolumab (anti-PD-1). However, the number of patients who develop high grade irAEs is drastically higher (40-50%) among those who receive combination anti-PD-1 and anti-CTLA-4 checkpoint blockade (CCB)[74,75].

irAEs can manifest in a number of different ways, with the pattern and onset differing based on the therapeutic target (CTLA-4 vs PD-1) or the combination of the two. Early studies in murine models described differing immune effects of ICIs. Genetic depletion of CTLA-4 in mice resulted in multiorgan autoimmunity and severe lymphoproliferative disorders that led to early death[36,37]. Alternatively, PD-1 knockout mice demonstrated a milder phenotype with strain-specific autoimmunity developing later in life[47,76]. Data from the clinic also show similar phenomena. Anti-CTLA-4 is associated with higher rates of toxicities in the GI tract and the endocrine system while anti-PD-1 leads to fewer overall toxicities but higher rates in the thyroid and pulmonary system. In combination therapy, the most common toxicities are reported to be hepatitis and colitis[75]. Consistent with clinical findings, ex vivo studies show that each of the ICI strategies result in

distinct genomic signatures in patient immune cells[61,62,77]. These data collectively demonstrate the varying patterns of toxicities with CTLA-4 and/or PD-1 blockade and offer insight into the possible mechanisms by which irAEs develop.

Most irAEs develop quickly, often presenting following the first treatment cycle. A pooled analysis of patients receiving ICI therapy noted the median time to onset of all irAEs is 2.2-14.8 weeks. This median time was shorter in CTLA-4 monotherapy and CCB, as irAEs in PD-1 monotherapy took slightly longer to develop[78]. Previous studies from our lab and others describe early changes in B cells observed shortly after patients begin treatment. Following one cycle of anti-PD-1 or CCB, patients with melanoma, renal cell carcinoma, liver cancer, and lung cancer showed decreased levels of overall circulating B cells accompanied by increased levels of $CD21^{lo}$ B cells and plasmablasts. In particular, the phenotype of the expanded $CD21^{lo}$ B cells appeared to be similar to a subset of Tbet+ B cells that have been described in patients with autoimmune diseases. Additionally, these B cell changes correlated with the onset of severe irAEs, implicating B cells in the pathogenesis of irAE development[79-84]. This information gives some insight into the potential mechanisms by which irAEs develop and suggest that some patients may have an underlining predisposition to autoimmunity. Ultimately, it is of great interest to identify patients at risk of developing severe irAEs prior to treatment in order for preemptive measures to be taken.

Multiple irAE mechanisms have been proposed, however the exact pathophysiology of these toxicities is not fully understood. CTLA-4 and PD-1 are key players in maintaining peripheral tolerance and controlling autoreactive T and B cells[76,85-87]. It is generally thought that by blocking these checkpoint molecules, irAEs develop as the result of immune imbalance and the loss of

peripheral tolerance[84]. While the aberrant activation of both autoreactive T and B cells are believed to be central to this process (Figure 1.2), much of the focus has been on studying the role of T cells. Several studies have outlined potential T cell-related mechanisms of irAE development. One proposed mechanism suggests that as tumor cells die and release antigen, T cells become activated against both tumor tissue and healthy tissue that share the same released antigens. This is supported by data demonstrating the presence of shared TCRs between both tumor and autoimmune tissue, such as in the skin and cardiac muscle[88,89]. Alternatively, other studies suggest that in some cases, there is a clear difference between the T cells that target the tumor versus those that target healthy tissue. These findings show that in ICI-induced colitis and dermatitis tissue, there is a high proportion of inflammatory, activated T cells originating from tissue-resident memory (T_{RM}) cells[90,91]. Currently, most studies conducted focus on identifying mechanisms among specific irAEs. It is unclear whether there are differing mechanisms of irAE development based on the affected organ, or if there are general, systemic changes occurring that lead to autoimmunity.

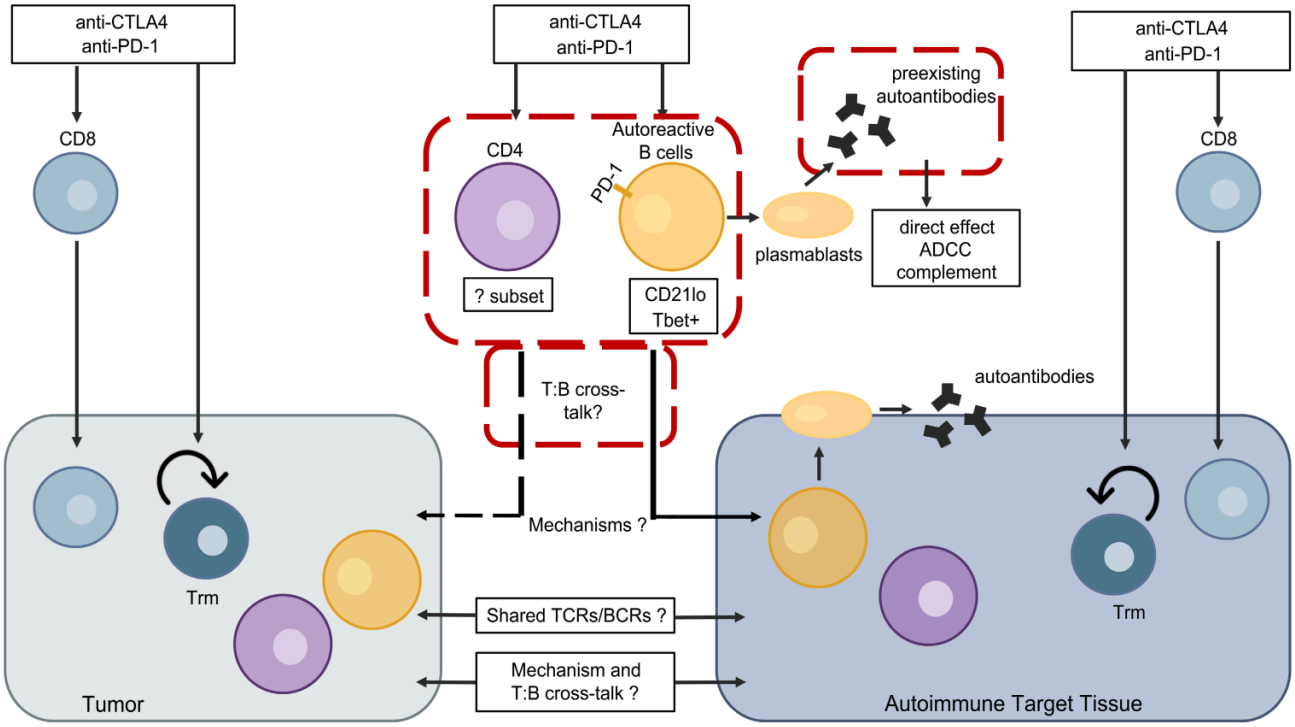

Figure 1.2: Role for B cells and T:B cross talk in immune-related adverse events (irAEs) following immune checkpoint blockade. Activation of autoreactive B cells as well as T cells following checkpoint blockade contributes to irAEs. Baseline levels of CD4 cells as well as changes in CD21loTbet+ B cells have been linked to the development of high-grade irAEs. Cross talk between these cells may contribute to tissue inflammation in autoimmune tissues. Highlighted boxes represent some potential areas of intervention for preventing these irAEs.

1.5 Summary, scope, and goals for this project

In summary, immune checkpoint inhibitors have transformed the treatment landscape for several types of cancers, particularly for tumor types with previously poor responses to other therapies. However, it is imperative to develop a more robust understanding of the cellular mechanisms underlying these therapies in order to fully optimize treatment and rationally design new combinations. Thus, the overall goal of this project was to provide new insights into the systemic impact of ICIs beyond the well documented anti-tumor T cell-mediated activity. While the mechanisms of anti-tumor response when administering anti-CTLA-4, anti-PD-1, or the combination of both have been well documented[61,62], the differences between anti-PD-1 and anti-PD-L1 remained understudied. Therefore, focusing first on efficacy of ICIs, this project sought to differentiate the cellular effects of PD-1 versus PD-L1 blockade in patients based on the distinct genomic profiles generated by each treatment. The second goal of this work was to tackle another major clinical challenge through investigating mechanisms of toxicity. Clinical data thoroughly reports the prevalence of irAEs associated with ICIs, particularly in patients receiving CCB with anti-CTLA-4 and anti-PD-1[72-75]. As irAEs remain a significant challenge with ICI therapy, this project sought to uncover the mechanisms by which these toxicities develop. Additionally, it was important to highlight phenotypic and/or functional immune cell differences between patients to understand why some develop severe toxicities while others do not. Thus, in this text herein, I discuss my efforts and scientific findings contributing to the advancement of ICI therapy. Ultimately, with this work, our aim is to further the understanding of ICI mechanisms of efficacy and toxicity, leading to improved patient outcomes.

Chapter 2: Differential effects of PD-L1 versus PD-1 blockade on myeloid inflammation in human cancer

Noffar Bar,[1] Federica Costa,[2,3] Rituparna Das,[2] Alyssa Duffy,[2] Mehmet Samur,[4] Samuel McCachren,[2] Scott N. Gettinger,[1] Natalia Neparidze,[1] Terri L. Parker,[1] Jithendra Kini Bailur,[2] Katherine Pendleton,[2,5] Richa Bajpai,[2] Lin Zhang,[1] Mina L. Xu,[6] Tara Anderson,[1] Nicola Giuliani,[3] Ajay Nooka,[2] Hearn J. Cho,[7] Aparna Raval,[8] Mala Shanmugam,[2,9] Kavita M. Dhodapkar,[5,9] and Madhav V. Dhodapkar[2,9]

Affiliations: [1]Department of Medicine, Yale University School of Medicine, New Haven, Connecticut, USA; [2]Department of Hematology/ Oncology, Emory University, Atlanta, Georgia, USA; [3]Department of Medicine and Surgery, University of Parma, Parma, Italy; [4]Department of Data Sciences, Dana-Farber Cancer Institute, Boston, Massachusetts, USA; [5]Department of Pediatrics, Children's Healthcare of Atlanta, Emory University, Atlanta, Georgia, USA; [6]Department of Pathology, Yale University School of Medicine, New Haven, Connecticut, USA; [7]Mount Sinai Medical Center, New York, New York, USA; [8]Oncology Biomarker Development, Genentech, South San Francisco, California, USA; [9]Winship Cancer Institute, Emory University, Atlanta, Georgia, USA

Authorship note: NB, FC, RD, and AD are co–first authors. KMD and MVD are co–senior authors.

The work contained in this chapter is reproduced with minor edits and was originally published in JCI Insight in 2020.

Citation:

Bar N, Costa F, Das R, **Duffy A**, Samur M, McCachren S, Gettinger SN, Neparidze N, Parker TL, Bailur JK, Pendleton K, Bajpai R, Zhang L, Xu ML, Anderson T, Giuliani N, Nooka A, Cho HJ, Raval A, Shanmugam M, Dhodapkar KM, Dhodapkar MV. Differential effects of PD-L1 versus PD-1 blockade on myeloid inflammation in human cancer. JCI Insight. 2020;5(12). doi: 10.1172/jci.insight.129353.PMID:32427579 ; PMCID: PMC7406262

2.1 Abstract

BACKGROUND. PD-1 and PD-L1 have been studied interchangeably in the clinic as checkpoints to reinvigorate T cells in diverse tumor types. Data for biologic effects of checkpoint blockade in human premalignancy are limited. METHODS. We analyzed the immunologic effects of PD-L1 blockade in a clinical trial of atezolizumab in patients with asymptomatic multiple myeloma (AMM), a precursor to clinical malignancy. Genomic signatures of PD-L1 blockade in purified monocytes and T cells in vivo were also compared with those following PD-1 blockade in lung cancer patients. Effects of PD-L1 blockade on monocyte-derived DCs were analyzed to better understand its effects on myeloid antigen presenting cells. RESULTS. In contrast to anti–PD-1 therapy, anti–PD-L1 therapy led to a distinct inflammatory signature in CD14+ monocytes and increase in myeloid-derived cytokines (e.g., IL-18) in vivo. Treatment of AMM patients with atezolizumab led to rapid activation and expansion of circulating myeloid cells, which persisted in the BM. Blockade of PD-L1 on purified monocyte-derived DCs led to rapid inflammasome activation and synergized with CD40L-driven DC maturation, leading to greater antigen-specific T cell expansion. CONCLUSION. These data show that PD-L1 blockade leads to distinct systemic immunologic effects compared with PD-1 blockade in vivo in humans, particularly manifest as rapid myeloid activation. These findings also suggest an additional role for PD-L1 as a checkpoint for regulating inflammatory phenotype of myeloid cells and antigen presentation in DCs, which may be harnessed to improve PD-L1–based combination therapies.

2.2 Key Findings

- Distinct genomic signature of PD-L1 blockade in human cancer, characterized by changes in myeloid cells.

- PD-L1 blockade leads to enhanced DC maturation and in synergy with CD40L signal, promotes expansion of antigen-specific T cells.
- Role for PD-L1 in the afferent arm of the cancer immunity cycle.
- One of the first clinical studies for PD-L1 blockade in cancer precursor states.

2.3 Introduction

Antibody-mediated blockade of PD-1 or PD-L1 has led to tumor regression and improved survival in a subset of patients with diverse tumor types[92]. PD-L1–expressing tumor cells and antigen-presenting cells (APCs) engage PD-1+ T cells, leading to T cell dysfunction. In view of the dominant role of T cells in tumor immunity, blockade of PD-1 or PD-L1 has been studied interchangeably in clinical cancer immunotherapy as a strategy to activate T cells. However, both molecules have alternate ligands/receptors; it has also been suggested that PD-L1 can act as a receptor to back-transmit signals into T cells[53] and tumor cells[93]. PD-L1 is constitutively expressed on a subset of myeloid APCs, including DCs, and prior studies in murine models have suggested a functional role for PD-L1 in myeloid cells or DCs[94-96]. Direct comparison of signaling pathways altered in vivo following PD-1 or PD-L1 blockade in T cells and APCs in humans are limited and may help optimal design of combination therapies with these antibodies (Figure 2.1A). While the PD-L1 axis has been extensively studied in the context of immunotherapy of established cancer, data about the effects of PD-L1 blockade on premalignant states are limited.

Multiple myeloma (MM) is a common hematologic malignancy, which is preceded in all cases by well-defined precursor states, monoclonal gammopathy of undetermined significance (MGUS), and asymptomatic MM (AMM)[97]. In spite of major therapeutic advances, there is an unmet need

to achieve durable unmaintained responses in this malignancy, prompting the need to pursue strategies to engage long-term immunologic memory against tumor cells. Antibody-mediated blockade of PD-1 as a single agent did not lead to tumor regression in relapsed MM[98]. Prior studies have demonstrated immune recognition of preneoplastic MGUS cells by T cells[99,100]. In a prospective trial, the presence of preexisting T cell immunity to an embryonal stem cell antigen SOX2 was associated with reduced risk of progression to clinical MM[101]. MM tumor cells commonly express PD-L1, and the expression of PD-L1 on MGUS/AMM cells correlated with an increased risk of transformation to clinical malignancy[101,102]. These considerations prompted us to initiate a clinical trial of single-agent anti–PD-L1 antibody (atezolizumab) in patients with AMM (Figure 2.1B).

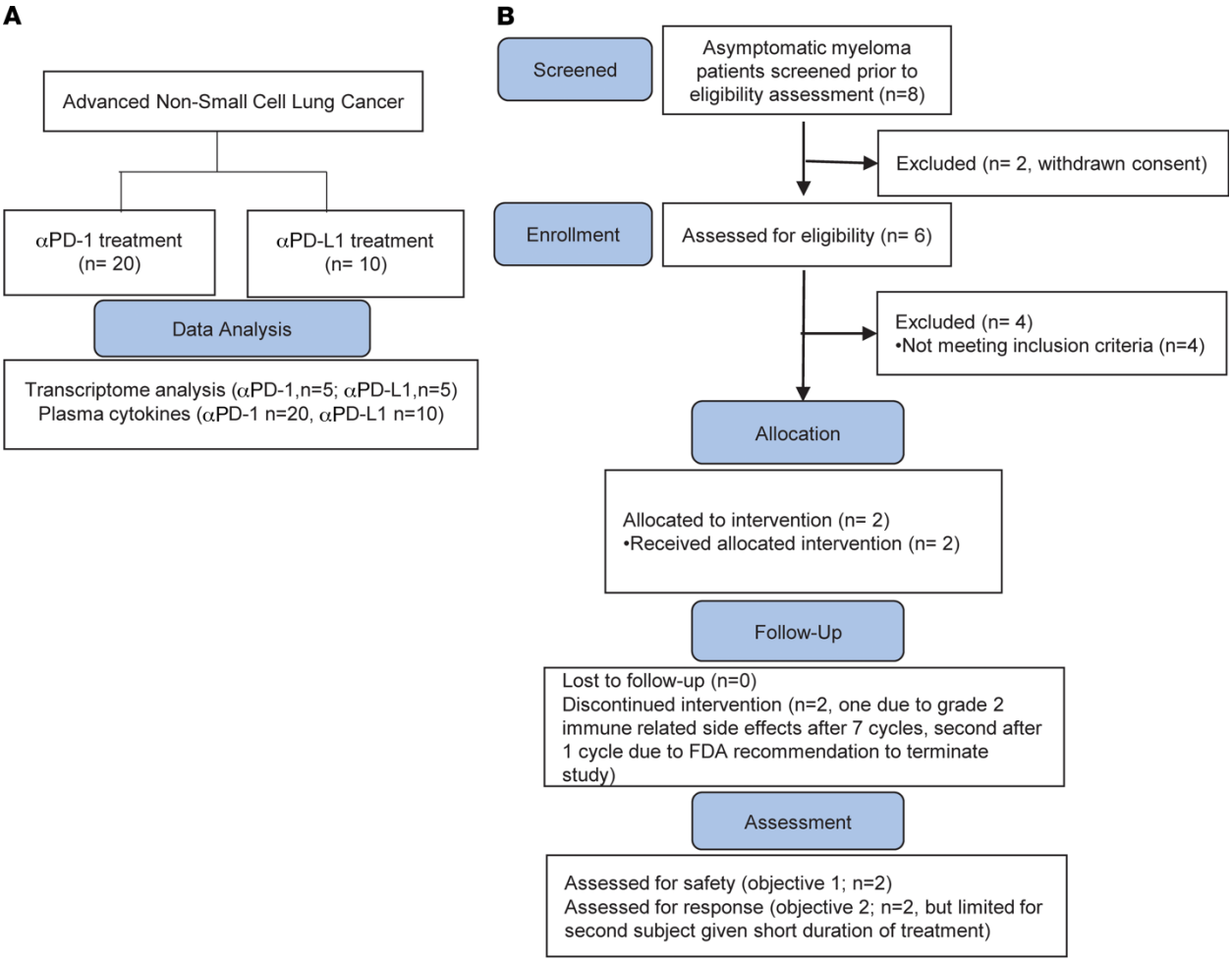

Figure 2.1: CONSORT flow diagram for non-small cell lung cancer and asymptomatic myeloma clinical trials. (A) Diagram reporting the distribution of anti-PD-L1 and anti-PD-1 treatment in patients with non-small cell lung cancer and subsequent data analysis. (B) Flow diagram reporting the process of screening, enrollment, allocation, follow-up, and assessment through the phases of the clinical trial of single-agent atezolizumab in patients with asymptomatic myeloma.

2.4 Results

Prior studies have shown that therapy with anti–CTLA-4, anti–PD-1, or combination leads to distinct genomic signatures in purified human T cells and monocytes in vivo[62]. In order to compare the genomic and proteomic profiles of anti–PD-1 and anti–PD-L1 therapies, we isolated T cells and CD14+ monocytes from peripheral blood before and after anti–PD-L1 therapy in patients with advanced non–small cell lung cancer and analyzed changes in gene expression using Affymetrix HTA v2.0 array (Figure 2.1A). In direct contrast to prior studies with anti–PD-1 therapy, which predominantly leads to gene expression changes in T cells[62], anti–PD-L1 therapy led to dominant gene expression changes in CD14+ monocytes (Figure 2.2A). Importantly, changes in gene expression following anti–PD-L1 therapy in both T cells and monocytes were nonoverlapping with those observed following anti–PD-1 therapy (Figure 2.2A). Top differentially expressed genes [103] in myeloid cells following PD-L1 blockade included inflammation-associated genes such as heparin-binding EGF-like growth factor (HBEGF), thrombospondin-1 (THBS), IL-1β, CXCL1/GROα, CXCL2, and NLRP3 (Figure 2.2B). Pathway analysis of DEGs ($q < 0.01$) in monocytes revealed pathways related to inflammation and inflammasome-associated cytokines (IL-1 and IL-18) (Table 2.1). In order to further validate these data in the context of samples analyzed together and determine if these signals were derived from only a subset of monocytes, we analyzed purified monocytes from patients before and after anti–PD-1/PD-L1 therapy using single cell RNA sequencing (RNA-seq). These data demonstrate that early changes in myeloid cells were again more prominent following PD-L1 blockade (Figure 2.2C) and involved nearly all

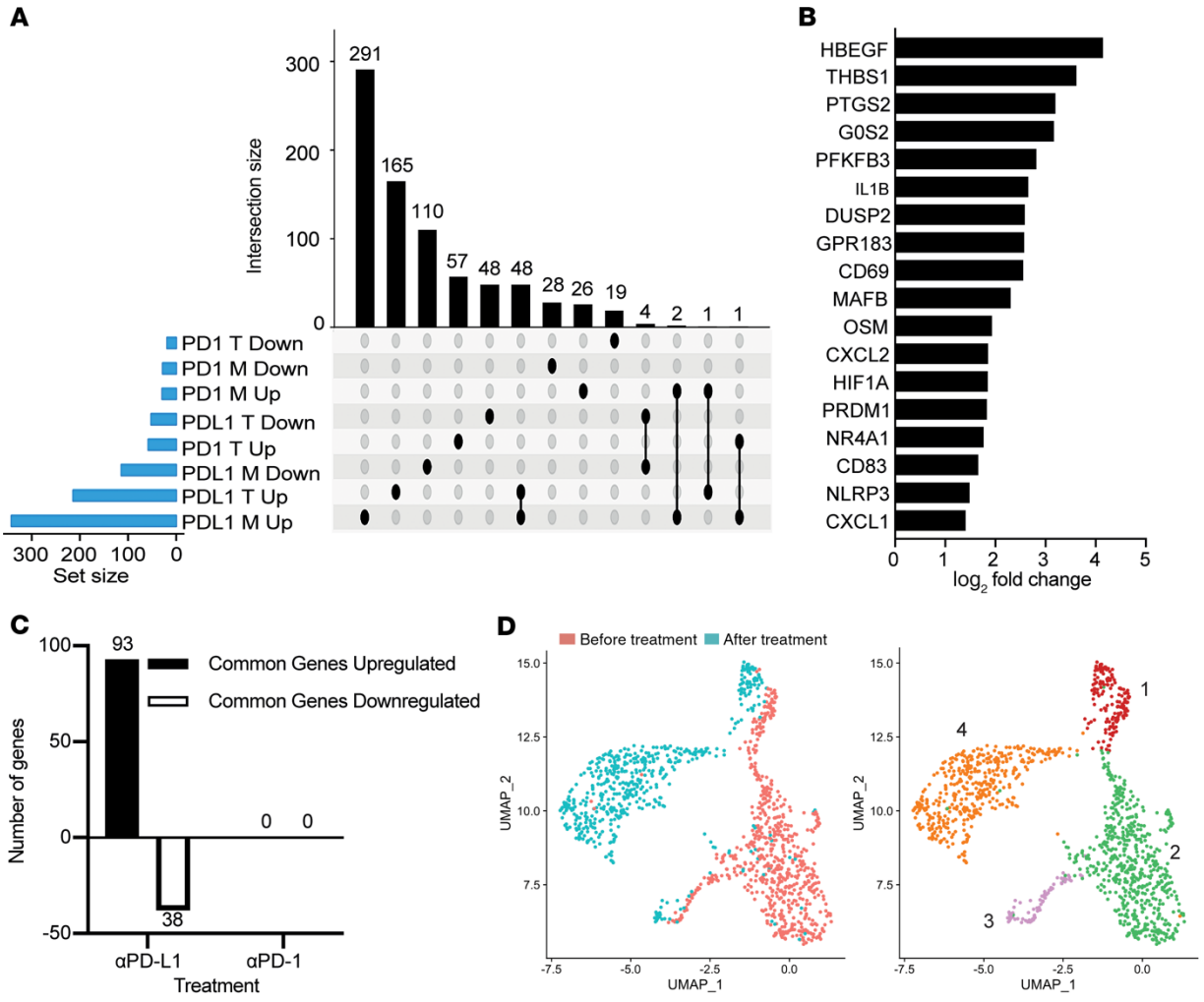

Figure 2.2: PD-L1 blockade leads to distinct transcriptomic changes in circulating monocytes and T cells. RNA was extracted from magnetic bead isolated CD14+ monocytes and CD3+ T cells from patients with lung cancer before and after therapy with either anti–PD-L1 (atezolizumab; *n* = 5) or anti–PD-1 (nivolumab; *n* = 6 previously published)[100] and analyzed using affymetrix human transcriptome array 2.0. (A) Distribution of differentially regulated genes upregulated and downregulated in monocytes and T cells following therapy with anti–PD-L1 or anti–PD-1. (B) Differentially regulated genes in monocytes following therapy with anti–PD-L1 (selected from top 50 differentially regulated genes). (C) Single cell RNA sequencing was performed before and after therapy with either anti–PD-L1 (*n* = 3) or anti–PD-1 (*n* = 4). Figure shows the number of shared

differentially expressed (Wilcoxon rank-sum with Bonferroni's correction, $p < 0.05$) genes after versus before treatment between all anti–PD-L1 treated monocytes and all anti–PD-1–treated monocytes. (D) Uniform manifold approximation and projection (UMAP) plots of monocytes from single cell RNA sequencing of anti–PD-L1 monocytes before and after treatment (left panel: blue, after treatment; red, before treatment) and monocyte groups identified by unsupervised clustering (right panel). Cluster 1 represents CD16+ monocytes; clusters 2, 3, and 4 represent CD16- monocytes.

Table 2.1: Pathways enriched in circulating monocytes following therapy with anti-PD-L1 in vivo.

Pathway	FDR
IL-1 signaling in melanoma	3.59E-07
Immune response IL-1 signaling pathway	4.81E-07
Cell adhesion_IL-8 family dependent cell migration and adhesion	1.82E-07
IL-1 production in melanoma	4.65E-06
Immune response_IL-18 signaling	2.99E-05
Immune response_IL-17 signaling pathways	2.99E-05
Macrophage and dendritic cell phenotype shift in cancer	6.45E-05

Table 2.2. Clinical characteristics.

	Patient 1	**Patient 2**
Age (years)	59	54
Sex	Male	Male
M spike IgH/L isotype	IgA kappa	IgG Lambda
Total number of cycles	7	1
IrAE (≥ grade 2)	Grade 2 adrenal insufficiency Grade 2 hypothyroidism	None
Best Response to therapy	Stable disease	Stable disease

classical monocytes (Figure 2.2D). Changes in gene expression in these monocytes were similar to those in earlier studies (Figure 2.3A) and also revealed pathways consistent with myeloid activation (Figure 2.3B). Analysis of sera before and after therapy demonstrated that, while both therapies led to an increase in IP-10 as a marker of immune activation, increases in serum IL-18, GROα, IFN-a2 typically derived from myeloid cells and sCD40L, are only observed following anti–PD-L1 therapy (Figure 2.4, A–E). Taken together, these data demonstrate that systemic immunologic changes following anti–PD-L1 therapy are surprisingly distinct from that following anti–PD-1 therapy, both at genomic and proteomic levels — in particular, with rapid activation of inflammation-associated genes in monocytes.

Expression of PD-L1 was previously correlated with the risk of progression to MM[101]. In order to evaluate the potential of targeting the PD-L1 axis to prevent MM, we enrolled AMM patients in a pilot trial of single-agent atezolizumab. The trial was closed prematurely based on FDA guidance after enrollment of only 2 patients due to safety concerns emerging in 2 clinical trials of pembrolizumab and lenalidomide in MM. Clinical data from these patients are summarized in Table 2.2. Both patients had stable disease at the time of study closure, after receiving 7 and 1 cycles, respectively, and remain progression-free off therapy with 23- and 18-month follow-up. Patient 1 developed grade 2 endocrinopathy with hypothyroidism and adrenal insufficiency after 7 cycles. Incidentally, this patient also experienced remission of prior gluten intolerance after enrolling in the study. Serial analysis of peripheral blood samples by mass cytometry revealed an early increase in blood monocytes and a decline in B cells in both patients, detected at 15 days after initiation of therapy (cycle 1 day 15; C1D15) (Figure 2.5A and Figure 2.6A). Phenotypic analysis revealed an increase in CD16+CD40+HLADRhi

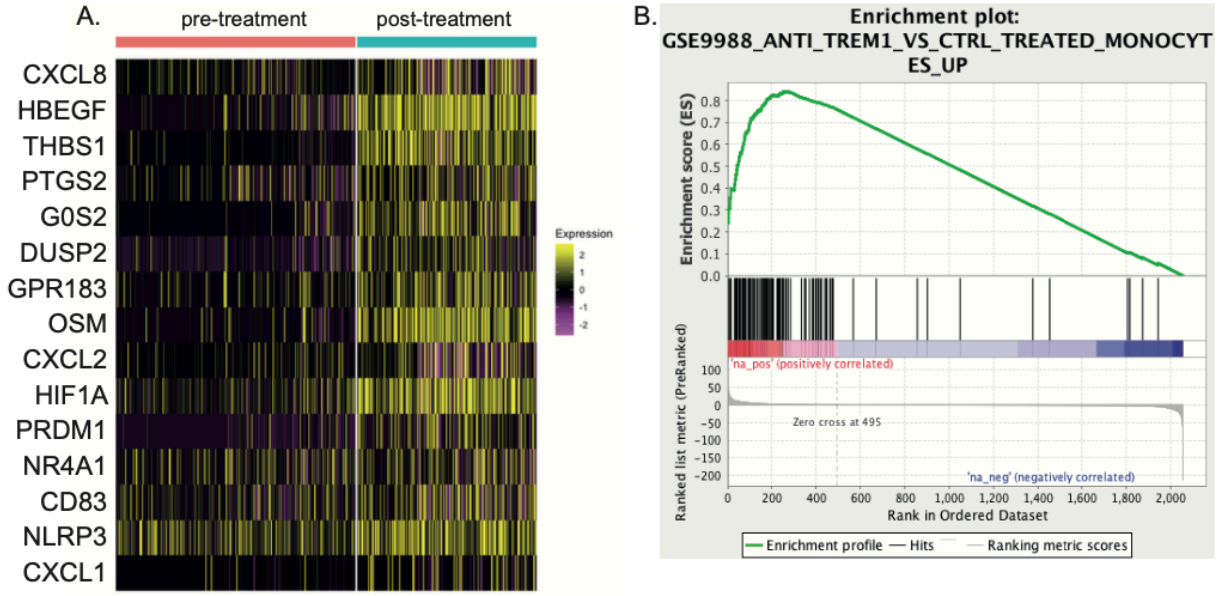

Figure 2.3: Single-cell RNA sequencing differential gene expression in classical (CD14+ CD16-) monocytes post vs. pre anti-PD-L1 treatment. (A) Heatmap of selected significantly differentially expressed genes (Wilcoxon rank-sum test Bonferroni corrected $p<0.05$) with increased expression in the CD16- monocyte cluster post-treatment relative to the baseline CD16- monocyte cluster. (B) Gene Set Enrichment Analysis (GSEA) pathway analysis of all significantly differentially genes in CD16- monocytes post- versus pre-treatment revealed enrichment of gene sets associated with activated/stimulated monocytes after treatment relative to baseline. Representative enriched pathway: anti-TREM1 stimulated monocytes (corresponding to post-treatment monocytes) versus control unstimulated monocytes (corresponding to pre-treatment monocytes).

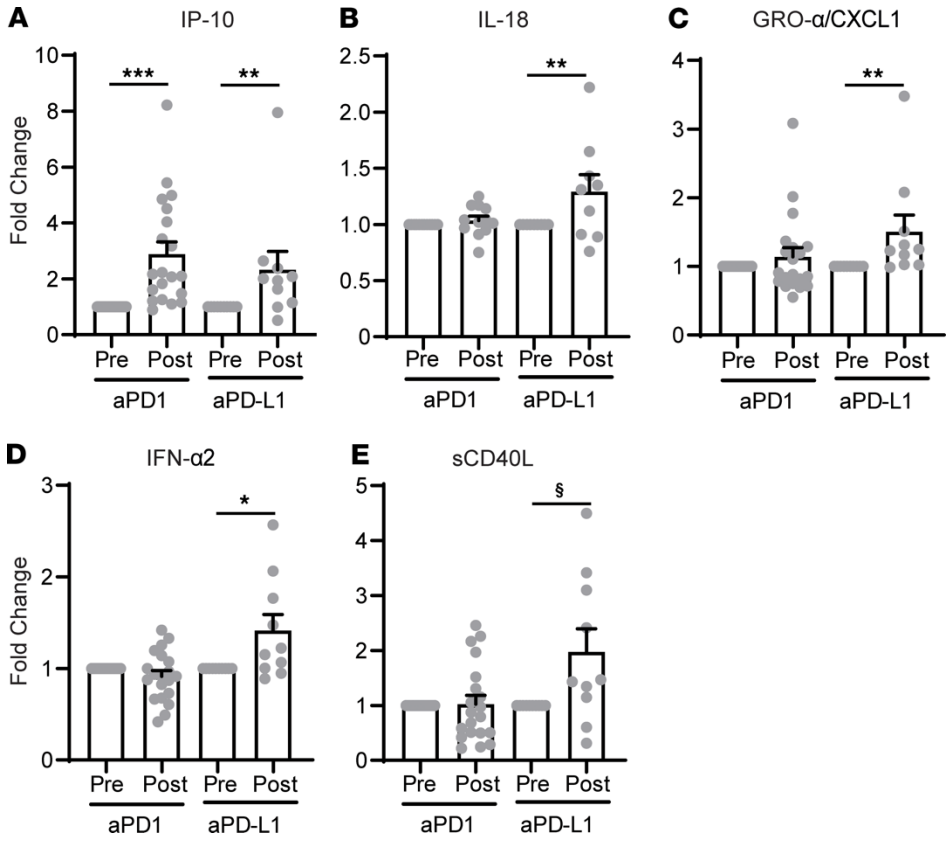

Figure 2.4. PD-L1 blockade leads to distinct plasma cytokine profiles. Plasma collected before and after therapy with anti–PD-L1 (*n* = 10) or anti–PD-1 (*n* = 20, as previously published(Spisek, 2007 #523)) was analyzed using Luminex multiplex/ELISA. Figure shows changes in plasma IP-10 (A), IL-18 (B), GRO-α/CXCL1 (C), IFN-a2 (D), and sCD40L (E) following therapy with anti–PD-L1 or anti–PD-1. (*p< 0.05, **p< 0.01, ***p< 0.001, §p= 0.06 by Mann-Whitney U test).

monocytes (Figure 2.5B). In order to validate these findings in an independent data set, we analyzed early changes in blood monocytes from another clinical trial in MM (NCT02431208), wherein a cohort received single-agent atezolizumab. These data also corroborate our prior studies and demonstrate a similar pattern of rapid increase in circulating activated monocytes in vivo (Figure 2.5C). Taken together, data from both lung cancer and MM patients show that PD-L1 blockade leads to early activation of myeloid cells with a transient increase in activated circulating monocytes in vivo.

Evaluation of T cells in AMM patients treated with atezolizumab revealed an early increase in circulating CD8+ and CD4+ memory T cells detectable by C1D15 (Figure 2.8A and Figure 2.6B). Single cell mass cytometry revealed proliferation of CD8+ and CD4+ effector memory [104] compartment, as well CD8+ central memory (Tcm) compartment, manifest as upregulation of Ki-67 (Figure 2.8B). In prior studies, we have shown that SOX2 is a common antigenic target of T cells in MGUS[100]. Evaluation of antigen-specific T cells at C1D15 also revealed an increase in antigen-reactive IP10 production following stimulation with SOX2-peptide library (Figure 2.8C). However, therapy-induced changes in circulating T cells were transient and returned to baseline by cycle 2. Although the number of total B cells declined, therapy was also associated with an increase in the CD21lo B cell subset implicated in autoimmunity[83] (data not shown). Analysis of serum cytokines also revealed early but transient changes in inflammatory cytokines (IL-18, IP-10, GROα, and TNF-α), which returned closer to baseline by cycle 2 (Figure 2.7). Together, these data show that atezolizumab leads to rapid but only transient systemic immune activation in vivo in AMM patients.

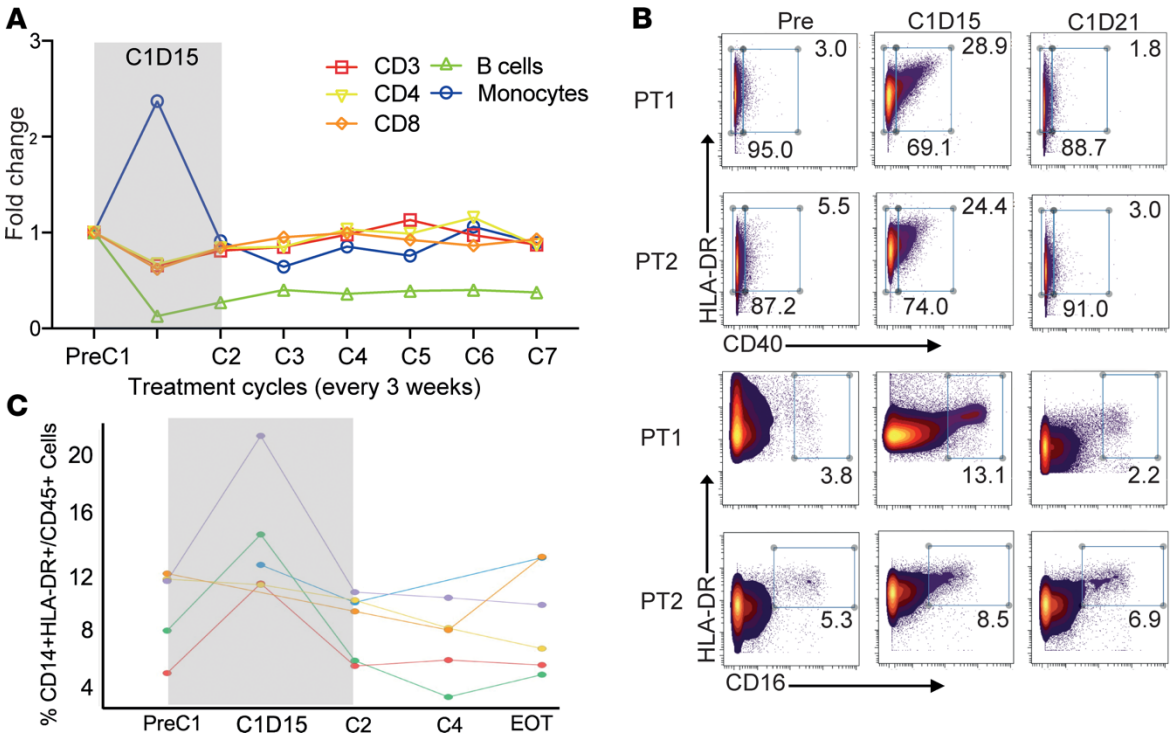

Figure 2.5: Changes in circulating immune cells following therapy with anti–PD-L1 in asymptomatic myeloma (AMM). PBMCs isolated from blood of AMM patients before therapy (PreC1) and following therapy with atezolizumab on day 15 (C1D15), as well as before cycles 2–7 (C2–C7) were analyzed using single cell mass cytometry or CyTOF. (A) Changes in circulating CD3+, CD4+, CD8+ T cells, monocytes, and B cells. Data are shown as fold change compared with pretherapy (PreC1) levels. (B) Expression of CD40, HLA-DR, and CD16 on circulating monocytes before therapy (Pre), on day 15 following first dose (C1D15), and before second dose of atezolizumab (C1D21) in 2 different patients (PT1 and PT2). (C) Changes in circulating monocytes in MM patients receiving atezolizumab in another clinical trial (NCT02431208). Each line represents an individual patient. EOT, end of therapy.

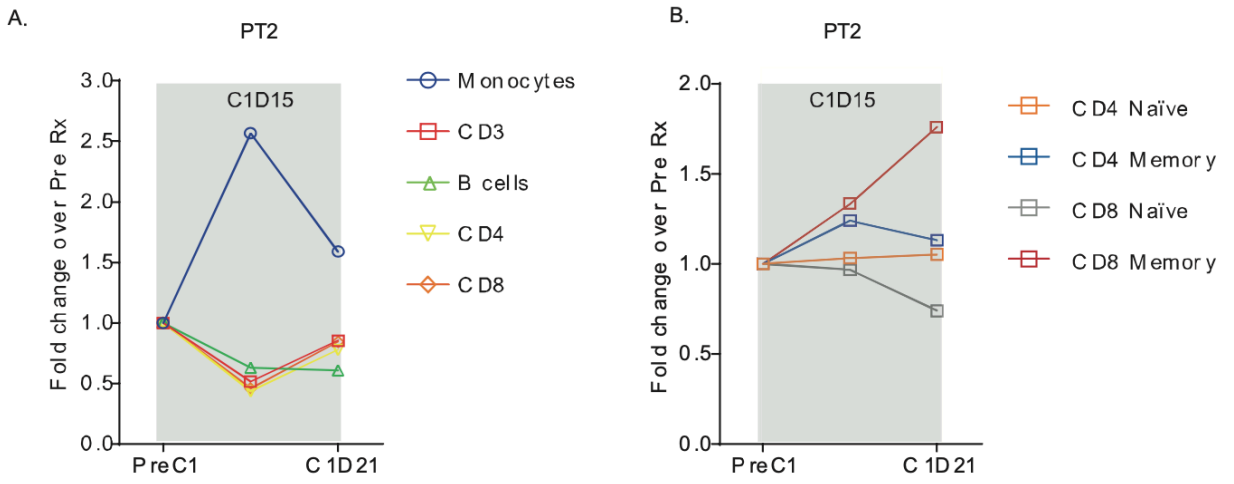

Figure 2.6: Changes in circulating immune cells of AMM patient following therapy with atezolizumab. (A) Changes in circulating CD3+, CD4+, CD8+ T cells, monocytes and B cells at day 15 (C1D15) and 21 (C1D21) following therapy with atezolizumab. Data shows fold change compared to pre therapy (PreC1). (B) Change in circulating CD4+ and CD8+ naïve and memory T cells at day 15 (C1D15) and 21 (C1D21) following therapy with atezolizumab. Data shows fold change compared to pre therapy (PreC1).

Evaluation of posttreatment BM specimens was planned after the completion of 2 cycles and, therefore, was obtained in only 1 patient. Post-treatment BM revealed a decline in T and B cells but clear increase in the proportion of CD14+ myeloid cells (Figure 2.9, A and B), which also exhibited some evidence of activation manifest with upregulation of HLA-DR (Figure 2.9C). Although reduced in number, BM memory T cells from posttreatment biopsies did demonstrate an increase in granzyme and Tbet relative to baseline samples, particularly within the Tem subset (Figure 2.9D). In order to understand the observed changes in immune cells in further detail, we analyzed single cell transcriptomes of circulating as well as BM mononuclear cells. In the BM, single cell RNA-seq (scRNA–seq) identified 6 major T/NK cell clusters (Figure 2.10, A and B). Of these, the proportion of T cell clusters 0 and 3 declined in the post-treatment biopsy, consistent with reduction in T cells detected by mass cytometry. In contrast, there was an increase in the proportion of cells in several myeloid clusters, including classical CD14+ myeloid cells (cluster 5), CD16+ myeloid cells (cluster 7), and DCs (cluster 8). Pathway analysis of DEGs in these clusters demonstrated an increase in TNF-α signaling and IFN-a response in myeloid cells, as well as other cell types, consistent with evidence of inflammatory signaling in post-treatment BM (Table 2.3). scRNA–seq analysis of paired blood samples from baseline and C1D15 from both patients also demonstrated systemic changes in gene expression, particularly in cluster 2 (myeloid cells) and cluster 5 (B cells), consistent with prior results using mass cytometry (Figure 2.11 and Table 2.4). Pathway analysis revealed an enrichment of IFN response and inflammation-associated pathways after therapy in several major circulating cell types (T cells, B cells, monocytes, and NK cells), consistent with systemic immune activation and changes in serum cytokines at this time point (Table 2.4).

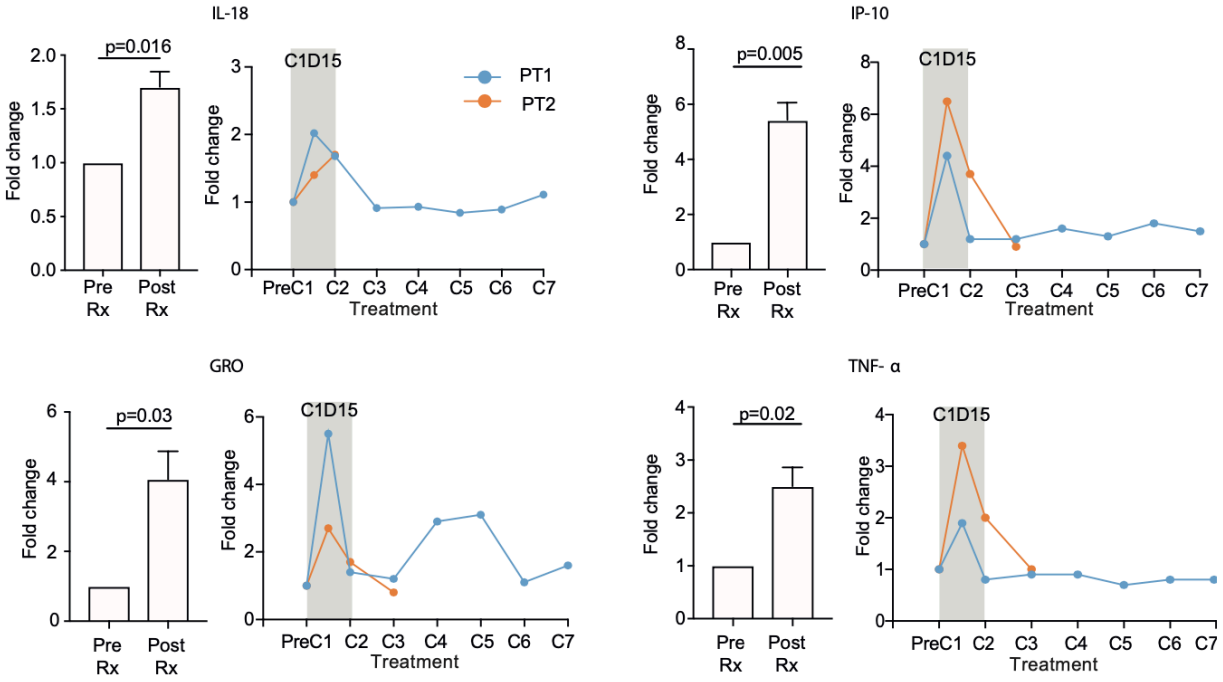

Figure 2.7: Changes in plasma cytokines following therapy with atezolizumab in AMM patients. Plasma obtained pre therapy (PreC1), 15 days following first dose of atezolizumab (C1D15) and prior to cycles 2-7 (C2-C7) was analyzed for presence of IL-18, IP-10, GRO and TNF-α. Bar graph shows plasma levels pre (PreRx) and post cycle 1 (PostRx; n=2 patients) as fold change compared to pre therapy. The line graphs show changes in cytokines over time.

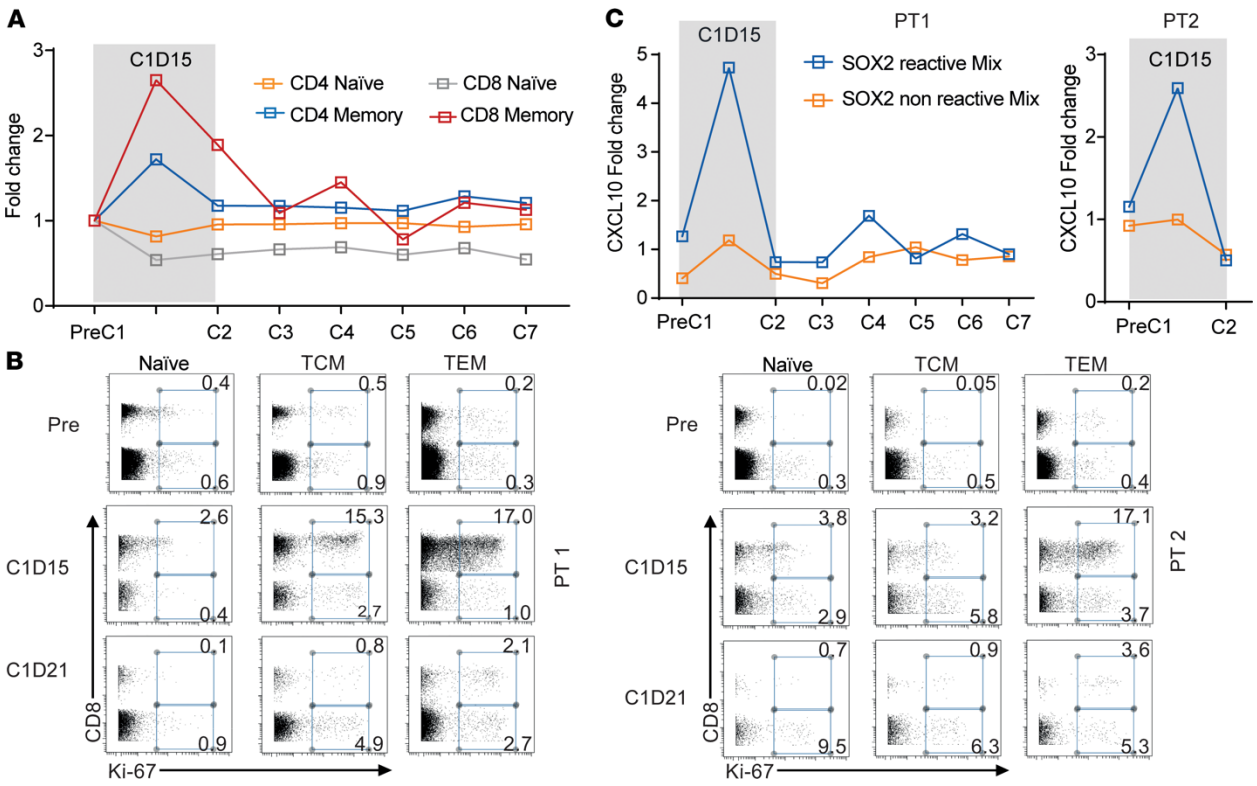

Figure 2.8. Changes in circulating T cells following therapy with anti–PD-L1 in asymptomatic myeloma (AMM). PBMCs isolated from blood of AMM patients before therapy (PreC1) and following therapy with atezolizumab on day 15 (C1D15), as well as before cycles 2–7 (C2–C7), were analyzed using single cell mass cytometry or CyTOF. (A) Changes in CD4+ and CD8+ naive and memory T cells during therapy with atezolizumab. Data are shown as fold change compared with levels before starting therapy (PreC1). (B) Ki-67+ proliferating naive (CCR7+RO-), central memory (Tcm; CCR7+RO+), and effector memory (Tem; CCR7-RO+) T cells before (Pre), 15 days following start of therapy (C1D15), and before cycle 2 (C1D21) of therapy with atezolizumab. Figure shows data from 2 separate patients. (C) PBMCs obtained pre therapy (PreC1), 15 days after starting therapy (C1D15), or before cycles 2–7 (C2-C7) were evaluated for

the presence of SOX2-specific T cell reactivity using overlapping peptides encompassing the entire SOX2 antigen as previously described[100]. Figure shows SOX2 T cell reactivity in the 2 patients. Data reported as fold change compared with before therapy (PreC1) for SOX2 reactive submix versus nonreactive mix as control.

Among myeloid cells, DCs constitutively express high levels of PD-L1. Prior studies have mostly focused on effects of PD-L1 blockade in the context of D:T cell interactions[92]. In order to test if PD-L1 may directly impact the biology of human monocyte-derived DCs (Mo-DCs) independent of DC:T cell interactions, we cultured purified Mo-DCs with anti–PD-L1 antibodies. Culture of Mo-DCs with anti–PD-L1, but not anti–PD-1, led to modest increases in CD80 and CD83 as markers of DC maturation (Figure 2.12A). This was associated with an increase in the secretion of several inflammatory cytokines— notably, IL-6, IL-8, TNF-α, and IL-1β — in the culture supernatants (Figure 2.12B), as well as rapid (within 4 hours) activation of caspase-1 (Figure 2.12C) and changes in cellular energetics associated with DC maturation, manifest as an increase in spare respiratory capacity (Figure 2.12D). In the setting of DC:T cell interaction, CD40L-mediated licensing of DCs is a critical regulator of antigen presentation[105]. Therefore, we examined the impact of PD-L1 blockade on DC maturation following suboptimal concentration of CD40L. PD-L1 blockade led to an increase in CD40L-driven DC maturation, as detected by the expression of CD80 and CD83 (Figure 2.13, A and B), but also greater expansion of influenza-matrix peptide–specific (Flu-MP–specific) T cells by Flu-MP–loaded DCs (Figure 2.13C). Expression of PD-L1 in human Mo-DCs can vary in a donor-dependent fashion. Expression of PD-L1 on DCs correlated with the observed synergy for DC maturation with CD40L and atezolizumab (Figure 2.14A). In order to further evaluate the effects of PD-L1 blockade on naturally occurring BM myeloid cells, we cultured these cells with atezolizumab. Consistent with our in vivo data, atezolizumab also led to an increase in CD16+HLADR+CD14+ BM myeloid cells in culture (Figure 2.14B).

Table 2.3. Differentially regulated pathways in bone marrow immune cells following therapy with anti-PD-L1.

	Pathway	FDR q-value
T cells		
Cluster 0	ALLOGRAFT_REJECTION	3.13E-18
	TNFA_SIGNALING_VIA_NFKB	4.63E-17
	HYPOXIA	2.31E-10
	APOPTOSIS	3.09E-10
	COMPLEMENT	2.55E-09
	INFLAMMATORY_RESPONSE	3.55E-08
	INTERFERON_GAMMA_RESPONSE	4.00E-07
Cluster 1	TNFA_SIGNALING_VIA_NFKB	3.11E-16
	HYPOXIA	1.31E-12
	APOPTOSIS	2.50E-03
	INFLAMMATORY_RESPONSE	3.14E-03
	INTERFERON_GAMMA_RESPONSE	3.14E-03
Cluster 3	TNFA_SIGNALING_VIA_NFKB	1.41E-14
	COMPLEMENT	4.22E-07
	INFLAMMATORY_RESPONSE	4.22E-07
	APOPTOSIS	6.24E-05
	INTERFERON_GAMMA_RESPONSE	1.42E-03
Cluster 4	HYPOXIA	3.37E-13
	TNFA_SIGNALING_VIA_NFKB	3.37E-13
	INTERFERON_GAMMA_RESPONSE	8.76E-04
NK cells		
Cluster 2	TNFA_SIGNALING_VIA_NFKB	3.27E-21
	ALLOGRAFT_REJECTION	1.19E-16
	COMPLEMENT	1.93E-09
	HYPOXIA	6.29E-06
	INTERFERON_GAMMA_RESPONSE	6.29E-06
Myeloid cells		
Cluster 5	COMPLEMENT	2.43E-02
	INFLAMMATORY_RESPONSE	2.43E-02
	INTERFERON_GAMMA_RESPONSE	2.43E-02
	TNFA_SIGNALING_VIA_NFKB	2.43E-02
Cluster 7	INFLAMMATORY_RESPONSE	2.53E-02
Cluster 8	IL2_STAT5_SIGNALING	1.40E-02

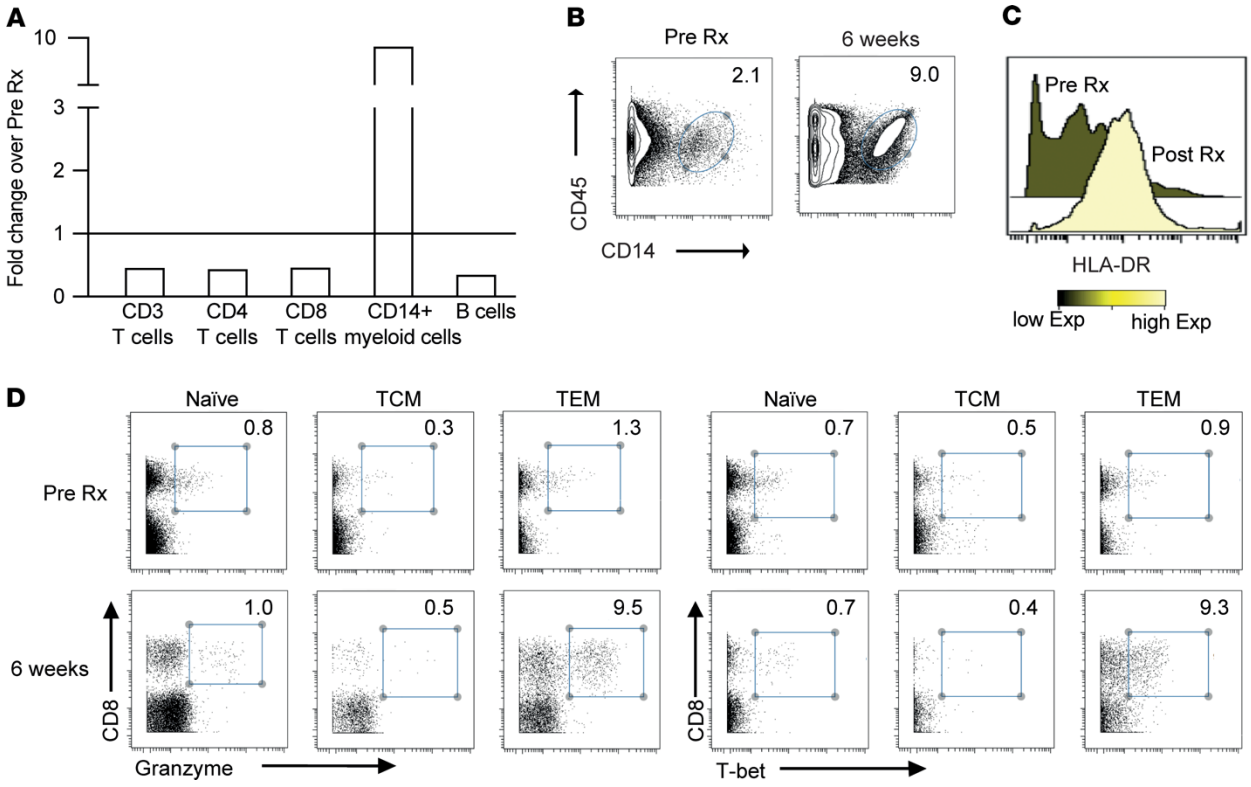

Figure 2.9. Changes in monocytes and effector T cells in BM following therapy with anti–PD-L1 in AMM by mass cytometry. BM was collected from AMM patient before and after 2 cycles (6 weeks) of therapy with atezolizumab. Mononuclear cells were isolated and analyzed using single cell mass cytometry, as well as single cell RNA sequencing. (A) Bar graph shows changes in CD3+, CD4+, CD8+ T cells, CD14+ myeloid cells and B cells at 6 weeks following therapy with atezolizumab. (B) Changes in CD14+ myeloid cells. (C) Histogram showing changes in HLA-DR expression in CD14+ myeloid cells following therapy with atezolizumab. (D) Proportions of granzyme and Tbet positive naive, Tcm, and Tem cells in the marrow before start of therapy, as well as 6 weeks following therapy with atezolizumab.

Table 2.4. Differentially regulated pathways in peripheral blood immune cells following therapy with anti-PD-L1.

	Pathway	FDR q-value
T cells		
Cluster 0	INTERFERON_GAMMA_RESPONSE	1.26E-59
	INTERFERON_ALPHA_RESPONSE	3.38E-53
	INFLAMMATORY_RESPONSE	5.68E-10
	IL2_STAT5_SIGNALING	1.00E-07
	TNFA_SIGNALING_VIA_NFKB	1.00E-07
Cluster 3	INTERFERON_GAMMA_RESPONSE	6.29E-63
	INTERFERON_ALPHA_RESPONSE	1.67E-56
	COMPLEMENT	7.21E-09
	TNFA_SIGNALING_VIA_NFKB	2.35E-06
Cluster 4	INTERFERON_ALPHA_RESPONSE	7.16E-61
	INTERFERON_GAMMA_RESPONSE	1.34E-60
	INFLAMMATORY_RESPONSE	2.70E-06
	TNFA_SIGNALING_VIA_NFKB	2.70E-06
Cluster 6	INTERFERON_GAMMA_RESPONSE	1.53E-16
	INTERFERON_ALPHA_RESPONSE	9.58E-16
	TNFA_SIGNALING_VIA_NFKB	5.42E-06
NK cells		
Cluster 1	INTERFERON_GAMMA_RESPONSE	1.10E-73
	INTERFERON_ALPHA_RESPONSE	3.26E-62
	COMPLEMENT	1.70E-12
	IL2_STAT5_SIGNALING	5.86E-09
	TNFA_SIGNALING_VIA_NFKB	6.88E-08
Cluster 8	INTERFERON_GAMMA_RESPONSE	1.28E-44
	INTERFERON_ALPHA_RESPONSE	3.03E-35
Myeloid cells		
Cluster 2	INTERFERON_GAMMA_RESPONSE	3.75E-118
	INTERFERON_ALPHA_RESPONSE	4.23E-85
	TNFA_SIGNALING_VIA_NFKB	3.44E-32
	INFLAMMATORY_RESPONSE	1.89E-26
	COMPLEMENT	3.43E-11
	REACTIVE_OXYGEN_SPECIES_PATHWAY	2.51E-06
	FATTY_ACID_METABOLISM	2.77E-05
Cluster 7	INTERFERON_GAMMA_RESPONSE	1.28E-44
	INTERFERON_ALPHA_RESPONSE	3.03E-35
B cells		
Cluster 5	INTERFERON_ALPHA_RESPONSE	1.71E-34
	INTERFERON_GAMMA_RESPONSE	6.09E-31
	COMPLEMENT	7.41E-04

2.5 Discussion

Together, these data demonstrate that PD-L1 blockade leads to a distinct genomic signature characterized by early activation and expansion of myeloid compartment in vivo. Therefore, while both PD-1 and PD-L1 blockade share well-studied effects in terms of reinvigoration of T cells, PD-L1 blockade also unleashes an underappreciated myeloid inflammatory checkpoint in vivo in humans. These findings are also consistent with recent data on PD-L1–mediated regulation of macrophage activation and proliferation in PD-L1–deficient mice[106].

Understanding differences between PD-1 and PD-L1 blockade will be essential for optimal design of rational combination therapies with these approaches and may differ for each of these targets. Differential effects of PD-1 versus PD-L1 blockade on myeloid cells in vivo may also help explain why PD-L1 expression on myeloid cells better predicts responsiveness to PD-L1 than PD-1 blockade in the clinic[107]. PD-L1 blockade of human DCs led to rapid activation of caspase-1/inflammasome, with upregulation of NLRP3 and inflammasome-dependent cytokines such as IL-18. Inflammasome activation plays a complex and context-dependent protumor/antitumor role in tumor immunity[107]. Activation of NLRP3 inflammasome in DCs was shown to be critical for induction of adaptive immunity to dying tumor cells following chemotherapy[108]. Therefore, PD-L1 may play an important role in the afferent arm of tumor-immunity cycle in regulating antigen presentation. The finding that PD-L1 blockade may enhance CD40L/T cell–mediated DC maturation may provide the rationale for combinations of PD-L1 blockade with agents targeting agonistic CD40 signaling.

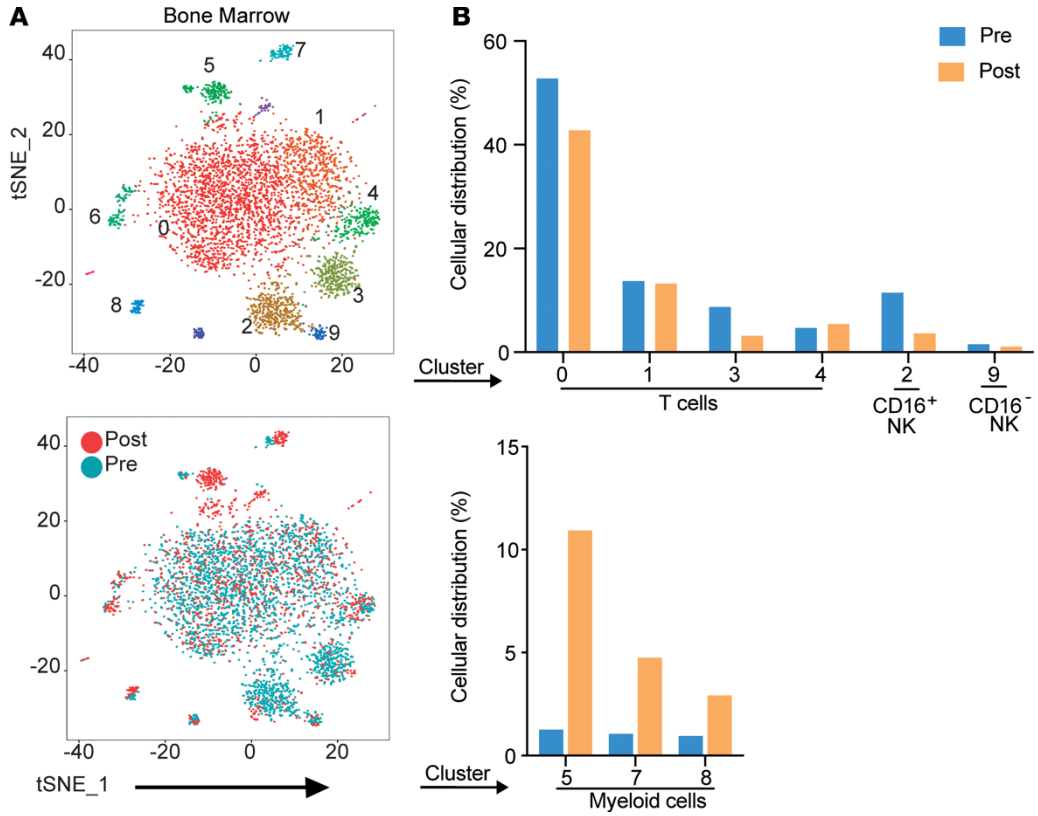

Figure 2.10. Changes in monocytes and effector T cells in BM following therapy with anti–PD-L1 in AMM by single cell RNA sequencing. BM was collected from AMM patient before and after 2 cycles (6 weeks) of therapy with atezolizumab. CD138- BM cells obtained before therapy and 6 weeks after therapy were characterized using scRNA–seq. (A) t-SNE plot with 9 distinct populations determined by unsupervised clustering. Figure also shows distribution of the immune cells from before therapy BM (Pre) and after therapy BM (Post). (B) Percent of immune cells from before therapy (Pre) and after atezolizumab therapy (Post) within the clusters shown in A.

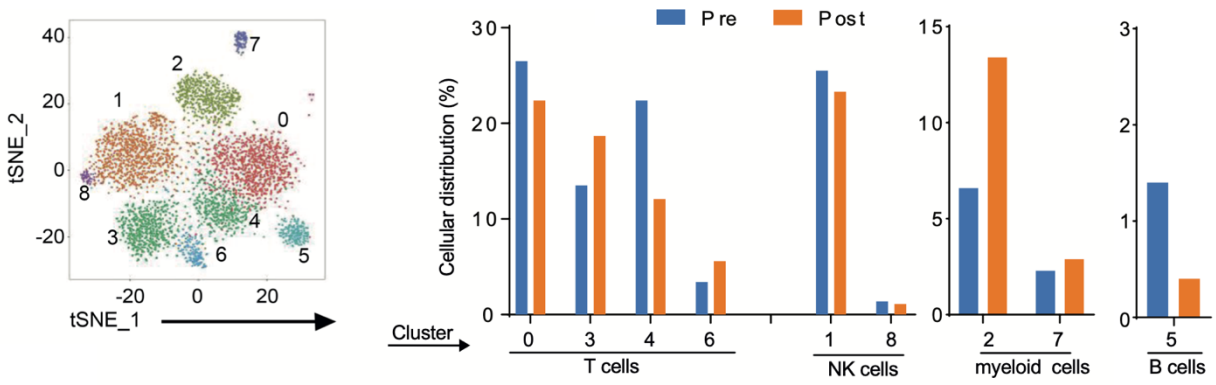

Figure 2.11: Changes in transcriptome profile in PBMCs following therapy with atezolizumab. scRNA-seq analysis was performed on PBMCs obtained prior to therapy and 15 days following start of atezolizumab (Patient 1 as in figure 2.4E). t-SNE plot shows distinct cell clusters as determined by unsupervised cluster analysis. Bar graph shows the percent of cells in each of these distinct populations pre- and post-treatment.

Effect of PD-L1 blockade on myeloid cells in vivo could, however, also have potential undesired effects. Enrichment and activation of myeloid cells following PD-L1 blockade may lead to T cell exclusion and resistance to PD-L1 blockade in myeloid-rich tumors[109]. Effects on myeloid cells could also have contributed to the lack of persistent T cell activation following atezolizumab that we observed in AMM patients, and this suggests that combinations with therapies that inhibit enrichment of myeloid compartment may be explored to improve PD-L1 blockade. Recent studies have also suggested the potential for myeloid cells to mediate hyperprogression in some tumors[110]; prior studies have, indeed, shown the capacity of myeloid cells to promote MM growth[111,112].

While the small number of patients treated due to regulatory issues limits interpretation, the correlative immunologic data in this earlier stage do demonstrate the feasibility to achieve immune activation in the tumor bed. The bar for acceptable complications is lower in this setting than in clinical myeloma. Therefore, careful selection of patients more likely to respond to immune therapies would be important for future investigations in immune prevention based on checkpoint blockade. In this regard, recent studies show that loss of stem-like and marrow-resident T cells is an early feature of MM, which may restrict the efficacy of checkpoint blockade in this setting[113]. It is, however, notable that the finding of increase in inflammasome-dependent cytokines such as IL-18 has been prominently demonstrated in large cohorts of patients treated with anti–PD-L1 but not anti–PD-1 antibodies, which is consistent with our data[107].

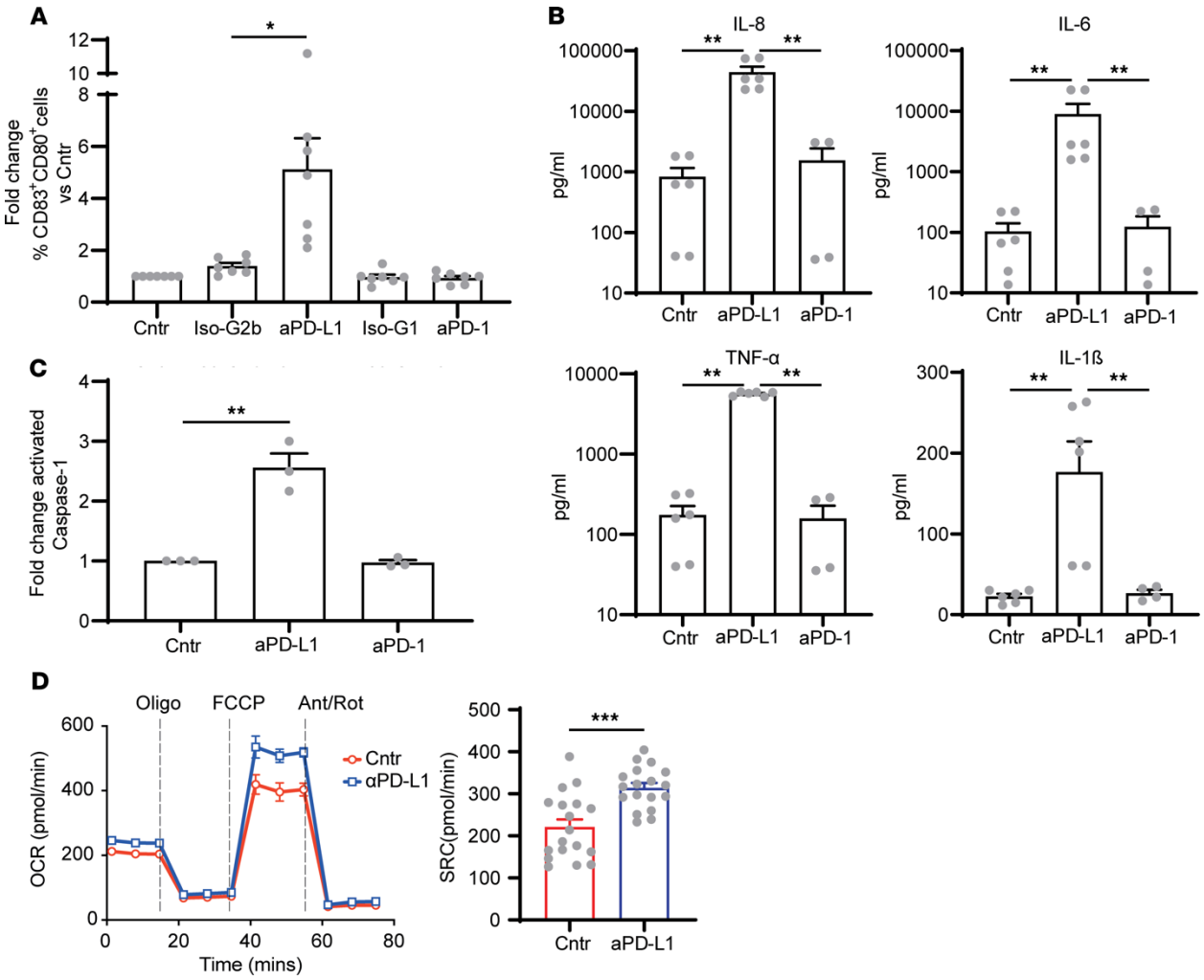

Figure 2.12. PD-L1 blockade leads to functional changes in DCs. Immature Mo-DCs generated from healthy blood donors were either left untreated (control, Cntr) or treated with either anti–PD-L1 antibody (200 µg/mL), anti–PD-1 antibody (200 µg/mL), or their respective isotype control antibodies (Ig-G2b and Ig-G1) at 200 µg/mL or CD40L (250 ng/mL). Culture supernatants were analyzed for changes in cytokines using Luminex assay. Representative data from 7 healthy donors (HDs). (A) DC maturation following treatment with either anti–PD-L1, anti–PD-1, or isotype control. Figure shows fold change in CD83 and CD80 double-positive DCs compared with untreated cells. (B) Changes in secreted IL-8, IL-6, TNF-α, and IL-1β following treatment with anti–PD-L1 or anti–PD-1. (C) Treatment with anti–PD-L1 leads to early activation of caspase-1.

Fold change of activated caspase-1 in immature Mo-DCs following treatment with anti–PD-L1 or anti–PD-1 for 4 hours. Figure shows fold change compared with untreated cells (Cntr). (D) Changes in respiratory capacity of DCs following treatment with anti–PD-L1. Immature Mo-DCs (n = 3 HDs) were either left untreated (control; Cntr) or were treated with anti–PD-L1 (200 μg/mL for 3 hours), and their spare respiratory capacity was analyzed using Seahorse XFe96 analyzer. Basal, coupled, maximal, and spare respiratory capacities were analyzed. Line graph shows data from a representative patient. Bar graph on the right shows data from all 3 different donors (mean ± SEM). (*p< 0.05, **p< 0.01, ***p< 0.001; A, C, D used Mann-Whitney U test, and B used Kruskal Wallis test).

An important limitation of these data is the small number of patients studied, due to early closure of the trial linked to regulatory concerns about PD-1 blockade in a different myeloma trial. In addition, comparison between effects of PD-1 and PD-L1 blockade is based on patients treated in different clinical studies and not as a part of a prospective randomized clinical trial directly comparing PD-1 and PD-L1 blockade. Such a clinical trial may now be feasible in malignancies wherein both PD-1 and PD-L1 blockade are now clinically approved and would be useful to dissect biologic differences between these therapies in humans.

The finding that PD-L1 blockade leads to rapid activation of inflammatory signatures on human myeloid cells in vivo suggests that the PD-L1 axis may be an important regulator of myeloid inflammation and impact emergency myelopoiesis and trained immunity in the clinic. While studies in human subjects described here are mostly correlative, a possible role of PD-L1 axis in regulating myeloid inflammation is also supported by emerging data from murine models, which is consistent with our studies. Engaging these pathways may be important for improving combination therapies with PD-L1 blockade, particularly harnessing the afferent arm of the cancer immunity cycle. Finally, differences in pharmacodynamic effects of PD-1 and PD-L1 blockade, as shown here, also have important implications for optimal combinations in the clinic, which may differ between these targets.

2.6 Materials & Methods

Patients and samples. For studies comparing genomic signatures of PD-1 and PD-L1 blockade, blood samples were obtained before and after 1 cycle of therapy from patients with advanced non–

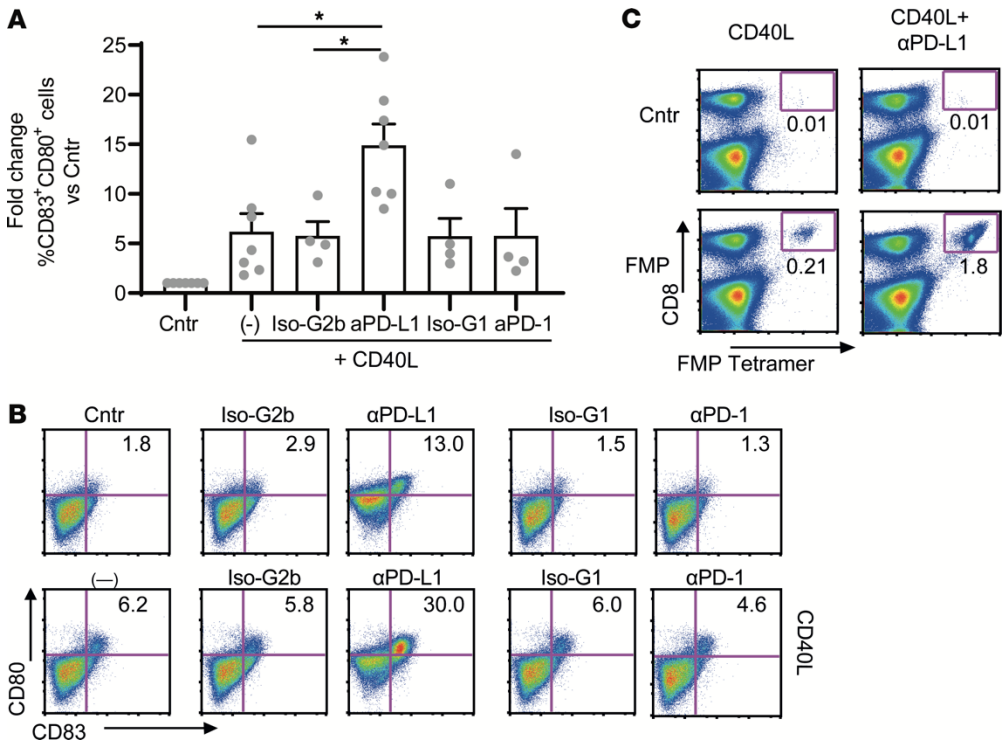

Figure 2.13. PD-L1 blockade synergizes with CD40L to improve antigen-specific T cell expansion. Immature Mo-DCs generated from healthy blood donors were either left untreated (control, Cntr) or treated with CD40L (250 ng/mL) alone (–) or with anti–PD-L1 antibody (200 μg/mL), anti–PD-1 antibody (200 μg/mL), or their respective isotype control antibodies (Ig-G2b and Ig-G1) at 200 μg/mL. (A) Anti–PD-L1 treatment synergizes with CD40L to improve DC maturation. Figure shows fold change in DC maturation (assessed by increase in CD83 and CD80 double-positive cells) compared with control cells. (B) Representative data from one donor showing increased DC maturation with concurrent treatment with CD40L and PD-L1. (C) Immature Mo-DCs (*HLA-A*2.1^{+}) were stimulated with CD40L alone or CD40L plus anti–PD-L1 antibody. After overnight culture, DCs were loaded with *HLA-A*2.1-specific influenza matrix peptide (FMP) at 0.1 μg/mL and used to stimulate autologous T cells.

After 10–12 days of DC–T cell coculture, expansion of influenza-specific T cells was analyzed using FMP-specific tetramer. (*$p < 0.05$, Kruskal Wallis test).

small cell lung cancer undergoing therapy with anti–PD-1 (nivolumab)[62] or anti–PD-L1 (atezolizumab).

Study design and monitoring. In the pilot study of atezolizumab in AMM (NCT02788843), patients were eligible if they met criteria for AMM based on BM clonal plasmacytosis of > 10% and/or levels of monoclonal immunoglobulin > 3 g/dL. Patients were also required to have an abnormal serum free light chain ratio (but < 100) and absence of end organ damage based on CRAB criteria (hypercalcemia, renal dysfunction, anemia, bone disease), < 60% BM plasma cells, and no more than 1 known focal lesion on MRI. Other key eligibility criteria included the presence of measurable disease and adequate hematologic and organ function. Patients with any prior therapy for plasma cell disorder and history of active autoimmune disease were excluded. All eligible patients received atezolizumab 1200 mg i.v. every 3 weeks. Blood samples for immune monitoring were collected at baseline, C1D15, and then before each cycle of therapy while in the study. BM biopsies were planned at baseline and after completion of 2 cycles of therapy.

Gene expression profiling of purified T cells and monocytes. Gene expression profiling of purified monocytes and T cells was performed as previously described[62]. Briefly, CD14+ monocytes cells were isolated from PBMCs using immunomagnetic separation with anti–human CD14 microbeads (Miltenyi Biotec, 130-050-21), and T cells were isolated with human Pan–T cell isolation kit (Miltenyi Biotec, 130-096-535) following manufacturer instructions. RNA isolated from purified cells was analyzed using Affymetrix GeneChip Human Transcriptome Array (v2.0) as described[62].

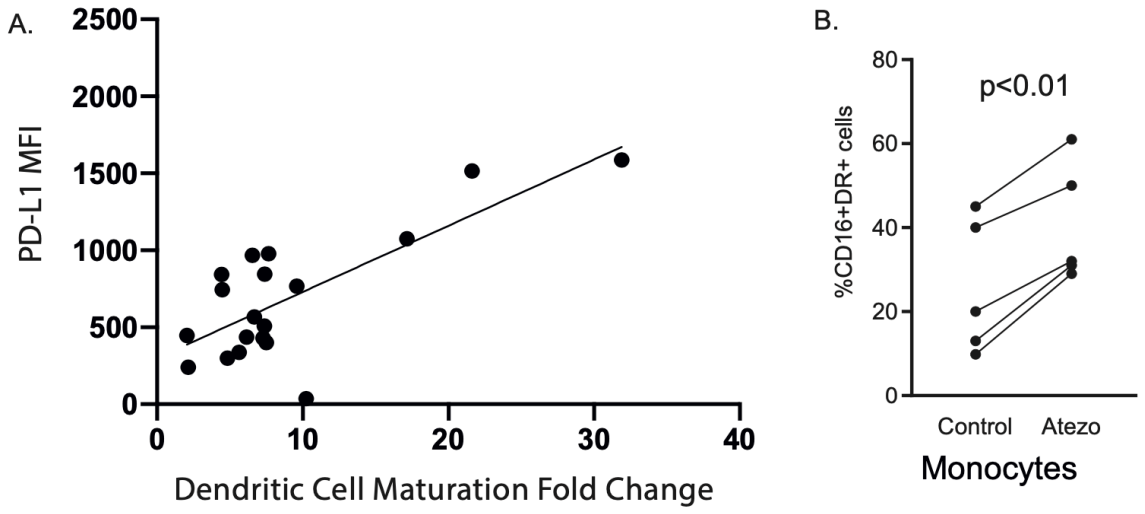

Figure 2.14: Atezolizumab-induced changes in myeloid cells in culture. (A) Correlation of PD-L1 expression and changes in dendritic cell maturation markers (CD83, CD80) following exposure of monocyte-derived dendritic cells to CD40L + atezolizumab compared to untreated control. (B) Changes in CD14+ CD16+ HLA-DR+ myeloid cells in bone marrow mononuclear cells cultured with atezolizumab versus control.

Mass cytometry. Peripheral blood and BM mononuclear cells were immunophenotypically characterized using mass cytometry as described[114]. The panel of antibodies used is shown in Table 2.5. Data were acquired on Helios instrument (Fluidigm Sciences Inc.) and analyzed using Cytobank software (Cytobank Inc., Fluidigm).

scRNA–seq. scRNA–seq of peripheral blood or BM mononuclear cells was performed using the 10x Genomics platform chromium single cell 3′ kit following manufacturer's protocol as described[83,115]. Libraries were sequenced. Reads were aligned, filtered, deduplicated, and converted into a digital count matrix using Cell Ranger 1.2 (10x Genomics). All downstream quality control and analyses were performed using Seurat[116]. Cells with ≥ 200 expressed genes were used for analysis.

For analysis of scRNA–seq from lung cancer patients treated with either anti–PD-1 or PD-L1, pre- and post-treatment samples for each patient were merged, and gene expression for each cell was log-normalized to total expression per cell. To reduce noise due to batch effects and interpatient heterogeneity, each patient was aligned and integrated with all other patients receiving the same treatment (anti–PD-L1, n = 3; anti–PD-1, n = 4) via canonical correlation analysis (CCA) using the Seurat Find- IntegrationAnchors and IntegrateData functions. Gene expression data were then scaled such that each gene had a mean expression of 0 and a variance of 1 across all cells using the ScaleData function, and principal component analysis was performed using the RunPCA function. Data were visualized in 2 dimensions using uniform manifold approximation and projection (UMAP) based on the first 20 principal components. Significant DEGs were identified by the Wilcoxon rank-sum test with a Bonferroni's correction ($p < 0.05$). Cluster identity was

Table 2.5. List of antibody clones used for CyTOF.

	Antibody	Clone
1	41BB	4B4-1
2	B7H3	MIH42
3	BTLA	MIH26
4	CCR7	G043H7
5	CD11b	ICMF44
6	CD11c	Bu15
7	CD123	6H6
8	CD138	M15
9	CD15	W6D3
10	CD155	SKIL4
11	CD16	3G8
12	CD19	HIB19
13	CD20	S2H7
14	CD200	OX-104
15	CD21	BL13
16	CD23	EBVCS-5
17	CD24	ML5
18	CD25	2A3
19	CD27	L128
20	CD28	CD28.2
21	CD3	UCHT1
22	CD33	WM53
23	CD38	HIT2
24	CD4	RPA-T4
25	CD44	IM7
26	CD45RO	UCHL1
27	CD56	HCD56
28	CD57	HCD57

	Antibody	Clone
29	CD69	FN50
30	CD8	RPA-T8
31	CD80	2D10.4
32	CD81	5A6
33	CD95	DX2
34	CTLA4	14D3
35	CXCR4	12G5
36	CXCR5	RF8132
37	DNAM-1	TX25
38	FOXP3	PCH101
39	Granzyme	GB11
40	HLADR	L243
41	HVEM	122
42	ICOS	C398.4A
43	Ig Kappa	MHK-49
44	Ig Lamba	MHK-38
45	IgM	MHM-88
46	Ki67	Ki-67
47	LAG3	11C3C65
48	NKG2D	OW72
49	OX-40	ACT35
50	PD1	EH12.2H7
51	PD-L1	MIH1
52	SLAMF7	162.1
53	SOX2	030-678
54	T-Bet	4B10
55	TIGIT	MBSA43
56	TIM3	F38-2E2

determined by inspection of canonical marker genes (e.g., CD14 for monocytes), and identity was confirmed by automated cell type determination with SingleR (https://bioconductor.org/packages/release/bioc/html/SingleR.html) via comparison with the Human Primary Cell Atlas (http://biogps.org/dataset/BDS_00013/primary-cell-atlas). Pathway analysis was performed using Gene Set Enrichment Analysis (GSEA) software (https://www.gsea-msigdb.org/gsea/index.jsp) and the Molecular Signature Database (MSigDB; https://www.gsea-msigdb.org/gsea/msigdb/index.jsp) from the Broad Institute.

Whole transcriptome analysis. Gene expression profiles from monocytes and T cells before and after anti– PD-1 and anti–PD-L1 treatment were obtained using Affymetrix Human Transcriptome Array 2.0, and gene-level signal intensities were used for subsequent analysis. Preprocessing and normalization of data sets were carried out by Affymetrix Expression Console using gene level Signal Space Transformation–Robust Multiarray Average (SST-RMA) normalization. All downstream analyses were conducted using R and Bioconductor[117]. The "limma" package was used for differential gene expression[118]. GSEA was performed using Metacore (https://portal.genego.com) and MSigDB (Molecular Signatures Database v6).

Detection of antigen-specific T cells. In order to detect SOX2-specific T cells, PBMCs were stimulated for 48 hours with SOX2 peptide library as described[100]. Following stimulation, the presence of T cell activation was determined based on the detection of IP-10 in the culture supernatant by Luminex.

Detection of plasma cytokines. Plasma samples were used for the detection of a panel of 38 cytokines/chemokines using the Milliplex MAP Human Cytokine/Chemokine Magnetic Bead Panel kit (HCYTMAG-60K-PX38; Millipore Sigma) as described[62]. xPONENT software (Luminex Corp.) was used to detect, quantitate, and analyze the samples on the Luminex 100 instrument. Levels of IL-18 were analyzed using an ELISA kit (R&D Systems).

Generation of Mo-DCs. Purified CD14+ monocytes were cultured in 1% plasma in the presence of IL-4 (25 ng/mL; R&D Systems) and GM-CSF (20 ng/mL sagramostim [Leukine]; Genzyme) to yield Mo-DCs. Immature Mo-DCs were used to study the effects of anti–PD-L1 or anti–PD-1 antibodies. DCs were cultured with anti–PD-L1 (clone 29E.2A3; BioLegend), anti–PD-1 (clone EH12.2H7; Bio-Legend) or their respective isotype control antibodies (IgG2b and IgG1; BioLegend) (200 μg/mL). For some experiments, immature Mo-DCs were cultured with CD40L (250 ng/mL; R&D Systems).

Effects of PD-L1 blockade on BM myeloid cells. Bone marrow mononuclear cells (BMMNCs) were treated with atezolizumab (200 μg/mL) every 24 hours for 48 hours or left untreated. Following incubation, samples were stained with antibodies for CD14 (MφP9), CD19 (SJ25C1), and CD11c (B-ly6) (BD Biosciences); BDCA3 (AD5-14H12, Miltenyi Biotec); and PD-L1 (29E.2A3), CD40 (5C3), CD16 (3G8), and HLA-DR (L243) (BioLegend).

Antigen-specific T cell stimulation. For some experiments, immature Mo-DCs differentiated from HLA A2.1+ donors (n = 4) were stimulated with CD40L (250 ng/mL) in the presence or absence of anti–PD-L1 (200 μg/mL). After overnight culture, DCs were loaded with HLA A2.1–restricted

Flu-MP (sequence GILGFVFTL) at 0.1μg/mL for 2 hours. Flu-MP–loaded DCs were then used to stimulate autologous T cells at a DC/T cell ratio 1:30 in the presence of IL-2 (10 U/mL). Flow cytometry analysis was performed to detect the presence of Flu-MP–specific CD8+ T cells using MHC tetramers (MBL International).

Detection of caspase-1 activation. Immature Mo-DCs were treated with anti–PD-L1 (200 μg/mL), anti-PD-1 (200 μg/mL) or left untreated for 4 hours. Activation of caspase-1 was assayed with the FAMYVAD-FMK Caspase-1 Detection Kit (Cell Technology Inc). FAM-YVAD-FMK was added to the culture 1 hour before the end of culture period, following manufacturer protocol; washed twice with Caspase-1 kit wash buffer; and detected using flow cytometry.

Measurement of oxygen consumption and spare respiratory capacity. Basal, maximal, and coupled oxygen consumption rates were measured in a Mito stress assay using a Seahorse extracellular flux (XFe96) analyzer. Immature Mo-DCs were treated with anti–PD-L1 (200 μg/mL) or left untreated. After 3 hours, DCs were harvested, washed 1X with PBS, and plated at 200,000 cells per well in 5–8 replicates on Cell-Tak– precoated (Becton Dickinson) 96-well plates custom designed for XFe96 analysis. Oxygen consumption rate was evaluated over time with sequential injection of oligomycin (MilliporeSigma, catalog 495455; final concentration 2.5 μM), carbonyl cyanide p-trifluoro-methoxyphenyl hydrazone (FCCP; Enzo Life Sciences, BML-CM120-0010; final concentration 0.5 μM), and antimycin (Ant; MilliporeSigma, A8674) or rotenone (Rot; MilliporeSigma, R8875; final concentration 2 μM each). Spare respiratory capacity was calculated as the difference between maximal and basal respiration.

Statistics. Data from individual cohorts were compared using GraphPad analysis software. Paired 2-tailed t tests and nonparametric tests were used to analyze the data with significance set to $p < 0.05$ and Bonferroni's to correct for multiple comparisons.

Study approval. The clinical trial was approved by the Yale University IRB and monitored by data safety monitoring committee at Yale Cancer Center. All specimens were collected following informed consent under institutional IRB guidelines at Emory and Yale universities.

2.7 Acknowledgements

This work is supported, in part, by funds from NIH/NCI (NCI CA197603 to MVD, CA238471 to KMD, CA208328 to MS, and P30CA138292 to Winship Shared Resources.

Chapter 3: Tregs protect against combination checkpoint blockade toxicity induced by T_{PH} and B cell interactions

Alyssa Duffy[1], Maryam I. Azeem[1], Smriti Kanangat[1], Melinda Yushak[1], David Lawson[1], Madhav V. Dhodapkar[1], Kavita M. Dhodapkar[1]

Affiliations: [1] Emory University, Atlanta, GA

The work contained in this chapter is reproduced with some edits and was originally published in Journal of Clinical Investigation (JCI) in 2024.

Citation: Duffy A, Azeem MI, Kanangat S, Yushak M, Lawson D, Dhodapkar MV, Dhodapkar KM. Tregs protect against combination checkpoint blockade toxicity induced by TPH and B cell interactions. J Clin Invest. 2024 May 2:e174724. doi: 10.1172/JCI174724. PMID: 38696264.

3.1 Key Findings

- Alterations in CD11c+CD21loTbet+ B cells correlate with irAE following CCB.
- Novel role for distinct population of T helper cells— CXCR5- TPH cells in T:B crosstalk in irAEs.
- Role of IFNg and IL-21 signaling in T:B crosstalk.
- Differences in Treg induction and Treg-mediated suppression of TPH:B crosstalk in patients with/without irAE.

3.2 Introduction

Immune-related adverse events (irAEs) have emerged as a major challenge for combination checkpoint blockade (CCB) with anti-PD-1 and anti-CTLA-4[84]. Although CCB therapy for the treatment of melanoma leads to higher response rates compared to monotherapy, it is also associated with drastically higher rates of irAEs[73]. Notably, up to 50% of patients receiving CCB develop severe, high-grade toxicities, forcing a pause or discontinuation of therapy[74,75].

CTLA-4 and PD-1 checkpoints impact both B and T cell tolerance and both cells have been implicated in irAEs. Early changes in B cells, particularly in the CD21lo B cell subset, are reported to correlate with the onset of severe irAEs in melanoma patients[83]. It appears CD21lo B cells may be a distinct target of CCB, as treatment induces proliferation and an activation signature[83]. On the other hand, several groups have linked features of T cells to the development of irAEs. Of note, baseline elevation of activated memory CD4+ T cells is a determinant of ICI-induced irAEs[119]. Thus, it is clear that both B and T cells play a role in the pathogenesis of irAEs.

Recent advances in B cell biology and extrafollicular responses have led to a better understanding of autoimmunity and highlighted the importance of T:B crosstalk[84,120]. A distinct population of Tbet+CD21lo B cells have been shown to play an outsized role in autoimmunity, with reports of elevated autoantibody production, an increased presence in autoimmune tissues, and an enrichment of autoreactive B cell receptors (BCRs)[121-123]. While the importance of B cells in autoimmunity is evident, new insights describe the critical role of T:B interactions in the development and maintenance of these diseases. T peripheral helper (TPH) cells, a newly identified T cell population, are enriched in patients with autoimmunity and are responsible for providing B cell help in inflamed tissues, leading to activation and differentiation[124,125]. Considering the similarities between irAEs and autoimmune diseases, it is plausible that similar interactions may play a role in ICI-induced autoimmunity. However, the nature of specific T cells that help pathogenic B cells and underlying mechanisms remain unknown.

Table 3.1. Patient characteristics.

	No- HG irAEs; n=6	**HG* irAEs; n=8**
Median Age (yrs) (range)	67 (54-76)	65 (44-75)
Gender Male (%)	5/6 (83)	4/8(50)
Grade 3 irAE organ involved	NA	GI (6), Skin, Kidney and Joints (1 each)

* HG= ≥ Grade 3 by common toxicity criteria, v5.

3.3 Results

We analyzed blood specimens before/after first cycle of CCB therapy from a cohort of melanoma patients undergoing CCB (clinical characteristics in Table 3.1). CCB therapy led to an increase in CD21loCD11c+ B cells as well as plasmablasts and a decline in circulating B cells in patients who developed high-grade irAEs (HG-irAE) (Figure 3.1A-C)[83]. The phenotype of expanded CD21loCD11c+ B cells was consistent with CXCR5-Tbet+ B cells implicated in extra-follicular B cell responses and autoimmunity (Figure 3.1D). FlowSOM analysis identified two distinct metaclusters (MC) of Ki-67+ CD4+ T cells (MC3 and MC8) and a Ki-67+ CD8+ MC (MC4) that underwent early proliferation following therapy (Figure 3.1E-F). Notably, MC6 containing CXCR5+PD1+ CD4+ T cells (consistent with TFH cells) did not change following therapy (Figure 3.1F-G). Proliferating CD4+ T cells expressed ICOS but not CXCR5 (Figure 3.1H), similar to TPH cells[125].

Next we tested the capacity of purified ICOS+ or ICOS- CD4+ T cells expanded in CCB-treated patients to induce B cell differentiation in T:B co-cultures. Addition of ICOS+CD4+ T cells (but not ICOS-CD4+ T cells) to B cells led to the induction of CD27+CD38+ plasmablasts (Figure 3.2A) and h-IgG secretion (Figure 3.2B). Plasmablast induction was significantly greater in co-cultures with memory versus naïve B cells (Figure 3.2C). T cell subsets were adoptively transferred with human B cells into MISTRG6 mice and monitored for the development of plasmablasts and Ig secretion. Co-injection of B cells with ICOS+CD4+ T cells (but not ICOS- counterparts) led to plasmablast differentiation (Figure 3.2D,E) and hIgG production (Figure 3.2F). Together these data demonstrate that CCB therapy leads to proliferation of CD21loCD11c+

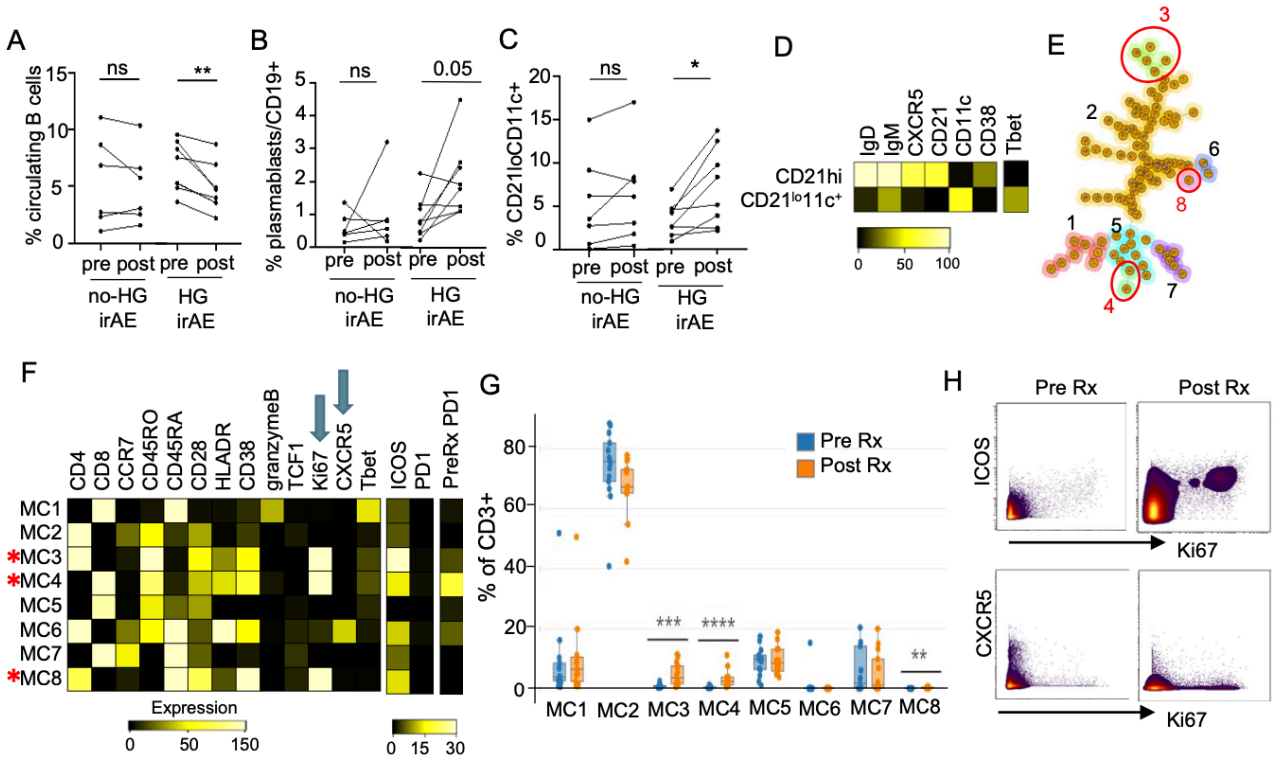

Figure 3.1. Changes in T and B cells following combination checkpoint blockade and the development of irAEs. (A-H) Peripheral blood mononuclear cells (PBMCs) obtained from patients before and after one cycle of combination anti-PD1 and anti-CTLA-4 therapy (n=14) were analyzed by mass cytometry. (A-C) Graphs showing the frequency of circulating B cells (A), plasmablasts (B), and CD21loCD11c+ B cells (C) as a percentage of total B cells. Patients were grouped into cohorts with high-grade irAEs (CTC grades 3-4; n=8) or no high-grade irAEs (CTC grades 0-2; n=6). (D) Phenotype of CD21lo B cells: Heatmap displays expression of IgD, IgM, CXCR5, CD21, CD11c, CD38, and Tbet on CD21hi versus CD21loCD11c+ B cells. (E-H) Phenotype of T cells before/after therapy: (E) FlowSOM analysis of CD3+ T cells identified 8 distinct T cell metaclusters (MC). Proliferating MCs that differ between pre- and post-treatment specimens are circled. (F) Heatmap showing phenotype of the MCs (*identifies Ki-67+ proliferating subsets). (G) Bar graph showing proportion of each MC (as percentage of T cells) in

patients before/after therapy. (H) Proliferating CD4+ T cells are ICOS+CXCR5-. Representative plots showing expression of ICOS and CXCR5 on proliferating CD4+ cells. *$p<0.05$, **$p<0.01$, ***$p<0.001$, ****$p<0.0001$, by 2-tailed Wilcoxon signed rank test.

B cells as well as ICOS+ TPH-like cells that help B cells, illustrating enhanced T:B cooperation following therapy.

ICOS+CD4+ T cell activation was associated with secretion of sCD40L, IL-21, and interferon-γ (IFNg) (Figure 3.3A-C). Plasmablast induction in T:B cocultures was inhibited by the blockade of CD40 (Figure 3.3D), IL-21 (Figure 3.3E), and IFNg-mediated signaling (Figure 3.3F). Increase in circulating ICOS+CD4+ T cells was similar in patients with or without HG-irAE (Figure 3.2G). However, ICOS+ T cells from patients with HG-irAE had greater capacity to provide help to B cells, suggesting functional differences in ICOS+ T cells (Figure 3.2H). FlowSOM analysis of ICOS+CD4+ T cells (Figure 3.4A-B) revealed that patients without HG-irAEs had a higher proportion of MC6 and MC10 in the post-treatment ICOS+CD4+ T cell population, which coexpressed FOXP3 and CD25, consistent with a Treg phenotype (Figure 3.2I). Patients with HG-irAEs trended towards a higher proportion of a CXCR3+ MC (MC7), expressing PD-1 at baseline (Figure 3.4B-C). Depletion of Tregs from ICOS+CD4+ T cells led to increased plasmablasts (Figure 3.2J). Together these data suggest that Tregs may suppress T:B interactions in patients without HG-irAEs.

The proportion of proliferating CD4+ and CD8+ T cells did not differ between patients with or without HG-irAE [83] (Figure 3.4E). However, patients with HG-irAE had higher expression of CXCR3 in proliferating CD4+ and CD8+ T cells and $CD21^{lo}$CD11c+ B cells, but not myeloid cells (Figure 3.4E). The expression of CXCR3 in ICOS+CD4+ T cells correlated with more effector/activated phenotype with higher expression of Tbet and HLA-DR (Figure 3.4F).

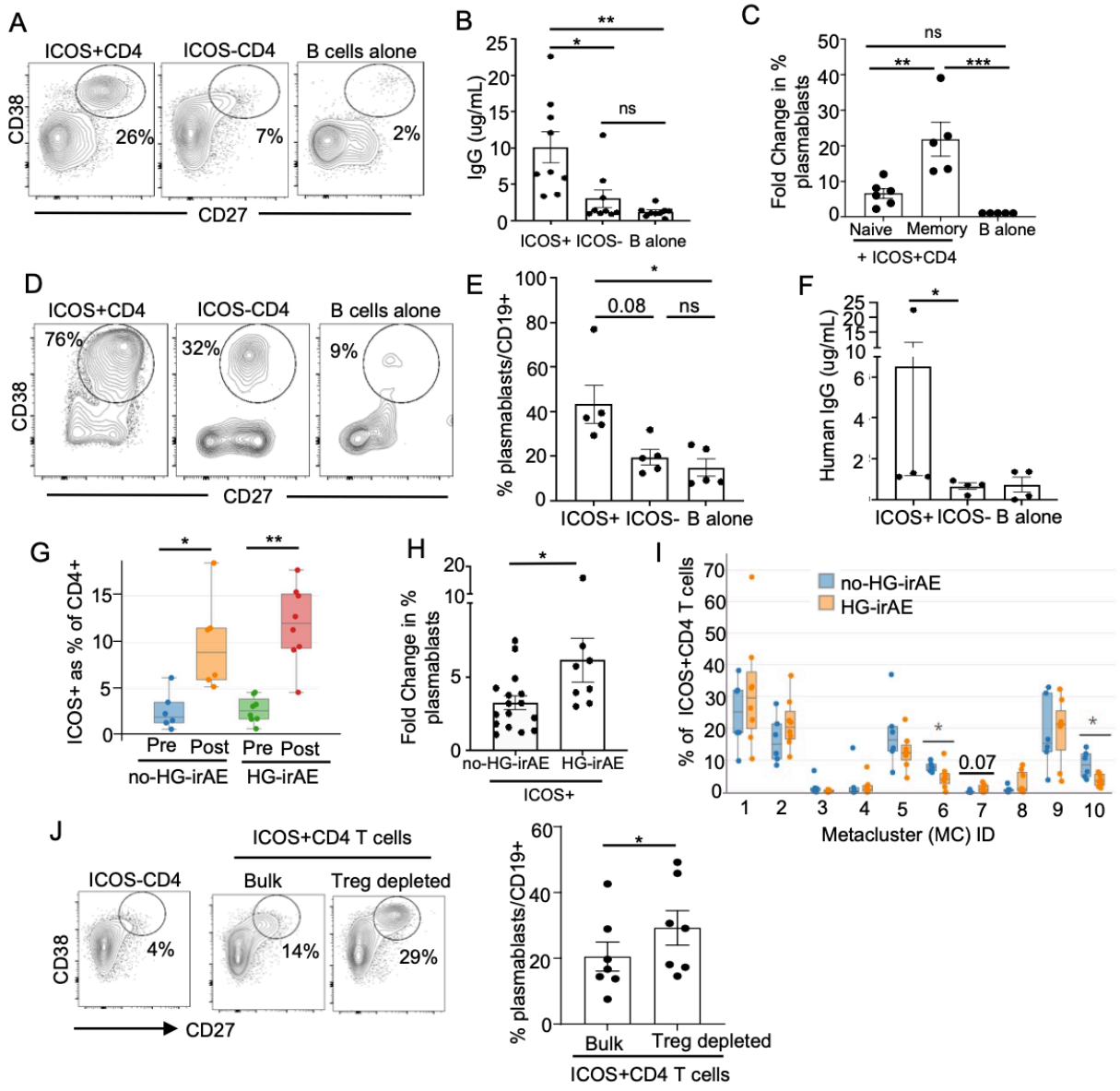

Figure 3.2. Mechanisms of T:B interactions. (A-C) T:B cocultures: Purified B cells were cultured alone or with flow-sorted ICOS+CD4+, ICOS-CD4+ T cells from melanoma patients post CCB treatment as described in methods. (A) Representative flow plot of CD38+CD27+ plasmablasts. (B) Human IgG levels by ELISA (n=9). Kruskal-Wallis with Dunn's multiple-comparisons correction. (C) Impact of B cell subsets: Flow-sorted post-treatment T cells were cultured with either memory(n=5) or naïve B cells (n=6). Bar graphs indicate fold change

compared to cultures with B cells alone. One-way Anova with Tukey's multiple-test correction. (D-F) Human T:B interactions in vivo: Sorted ICOS+ or ICOS- CD4+ T cells from melanoma patients (n=5) were injected into MISTRG6 mice along with purified human B cells, as described under methods. (D) Representative flow plots of plasmablast frequency in the spleen at two weeks post-injection, quantified in (E). One-way Anova with Dunn's multiple correction. (F) Human IgG levels detected by ELISA in mice from panel E. Wilcoxon matched-pairs signed rank test. (G) Bar graph shows expansion of ICOS+CD4+ T cells post-CCB therapy in patients with no HG-irAEs and those with HG-irAEs. Wilcoxon matched–pairs rank test. (H) B cells were cultured with flow-sorted ICOS+/- CD4+ T cells from patients with no-HG or HG-irAE. Bar graph shows fold change in plasmablasts in ICOS+ versus ICOS- co-cultures. Mann Whitney. (I) FlowSOM performed on ICOS+CD4+ T cells obtained following one cycle of combination therapy identified 10 metaclusters (MC). Bar graph shows proportions of these MCs in patients with HG-irAEs or no HG-irAEs. Mann-Whitney. (J) Depletion of Tregs in patients with no HG-irAEs leads to enhanced B cell activation by ICOS+CD4+ T cells. Purified B cells were cultured with either ICOS-, bulk ICOS+ or Treg-depleted ICOS+CD4+ T cells from patients with no HG-irAEs. Dot plot shows plasmablast frequency as percent of B cells. Bar graph shows data for 7 different experiments. Wilcoxon matched–pairs rank test. For all figures *$p<0.05$, **$p<0.01$, ***$p<0.001$ and ns=not significant.

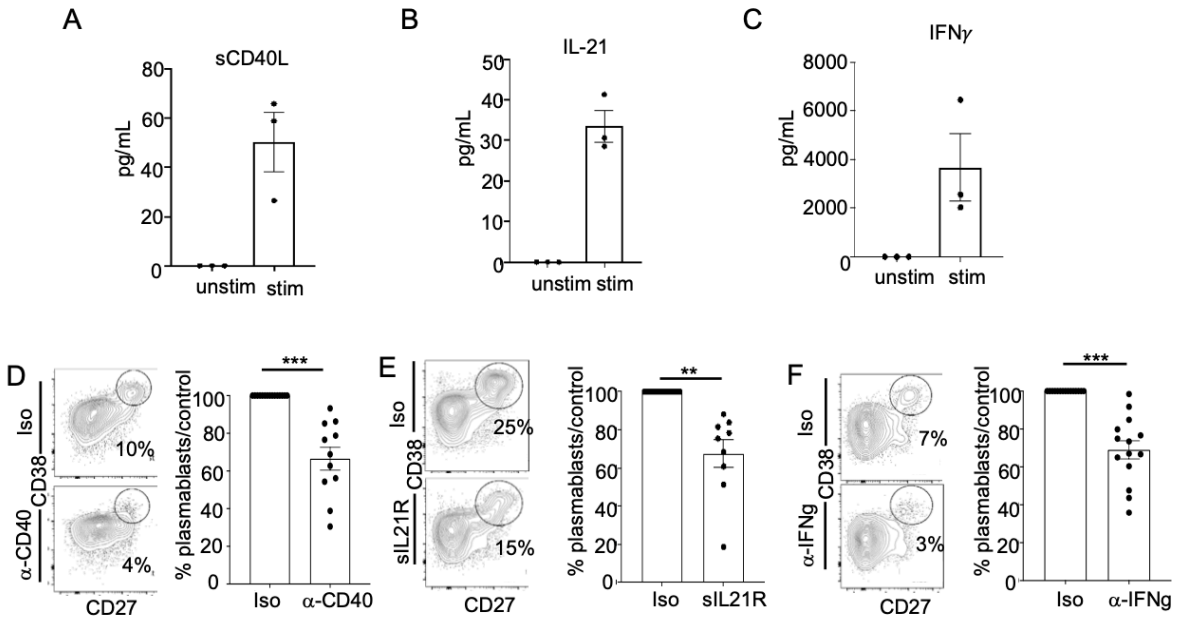

Figure 3.3. Mechanisms of T cell help. (A-C) ICOS+CD4+ T cells were flow sorted from peripheral blood of melanoma patients after CCB treatment and stimulated with PMA/Ionomycin for 24 hrs. Cell supernatant was analyzed for presence of sCD40L (A), IL-21 (B), and IFNg (C). [127] Flow-sorted ICOS+CD4+ T cells from post-CCB treated melanoma patients were cultured with purified human B cells in the presence of isotype control or CD40 blocking antibodies (D), soluble IL-21 receptor (E), or interferon-gamma blocking antibodies (F) as described in the methods. One week later, proportion of plasmablasts were assessed in these cocultures. Dot plots in D-F show data from a representative patient and bar graphs show data from all patient samples as a proportion of isotype control. Each dot represents a unique patient sample. For all panels: *p<0.05, **p<0.01, ***p<0.001, ****p<0.0001, by 2-tailed Wilcoxon signed rank test.

3.4 Discussion

In summary, we show that CCB therapy leads to expansion of ICOS+ TPH cells and CD21loCD11c+ B cells. Both cell types express PD-1 and play an outsized role in human autoimmunity[125]. However, irAE development depends on the induction of Tregs, which inhibit TPH:B interactions. Expansion of ICOS+ T cells by CTLA-4 blockade has also been implicated in mediating anti-tumor effects, suggesting potential overlap with mechanisms underlying irAEs. CXCR3 has been previously implicated in homing into autoimmune tissues[125]. Strengths of this work are analysis of uniformly treated patients and inclusion of in-vitro/in-vivo studies to dissect mechanisms. Limitations include small sample size and lack of analysis of autoimmune tissues. Underlying mechanisms may also differ by specific types of irAEs, which were not studied here. Blockade of specific pathways such as IL-21/IL-21R-mediated signaling and boosting Tregs may provide novel strategies to prevent or treat CCB-induced irAEs.

3.5 Materials & Methods

Patients and specimens. Blood specimens were obtained from melanoma patients receiving combination checkpoint blockade following informed consent approved by institutional review board. PBMCs were obtained utilizing Ficoll density gradient centrifugation, as described previously.

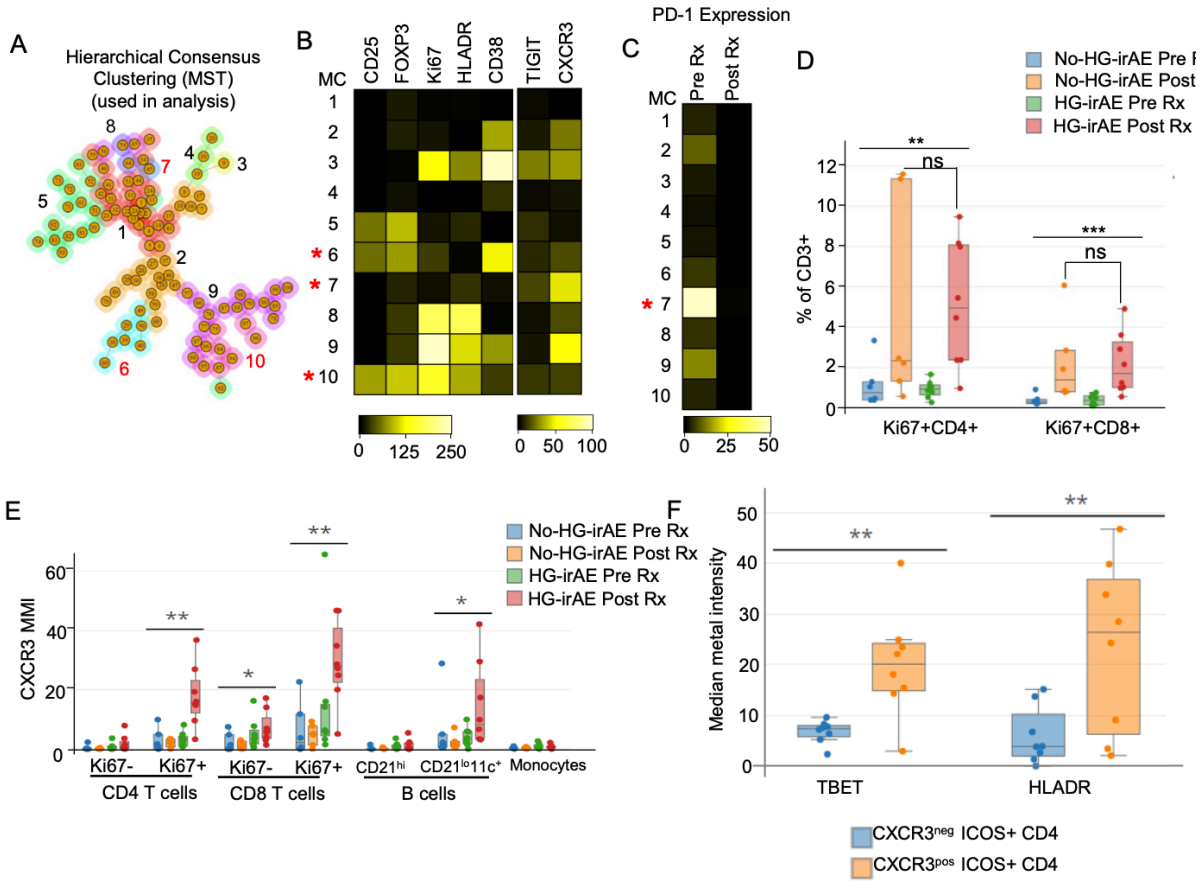

Figure 3.4 Phenotypic/functional profiles of T cells. (A-C) FlowSOM clustering analysis performed on ICOS+CD4+ T cells revealed 10 distinct metaclusters (MC). (A) Hierarchical clustering used in the analysis. (B) Heatmap showing phenotype of the metaclusters. (C) Detection of surface PD-1 on the ICOS+CD4+ T cell metaclusters pre and post therapy with CCB. (D) Proportion of proliferating (Ki-67+) CD4+ and CD8+ T cells in pre and post treatment patient samples. **p<0.01, ***p<0.001, by Kruskal-Wallis test and ns=not significant by Mann-Whitney. (E) Correlation between changes in CXCR3 expression (median metal intensity or MMI) on various cell populations before/after therapy in patients with/without HG-irAEs. *p<0.05, **p<0.01, Kruskal Wallis. (F) Expression of Tbet and HLA-DR on CXCR3+ICOS+CD4+ T cells

expanded in patients with HG-irAE, as compared to the CXCR3-ICOS+CD4+ T cell counterparts in these patients. **$p<0.01$, Wilcoxon matched-pairs signed rank test.

Sex as a biological variable. Study included both male and female patients with melanoma.

Single cell mass cytometry. PBMCs were thawed and stained with metal conjugated antibodies following manufacturer's recommendations as previously described[83]. Briefly, cells were labeled with extracellular antibodies to detect cell surface proteins followed by fixation and permeabilization for intracellular/intranuclear labeling using intracellular antibodies. Cells were stained with cisplatin to detect viability and were incubated with Intercalator (Ir) prior to analysis. Data were analyzed using Cytobank analysis software (Beckman Coulter Life Sciences).

Human T:B cocultures. B cells were isolated from PBMCs via immunomagnetic sorting using CD19 beads (Miltenyi). Flow-sorted ICOS+/- CD4+ T cells were cultured with B cells at a ratio of 1:10 (20,000 T cells:200,000 B cells) in 100 uL medium (cRPMI + 10% FBS) with SEB (1ug/mL, VWR) and LPS (5ug/mL, MD Bioproducts) for 1 week, based on methods adapted from prior studies[124,128]. Supernatant was collected for immunoglobulin analysis via ELISA (Bethyl Laboratories). After one week, cells were harvested and B cell phenotypes were analyzed via flow cytometry. In some experiments, either memory or naïve B cells were isolated using immunomagnetic sorting kits (Miltenyi) and cultured with patient ICOS+/- CD4+ T cells. For some experiments Tregs (CD4+CD127-CD25hi cells) were depleted from ICOS+CD4+ T cells prior to T:B coculture. For blocking experiments, 10ug/mL of anti-CD40 (clone 82102, R&D systems), 20 ug/mL of anti-IFNg (clone 25718, R&D Systems), 20 ug/mL of sIL-21R (R&D Systems), or isotype controls (IgG2B, IgG2A, R&D Biosystems or IgG1, Biolegend) were added at the start of the coculture.

Flow cytometry and cell sorting. Cryopreserved PBMCs were thawed and rested for 1 hour in cRPMI + 5% pooled human serum prior to sorting. To sort CD4+ T cell populations for T:B cocultures and in vivo experiments, cells were stained with Live/Dead® Fixable Dead stain from Thermo Fisher Scientific followed by antibodies to detect: ICOS (clone C398.4A), CD127 (clone A019D5), CD25 (clone M-A251), CD4 (clone RPA-T4), CD3 (clone SK7), CD19 (clone HIB19)(Biolegend), and CD8 (clone SK1)(BD Biosciences). Cells were sorted using BD FACSAria. To characterize B cell phenotypes after coculture, cells were harvested, washed with PBS and stained for 30 minutes at 4°C using the following markers: CD3 (clone HIT3a), CD38 (clone HIT2), CD19 (clone HIB19)(Biolegend), IgD (clone IA6-2), and CD27 (clone M-T271)(BD Biosciences). For in vivo studies, mouse cells were gated out using Ter119 (clone TER119)(BD Biosciences), mCD45 (clone 30-F11), and hCD45 (clone 2D1)(Biolegend). Live cells were identified using Live/Dead® Fixable Dead stain from Thermo Fisher Scientific. Samples were washed with cold PBS and acquired on a BDCelesta. Data was analyzed using FlowJo.

ELISA. Levels of IgG were measured in T:B coculture supernatant and in mouse serum using the Human IgG ELISA kits from Bethyl Laboratories following manufacturers protocol.

In vivo human T:B interactions in humanized mice. ICOS+/- CD4+ T cells and B cells were isolated as previously described. Cells were resuspended in a 1:1 ratio in sterile PBS and 0.1-1 million cells were injected retro-orbitally into MISTRG6 humanized mice. After 2 weeks, mice were euthanized and phenotype of human B cells /plasmablasts in the spleen was analyzed by flow

cytometry as previously described. Serum human immunoglobulins were analyzed using an ELISA kit, as previously described.

MesoScale Discovery Assay. U-PLEX custom immuno-oncology panel kits were used to measure supernatant cytokines (IFNg, sCD40L, and IL-21) following manufacturer's recommendations. Sort purified ICOS+ CD4+ T cells were cultured in the presence of 200 ng/mL PMA and 1 ug/mL Ionomycin for 24 hours. Following stimulation, supernatant was collected and used to measure cytokine secretion.

Statistics. Specific tests utilized for all comparisons are noted in the legends for each figure panel.

Data Availability. Supporting data for figures is included in supplementary materials appendix.

3.6 Acknowledgements

This work was supported in part by funds from NIH CA238471, AR077926 to KMD. MVD is supported in part by funds from NIH (R35CA197603). KMD and MVD are also supported in part by funds from Specialized Center for Research (SCOR) award from the Leukemia and Lymphoma Society. Collection of some of the patient samples was supported by the Yale SPORE in Skin Cancer, (NIH/NCI award# 1 P50 CA121974). Authors also acknowledge support of the Emory Flow Cytometry Core, the Immune Monitoring Shared Resource of Winship Cancer Institute of Emory University, and NIH/NCI under award number P30CA138292.

Chapter 4: General Discussion and Closing Remarks

4.1 Introduction

The advent of immunotherapies revolutionized the field of oncology, expanding the arsenal of tools available to treat patients with cancer. Unlike traditional cancer therapy, immunotherapies seek to harness the body's own immune system to create or enhance an anti-tumor response. This powerful therapy has demonstrated impressive clinical results and shows extreme promise. In particular, ICIs have emerged as a core pillar of cancer immunotherapy. Because this class of therapy does not target specific cancer antigens and instead helps to invigorate a T cell-mediated anti-tumor response, ICIs are broadly applicable across a range of tumor types and patients. Thus, ICIs enable long-term survival of patients with previously nonresponsive advanced disease and act as key tools for early interventions, which have dramatically improved clinical outcomes.

Despite the many advancements in the field of ICIs, several challenges still exist. A large proportion of patients do not respond to ICIs, which calls for the development of new checkpoint inhibitors and therapeutic combinations. To rationally design new therapies and combinations, the underlying mechanisms that drive ICI-induced anti-tumor responses must be fully understood. Many studies have demonstrated the differing modes of action of CTLA-4 and PD-1 blockade, however further studies delineating additional checkpoint targets are warranted. Furthermore, ICIs are associated with the development of irAEs, with especially high rates among patients receiving CCB therapy. To fully optimize ICI therapy and treat these toxicities, it is critical to develop a robust understanding of the pathogenesis of irAEs. With this project, we aimed to expand the knowledge of ICI efficacy and toxicity in human cancer patients and uncover distinct cellular mechanisms that contribute to these factors.

4.2 Effects of PD-L1 blockade on dendritic cell function

Blockade of the inhibitory PD-1/PD-L1 signaling axis has resulted in significant clinical outcomes in patients with a broad spectrum of tumor types including melanoma, colorectal cancer, and lymphoma[92]. Because both molecules are involved in the same signaling axis, anti-PD-1 and anti-PD-L1 have been studied interchangeably within the clinic. Both therapies enhance anti-tumor T cell responses, but the function and expression patterns of the molecules themselves differ greatly. Emerging studies have revealed distinct genomic and cellular mechanisms underlying the efficacy of anti-CTLA-4 and anti-PD-1[61,62], which prompted us to investigate the mechanistic differences between PD-1 and PD-L1 blockade.

Through a combination of transcriptomic and proteomic analyses, we assessed changes in T cells and myeloid cells from NSCLC patients after receiving one cycle of either single agent anti-PD-1 (nivolumab) or anti-PD-L1 (atezolizumab). Our findings indicate distinct, non-overlapping gene expression changes in patients receiving anti-PD-1 compared to anti-PD-L1 (Figure 2.2). As has been previously reported, anti-PD-1 primarily leads to transcriptomic changes within T cells[62]. However, it was interesting to see that anti-PD-L1 led to distinct changes in gene expression within CD14+ monocytes that was not seen with PD-1 blockade (Figure 2.2). Among these transcriptomic changes, we observed an increase in genes related to inflammation (e.g. HBEGF, NLRP3, and CXCL1) and inflammasome-associated cytokines (e.g. IL-1, IL-18), which was also reflected through increased inflammatory cytokines in patient sera (Figure 2.2, Figure 2.3). To further corroborate these findings, we studied patients with AMM who had received anti-PD-L1 treatment and found significant phenotypic changes in both circulating and TME myeloid cells within the BM. At early timepoints following anti-PD-L1 treatment, AMM patients displayed transient,

increased levels of monocytes (Figure 2.5, Figure 2.6, Figure 2.8, Figure 2.10, Figure 2.11). The enriched monocyte population expressed elevated levels of HLA-DR and CD40, both markers of activation (Figure 2.5, Figure 2.9). Together, these data clearly show that anti-PD-L1 specifically targets myeloid cells in cancer patients, leading to rapid, systemic myeloid inflammation.

Current knowledge of checkpoint molecules supports the notion of anti-PD-L1 targeting myeloid cells, as PD-L1 is found on a variety of cell types beyond tumor cells[96,129-131]. Expression of PD-L1 can be upregulated on several different cell types, such as myeloid cells, via inflammatory cytokine stimulation[129-131]. Additionally, and most notably, it is well known that PD-L1 is constitutively expressed on a subset of myeloid APCs, including DCs[94]. Although human studies are lacking, there have been several studies conducted in murine models that highlight a possible role of PD-L1+ myeloid cells in the anti-tumor response[94,96,132]. Considering the importance of DCs in the cancer immunity cycle and observed anti-PD-L1 induced myeloid cell changes, we interrogated the effect of PD-L1 blockade on the biology of human monocyte-derived DCs (Mo-DCs). Interestingly, we found that anti-PD-L1 had a drastic effect on Mo-DCs alone and in the context of DC:T cell interactions. When PD-L1 was blocked, Mo-DCs demonstrated elevated markers of maturation, increased secretion of inflammatory cytokines, and rapid activation of caspase-1, an important component in the inflammasome complex (Figure 2.12). Furthermore, anti-PD-L1 induced even greater levels of maturation of Mo-DCs in the context of DC:T cell interactions and led to a greater expansion of antigen specific T cells, suggesting enhanced DC function (Figure 2.13, Figure 2.14).

Targeting the PD-1/PD-L1 axis was previously thought to primarily exert an anti-tumor immune response through the reinvigoration of T cells within the tumor. While this mechanism still holds true, our work highlights a new, underexplored mode of action through the activation of myeloid cells during PD-L1 blockade. Anti-PD-L1 acts directly on DCs, inducing maturation and enhancing the expansion of antigen specific T cells, indicating a new mechanism of efficacy of PD-L1 blockade within the afferent arm of the cancer immunity cycle (Figure 4.1). This finding is critical, as it contributes to the understanding that the PD-1/PD-L1 signaling axis plays more than one role during tumor immune evasion. This inhibitory checkpoint not only dampens anti-tumor T cell responses within the TME, but it can also interfere with T cell priming and activation during the early stages of the cancer immunity cycle and may be involved in the regulation of myeloid inflammation. Specifically, this axis appears to restrict T cell responses during cross-presentation of tumor antigens by DCs. Consequently, through the blockade of PD-L1, we are able to enhance priming and expansion of tumor specific T cells, aiding in the anti-tumor response.

The findings reported in this study contribute to the growing body of work that defines a unique mechanism of action of anti-PD-L1 apart from that of anti-PD-1. Many studies previously linked the expression levels of PD-L1 in tumor tissue to the response rates of anti-PD-L1 or anti-PD-1 therapy[58,127,133-136]. However, clinical data demonstrates decent response rates in patients with tumors lacking PD-L1 expression[127,134], suggesting the impact of PD-L1 blockade is mediated in part by factors outside of the tumor itself. Additionally, patterns of PD-L1 expression that correlate with outcome differ for anti-PD-1 versus anti-PD-L1. In the context of PD-L1 blockade, expression levels of PD-L1 on myeloid cells and DCs are associated with patient response[107,137]. On the other hand, PD-L1 expression on tumor cells correlate with response to anti-PD-1[137].

Several recent studies in murine models support our findings, further demonstrating the essential role of PD-L1 expression on DCs in contributing to the efficacy of anti-PD-L1 therapy[96,126,132]. Additionally, in both human and murine samples, high levels of functional PD-L1 expression on DCs and macrophages were reported in the TME and in draining lymph nodes, both of which correlated with the efficacy of ICI[132].

In summary, we demonstrate a distinct mechanism of action of PD-L1 blockade in human cancer patients, through enhancement of DC-mediated T cell priming and activation. Developing a thorough understanding of the precise mechanisms that drive checkpoint inhibitor efficacy is crucial. Knowledge of molecular and cellular mechanisms that lead to tumor regression provides potential explanations as to why a large subset of patients do not respond to therapy. For example, studies show enrichment and inflammation of myeloid cells may actually suppress the T cell-mediated anti-tumor response[109,138], which offers one explanation as to why some patients do not respond to anti-PD-L1 therapy. As such, rational therapeutic combinations may be designed to improve patient outcomes. Data from our study suggests harnessing factors within the afferent arm of the cancer immunity cycle, such as agonists targeting CD40/CD40L signaling, may boost anti-PD-L1 efficacy.

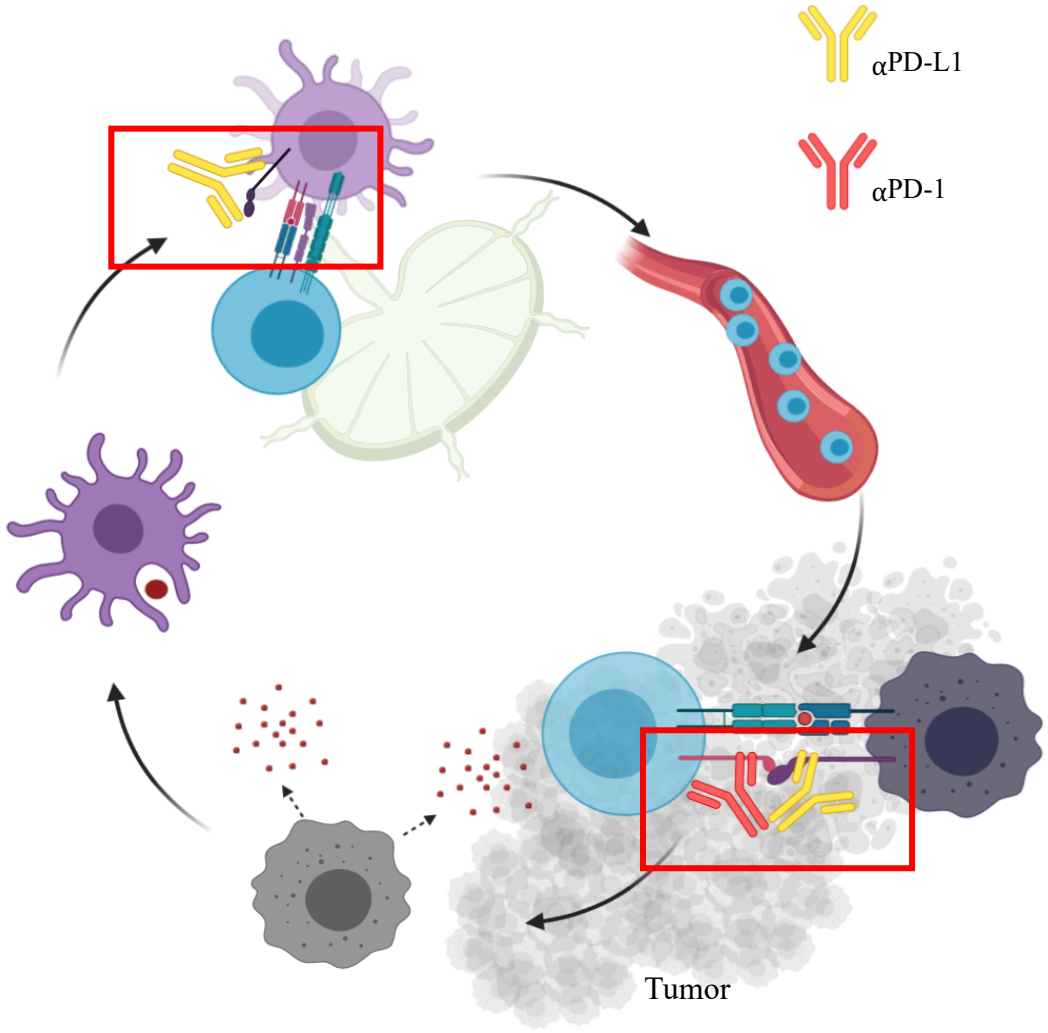

Figure 4.1. Anti-PD-L1 mechanisms of action. PD-L1 blockade induces an anti-tumor response through invigoration of T cells within the TME and within the affluent arm of the cancer immunity cycle, through enhancing T cell priming and activation via DCs.

4.3 Importance of T:B crosstalk in CCB-induced irAEs

The emergence of ICIs as a foundation of cancer therapy has afforded new treatment options for patients with previously nonresponsive tumors. Although clinical data shows impressive durable effects across a variety of tumor types, the development of irAEs remain a significant challenge. ICIs are associated with high rates of irAEs, with especially high rates of severe toxicities occurring in patients who receive combination anti-CTLA-4 and anti-PD-1 treatment. Most irAEs can be treated with the administration of steroids. However, high grade irAEs are more difficult to manage, often requiring patients to pause or completely come off ICI treatment. Ultimately, the disruption of treatment limits the optimal application of ICI and reduces patient outcomes.

Because irAEs pose a significant challenge to ICI treatment, it is crucial to understand the mechanisms by which these toxicities develop. The molecular and cellular components that contribute to the manifestation of irAEs is not yet fully understood. Both T and B cells have previously been individually implicated in the development of irAEs. Additionally, CTLA-4 and PD-1 checkpoints are involved in maintaining T and B cell peripheral tolerance. Therefore, we hypothesized that CCB induced T:B interactions may play a central role in the pathogenesis of irAEs, and sought to uncover the nature of specific cells involved.

To address this, we utilized pre- and post-treatment peripheral blood samples from melanoma patients receiving CCB therapy. Using single cell mass cytometry, we identified a distinct CD4+ memory T cell population that was significantly enriched following CCB, undergoing early proliferation as noted by the expression of Ki-67 (Figure 3.1). This population was characterized by the expression of ICOS and PD-1, markers previously linked to TFH cells, but surprisingly

lacked the expression of CXCR5, which is a key marker of TFH cells (Figure 3.1). Interestingly, the phenotype of this population appeared to be similar to that of another recently defined helper T cell population, termed T peripheral helper (TPH) cells, that have been described as key players in a number of autoimmune diseases including rheumatoid arthritis (RA) and systemic lupus erythematosus (SLE). Studies show that the function of these cells is similar to TFH cells, as they provide help to B cells to support activation and differentiation. However, unlike TFH cells, TPH cells do not function within germinal centers in secondary lymphoid organs, but instead interact with B cells in the periphery. In particular, TPH cells have been reported in circulation and within autoimmune inflamed tissue.

Having made this connection, we asked the question if the enriched ICOS+CD4+ T cells observed following CCB function in the same way as TPH cells. Indeed, we found that ICOS+CD4+ T cells do in fact provide help to B cells both in vitro and in vivo, leading to increased differentiation of B cells into plasmablasts with subsequent production of immunoglobulins (Figure 3.2). Notably, the ICOS+CD4+ T cells preferentially provide help to memory over naïve B cells suggesting that pre-existing autoreactive memory B cells may be targets of these cells (Figure 3.2). Furthermore, we report the importance of CD40, IL-21, and IFNg signaling in maintaining ICOS+CD4+ T cell help to B cells (Figure 3.3), highlighting some of the factors involved in this cellular interaction.

When looking at the patterns of irAE development, a significant question emerges- why do some patients develop severe, high grade toxicities while others do not? In an effort to answer this question, we stratified our patient samples based on irAE grading, categorizing patients with toxicities below grade 3 as low grade and those with grade 3-4 as high grade. Surprisingly, the

frequency of circulating ICOS+CD4+ T cells did not differ between low grade versus high grade patients (Figure 3.4). This led us to hypothesize that the phenotype and function of ICOS+CD4+ T cells may differ between patients with or without high grade irAEs. Indeed, ICOS+CD4+ T cells from high grade patients demonstrated a higher capacity to provide B cell help compared to those from low grade patients (Figure 3.2). Additionally, when looking at ICOS+CD4+ subpopulations, we found a higher proportion of FOXP3+CD25+ cells in patients with low grade toxicities, consistent with a Treg phenotype (Figure 3.2, Figure 3.4). Furthermore, when this Treg population was removed, we saw enhanced B cell help (Figure 3.2), suggesting Tregs may suppress pathogenic T:B interactions and provide a protective effect. In other words, patients with CCB-induced expansion of Tregs may not develop severe irAEs due to the immunosuppressive effects of this specific T cell population.

In addition, there was a significant increase in plasmablast and CD11c+CD21lo B cells specifically in high grade patients (Figure 3.1). This finding is consistent with previous studies, which noted a unique activation of CD21lo B cells post-CCB therapy in patients with high grade toxicities[83]. Notably, the CD11c+CD21lo B cell population we observed also expressed Tbet (Figure 3.1), another marker used to characterize B cell populations implicated in autoimmunity, further suggesting the potential pathogenic nature of this expanded population.

Furthermore, we observed elevated levels of CXCR3 expression in proliferating CD4+ and CD8+ T cells as well as CD11c+CD21lo B cells among patients with high grade irAEs (Figure 3.4). CXCR3 is a chemokine receptor associated with the homing of immune cells to inflamed tissues[139], suggesting in high grade patients, expression of CXCR3 on several activated cell populations may

lead to the migration of these cells to tissues where they contribute to the pathogenesis of various irAEs. Interestingly, the expression of CXCR3 in the ICOS+CD4+ population was associated with an effector/activated phenotype, as evidenced by higher expression of Tbet and HLA-DR (Figure 3.4), which may explain why these cells are able provide more help to B cells in high grade patients.

Collectively, the observed phenotypic and functional differences between low grade and high grade patients offer profound new insights into the mechanisms of irAE development. Enriched CD11c+CD21lo B cells, enhanced effector functions in ICOS+ TPH-like T cells, and CXCR3 expression all contribute to the manifestation of autoimmunity following CCB. Conversely, the presence of Tregs suppresses TPH:B cell interactions and prevents severe irAE development (Figure 4.2).

In summary, we show that both ICOS+CD4+ T cells and CD11c+CD21lo B cells are targets of combination anti-PD-1 and anti-CTLA-4, as evidenced by the proliferation and increased frequency observed following treatment. Our findings are corroborated by previous studies which demonstrated CTLA-4 blockade results in the expansion of ICOS+CD4+ T cells, although the function of these cells was not described[22]. Furthermore, other studies show elevated levels of CD11c+CD21lo B cells post CCB, noting increased proliferation and activation following therapy. Notably, this specific B cell population was associated with the onset of severe toxicities in melanoma patients[83], suggesting a central role of CD11c+CD21lo B cells in irAE development.

While our study did not explore which ICOS+CD4+ T cell and CD11c+CD21lo B cell clones are enriched post CCB, it is reasonable to assume there may be some expansion of pathogenic clones based on the current knowledge of these populations in autoimmune diseases. As previously mentioned, several studies have recently outlined the importance of T:B interactions in autoimmunity, particularly within sites of autoimmune inflamed tissue. In RA and SLE, elevated levels of both TPH and CD11c+CD21lo B cells are found in inflamed tissues and the frequency of these populations is highly associated with one another in circulation. Based on correlations between these cell populations, CD11c+CD21lo B cells are thought to be a potential target of TPH cells[140]. This further highlights the importance of our findings that CCB induces expansion of both ICOS+ TPH-like T cells and CD11c+CD21lo B cells, suggesting ICI therapy may promote the activation and interaction of autoimmune T and B cells. Furthermore, studies in murine models and in humans have described a similar population of CD11c+Tbet+ B cells expanded and enriched for autoreactive specificities in SLE[141-143]. Data shows IL-21 is able to promote the differentiation of these cells into Ig-secreting autoreactive plasma cells and loss of these cells leads to a reduction of autoimmune antibodies[141,144], identifying CD11c+Tbet+ B cells as a direct contributor to autoimmunity.

Finally, another important insight from our studies is the role of Tregs in suppressing T:B interactions involving TPH cells. Tregs have been extensively studied for their role in suppressing T cell responses. Our data suggest that induction of Tregs may also be critical in regulating interactions between TPH cells and preexisting autoreactive B cells to prevent autoimmunity. Thus, Tregs may play an important role in regulating autoimmunity by also impacting T:B help.

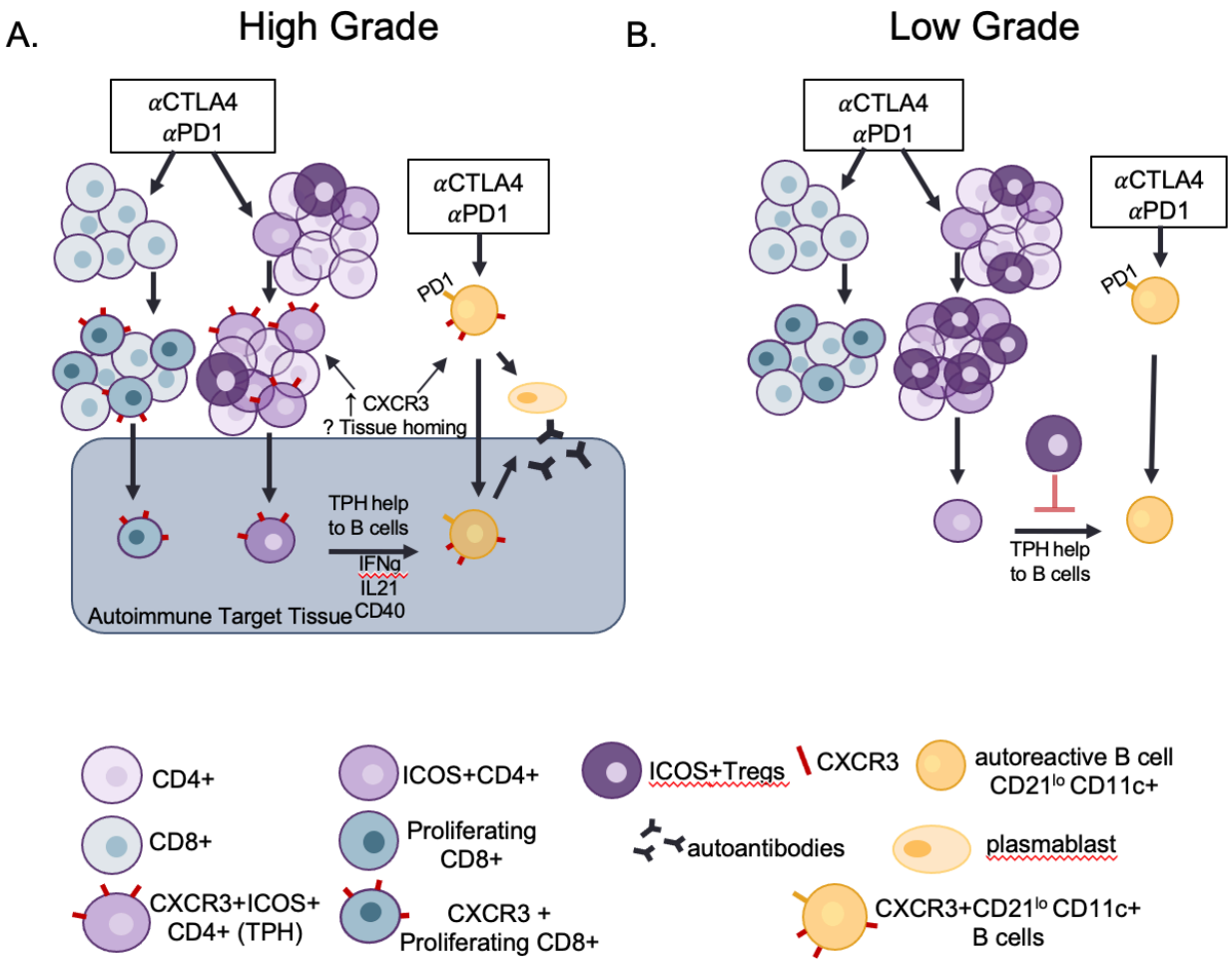

Figure 4.2. T:B interactions contribute to irAE development. Suggested mechanism of T:B interactions and tissue homing in the development of high grade versus low grade irAEs following combination checkpoint therapy with anti-CTLA-4 and anti-PD-1. CCB induces proliferation in a subset of CD8+ and CD4+ T cells. (A) High grade patients exhibit CXCR3 expression in proliferating CD8+ T cells, ICOS+CD4+ T cells, and CD11c+CD21lo B cells, suggesting trafficking to inflamed tissues where ICOS+CD4+ T cells interact with and provide help to

autoreactive B cells. (B) Low grade patients have an expansion of Tregs following CCB, which inhibits pathogenic T:B interactions and protects from the development of severe irAEs.

These data therefore point to Tregs as a potentially important target of therapeutic approaches to prevent CCB-induced irAEs.

4.4 Future Studies and Closing Remarks

The approval of the first ICIs ushered in a new era of cancer treatment, drastically improving patient outcomes and influencing the growth of the field of cancer immunology. However, the success of ICIs has not come without challenges, particularly surrounding efficacy and toxicity. The work presented herein uncovers some of the mechanisms of efficacy and toxicity in patients receiving ICI, contributing to the greater understanding of the effects of ICI on a wide range of immune cell populations. Here, we establish DCs as a direct target of anti-PD-L1 therapy, lending to the anti-tumor response through enhancement of T cell priming and activation. Thus, we describe the key role of PD-L1 blockade in the afferent arm of the tumor immunity cycle. Secondly, we identify a CCB-induced enrichment of a T helper cell population responsible for providing help to B cells, highlighting the role of these cells in the pathogenesis of irAEs. We also uncover factors that contribute to the development of severe toxicities, namely phenotypic and functional aspects of T and B cells may be pathogenic and the protective role of Tregs.

This work has high clinical relevance and translational potential as we primarily utilized patient samples, affording us the ability to study the effects of ICIs in real time. Our findings of the differential effects of PD-1 versus PD-L1 blockade provide insights into the complex mechanisms by which these therapies exert their action, particularly highlighting a new avenue of potential anti-PD-L1 combinations. Harnessing the afferent arm of the cancer immunity cycle, such as targeting components involved in DC mediated T cell priming, may be of particular interest.

Thoroughly deciphering distinct ICI mechanisms will help clinicians better understand why only a subset of patients respond to ICIs. Furthermore, as irAEs remain a significant challenge in the clinic, our findings contribute to the ongoing effort to uncover the mechanisms by which irAEs develop. We note several important factors that may be of interest as new methods to prevent or treat toxicities are developed. As such, our studies provide the rationale for further exploration into the differences between patients who experience low grade versus high grade toxicities, particularly focusing on distinct baseline features that may be used to identify patients with high risk of irAEs. Using biomarkers to predict toxicities will allow clinicians to select which patients will receive the most benefit of ICIs or afford the opportunity for preventative measures to be taken.

For years, the classic paradigm of the anti-tumor response driven by PD-1/PD-L1 blockade was based off the notion of reinvigoration of tumor specific T cells within the tumor. However, studies from our lab and others describe a more complex mechanism that exists. DC:T cell interactions appear to play a critical role in the formation of tumor immunity[126], by priming and activating novel or early memory T cell responses. Through disruption of the PD-1/PD-L1 signaling axis, checkpoint inhibitors enhance this cellular interaction, resulting in the expansion of effector T cells. Anti-PD-1 has also been shown to support effector T cell responses in chronic viral infections by promoting the activation of stem-like T cells in lymph nodes, a population essential for sustaining effector T cell responses[145,146]. Stem-like T cells have garnered great interest, as they have recently been reported as a critical component in mounting a successful anti-tumor response following ICI therapy[104,147-149], further highlighting the importance of DC:T cell interactions. Thus, PD-1/PD-L1 blockade may not only enhance cross-presentation of antigens to prime T cells, but

may also support stem-like T cells which give rise to effector T cells. Ultimately, the findings from our study add to the growing body of evidence that targeting the PD-1/PD-L1 axis induces an anti-tumor response heavily mediated by DC priming/activation of new T cells as opposed to invigorating exhausted, pre-existing intratumoral T cells.

While we emphasize the effect of anti-PD-L1 on DCs, the location of where these interactions occur remains unknown. The trafficking of DCs and T cells between the tumor and draining lymph nodes as well as expansion of T cells within lymph nodes have been implicated in anti-tumor immunity[132,150-154]. In particular, a subset of DCs in a melanoma mouse model were found to be the sole transporter of antigens to tumor draining lymph nodes and subsequently primed tumor-specific CD8+ T cells[152]. Importantly, these DCs were required for tumor control upon PD-L1 blockade[152]. Together, this data suggests tumor specific DC:T cell interactions take place within lymph nodes. However, alternative evidence indicates it is also possible that DC:T cell interactions occur within specific sites in the tumor. Proimmune intratumoral DCs have been characterized across multiple mouse models and human tumor biopsies[150]. Similarly, lymphoid aggregates containing high amounts of DCs have been found in several types of human tumors, arguing DC:T cell interactions can also occur within intratumoral antigen-presenting-cell niches[149]. As such, further studies are warranted to uncover the exact details of tumor specific DC:T cell interactions.

Our findings also provide new insights into the mechanisms of irAE pathogenesis, highlighting key cellular and molecular components. However, many important questions remain unanswered. A significant area of discourse within the field is whether patients who experience irAEs also have a higher likelihood of clinical ICI response. Several studies have indicated a positive association,

describing increased response rates among patients who develop irAEs, suggesting the development of these toxicities may be linked to or predict ICI response[155-157]. These findings are inconsistent among various studies, as several groups have reported conflicting results, indicating poorer outcomes among patients with specific irAEs and the observation of similar patterns of irAEs in patients who did not respond to ICI[158-161]. The correlation between irAEs and ICI response may ultimately differ based on the agent used, tumor type, and specific toxicities. Further studies are warranted to delineate the relationship between toxicity and anti-tumor response.

Management of irAEs remains a significant clinical challenge. Accordingly, there has been a great interest in developing tools to predict or prevent these toxicities. Many groups have focused on developing biomarkers to predict the risk of irAEs. One potential avenue is identification of specific human leukocyte antigen (HLA) genes that may predispose patients to ICI induced irAEs. A few studies have described different HLA alleles associated with the onset of organ specific toxicities, such as colitis, pruritis, and arthritis[162,163]. Similarly, ongoing work is assessing susceptible loci involved in various autoimmune diseases, with the hope this will inform the development of polygenic irAE risk scores for patients receiving ICIs[164]. Another potential source of biomarkers is the gut microbiota. Several studies have noted features of altered gut microbiome associated with ICI response and the protection against irAEs[165,166]. Currently, there is an ongoing clinical trial aiming to evaluate the role of the intestinal microbiome and autoimmune panels as a predictor of severe irAEs in solid tumor patients receiving ICIs[167]. Finally, a growing body of evidence, including data from our studies, suggests an early change in the immune signature in peripheral blood may be a useful biomarker. Several studies have assessed baseline immune cell alterations, indicating features that may predispose patients to irAEs and therefore, may be utilized

as biomarkers. Elevated levels of IL-17 and IL-6 prior to treatment have been associated with irAEs, as well as global cytokine dysregulation marked by elevated expression of several cytokines including GM-CSF and IL1B[168-170]. Furthermore, baseline abundance of an activated memory CD4 T cell subset and TCR diversity was also associated with severe irAE development[119]. We and others report an early increase in circulating CD21lo B cells and plasmablasts as well as elevated levels of CXCR3 after CCB therapy is associated with the development of severe irAEs[83]. Additionally, early diversification of the T cell repertoire in patients receiving anti-CTLA-4 preceded the onset of irAEs and was associated with increased levels of toxicity[171]. Studies to identify suitable biomarkers are ongoing, with the goal of developing a way to predict risk of irAEs and thus, improving the management of ICI induced toxicities.

Our discovery of a CCB-induced enrichment of TPH-like cells that provide help to B cells is significant, as it establishes important cellular players in irAE pathogenesis. However, there is a pressing need to further interrogate these interactions, particularly focusing on where they occur and if the cells involved are truly pathogenic. We show elevated levels of CXCR3, an inflammatory chemokine receptor involved in immune cell trafficking[139], on a subset of T and B cells in patients with high grade toxicities. Because we analyzed circulating lymphocytes, we cannot conclude that the cells we describe traffic to peripheral tissues. However, our characterizations are consistent with several other studies of TPH cells in autoimmune and inflammatory diseases. The seminal study defining TPH cells was conducted using pathogenic tissue samples from patients with RA, where they fully characterized the phenotype and function of TPH cells[124]. TPH cells from RA tissue expressed high levels of varying tissue-homing receptors, especially CXCR3, suggesting these cells do, in fact, migrate to peripheral sites of

inflammation[124]. Additionally, TPH cells were discovered in intestinal tissue of patients with inflammatory bowel disease (IBD), with a specific enrichment in sites of inflammation, and were associated with a pathogenic B cell response[172]. Thus, it is possible CCB-induced TPH-like cells and CD11c+CD21lo B cells migrate to sites of inflamed tissue, where they colocalize and mediate autoimmunity. Future studies should focus on analyzing these cell populations in irAE affected tissues, assessing colocalization and the presence of autoreactive clones.

To further the understanding of the mechanisms underlying irAE development, it is critical to study these toxicities in biologically relevant systems. Models to study ICI induced autoimmune toxicities are extremely limited, posing a unique challenge to the field. Currently, there are few models available that accurately recapitulate the biology of irAEs[167], which limits the ability to truly uncover mechanisms of irAE pathogenesis. Efforts to improve preclinical studies are ongoing. Recently, advancements have been made with the development of a genetic mouse model mimicking ICI induced myocarditis[173]. With the use of this model, investigators were able to interrogate the precise mechanisms of ICI myocarditis and establish modalities to mitigate the onset of this toxicity[173]. The emergence of this new model is promising, as it may pave the way for the creation of future models to study additional tissue specific irAEs.

In sum, the work presented herein contributes to the expanding body of work uncovering the mechanisms of ICI efficacy and toxicity. Through the use of clinical patient samples, we highlighted the role of PD-L1 blockade on enhancing DC:T cell interactions to exert an anti-tumor response, and established several key cellular and molecular components associated with CCB induced irAEs. We hope the insights described by this work will pave the way for future studies,

allowing for a more robust understanding of ICIs and advancing clinical practices to support optimal care for all patients.

Chapter 5: References

1. Zhang Y, Zhang Z. The history and advances in cancer immunotherapy: understanding the characteristics of tumor-infiltrating immune cells and their therapeutic implications. Cell Mol Immunol 2020;17(8):807-821. DOI: 10.1038/s41423-020-0488-6.
2. Tian T, Olson S, Whitacre JM, Harding A. The origins of cancer robustness and evolvability. Integr Biol (Camb) 2011;3(1):17-30. DOI: 10.1039/c0ib00046a.
3. Chen DS, Mellman I. Oncology meets immunology: the cancer-immunity cycle. Immunity 2013;39(1):1-10. DOI: 10.1016/j.immuni.2013.07.012.
4. De Plaen E, Lurquin C, Van Pel A, et al. Immunogenic (tum-) variants of mouse tumor P815: cloning of the gene of tum- antigen P91A and identification of the tum- mutation. Proc Natl Acad Sci U S A 1988;85(7):2274-8. DOI: 10.1073/pnas.85.7.2274.
5. Lurquin C, Van Pel A, Mariame B, et al. Structure of the gene of tum- transplantation antigen P91A: the mutated exon encodes a peptide recognized with Ld by cytolytic T cells. Cell 1989;58(2):293-303. DOI: 10.1016/0092-8674(89)90844-1.
6. Van den Eynde B, Lethe B, Van Pel A, De Plaen E, Boon T. The gene coding for a major tumor rejection antigen of tumor P815 is identical to the normal gene of syngeneic DBA/2 mice. J Exp Med 1991;173(6):1373-84. DOI: 10.1084/jem.173.6.1373.
7. Mandelboim O, Berke G, Fridkin M, Feldman M, Eisenstein M, Eisenbach L. CTL induction by a tumour-associated antigen octapeptide derived from a murine lung carcinoma. Nature 1994;369(6475):67-71. DOI: 10.1038/369067a0.
8. Monach PA, Meredith SC, Siegel CT, Schreiber H. A unique tumor antigen produced by a single amino acid substitution. Immunity 1995;2(1):45-59. DOI: 10.1016/1074-7613(95)90078-0.

9. Boon T, van der Bruggen P. Human tumor antigens recognized by T lymphocytes. J Exp Med 1996;183(3):725-9. DOI: 10.1084/jem.183.3.725.

10. Foley EJ. Antigenic properties of methylcholanthrene-induced tumors in mice of the strain of origin. Cancer Res 1953;13(12):835-7. (https://www.ncbi.nlm.nih.gov/pubmed/13116120).

11. Burnet FM. The concept of immunological surveillance. Prog Exp Tumor Res 1970;13:1-27. DOI: 10.1159/000386035.

12. Teng MW, Swann JB, Koebel CM, Schreiber RD, Smyth MJ. Immune-mediated dormancy: an equilibrium with cancer. J Leukoc Biol 2008;84(4):988-93. DOI: 10.1189/jlb.1107774.

13. Kim R, Emi M, Tanabe K. Cancer immunoediting from immune surveillance to immune escape. Immunology 2007;121(1):1-14. DOI: 10.1111/j.1365-2567.2007.02587.x.

14. Vajdic CM, van Leeuwen MT. Cancer incidence and risk factors after solid organ transplantation. Int J Cancer 2009;125(8):1747-54. DOI: 10.1002/ijc.24439.

15. Buell JF, Gross TG, Woodle ES. Malignancy after transplantation. Transplantation 2005;80(2 Suppl):S254-64. DOI: 10.1097/01.tp.0000186382.81130.ba.

16. Clark WH, Jr., Elder DE, Guerry Dt, et al. Model predicting survival in stage I melanoma based on tumor progression. J Natl Cancer Inst 1989;81(24):1893-904. DOI: 10.1093/jnci/81.24.1893.

17. Clemente CG, Mihm MC, Jr., Bufalino R, Zurrida S, Collini P, Cascinelli N. Prognostic value of tumor infiltrating lymphocytes in the vertical growth phase of primary cutaneous melanoma. Cancer 1996;77(7):1303-10. DOI: 10.1002/(SICI)1097-0142(19960401)77:7<1303::AID-CNCR12>3.0.CO;2-5.

18. Dunn GP, Bruce AT, Ikeda H, Old LJ, Schreiber RD. Cancer immunoediting: from immunosurveillance to tumor escape. Nat Immunol 2002;3(11):991-8. DOI: 10.1038/ni1102-991.

19. Coulie PG, Van den Eynde BJ, van der Bruggen P, Boon T. Tumour antigens recognized by T lymphocytes: at the core of cancer immunotherapy. Nat Rev Cancer 2014;14(2):135-46. DOI: 10.1038/nrc3670.

20. Campoli M, Chang CC, Ferrone S. HLA class I antigen loss, tumor immune escape and immune selection. Vaccine 2002;20 Suppl 4:A40-5. DOI: 10.1016/s0264-410x(02)00386-9.

21. Baitsch L, Baumgaertner P, Devevre E, et al. Exhaustion of tumor-specific CD8(+) T cells in metastases from melanoma patients. J Clin Invest 2011;121(6):2350-60. DOI: 10.1172/JCI46102.

22. Curran MA, Montalvo W, Yagita H, Allison JP. PD-1 and CTLA-4 combination blockade expands infiltrating T cells and reduces regulatory T and myeloid cells within B16 melanoma tumors. Proc Natl Acad Sci U S A 2010;107(9):4275-80. DOI: 10.1073/pnas.0915174107.

23. Ahmadzadeh M, Johnson LA, Heemskerk B, et al. Tumor antigen-specific CD8 T cells infiltrating the tumor express high levels of PD-1 and are functionally impaired. Blood 2009;114(8):1537-44. DOI: 10.1182/blood-2008-12-195792.

24. Chapon M, Randriamampita C, Maubec E, et al. Progressive upregulation of PD-1 in primary and metastatic melanomas associated with blunted TCR signaling in infiltrating T lymphocytes. J Invest Dermatol 2011;131(6):1300-7. DOI: 10.1038/jid.2011.30.

25. Iwai Y, Ishida M, Tanaka Y, Okazaki T, Honjo T, Minato N. Involvement of PD-L1 on tumor cells in the escape from host immune system and tumor immunotherapy by PD-L1 blockade. Proc Natl Acad Sci U S A 2002;99(19):12293-7. DOI: 10.1073/pnas.192461099.

26. Onizuka S, Tawara I, Shimizu J, Sakaguchi S, Fujita T, Nakayama E. Tumor rejection by in vivo administration of anti-CD25 (interleukin-2 receptor alpha) monoclonal antibody. Cancer Res 1999;59(13):3128-33. (https://www.ncbi.nlm.nih.gov/pubmed/10397255).

27. Shimizu J, Yamazaki S, Sakaguchi S. Induction of tumor immunity by removing CD25+CD4+ T cells: a common basis between tumor immunity and autoimmunity. J Immunol 1999;163(10):5211-8. (https://www.ncbi.nlm.nih.gov/pubmed/10553041).

28. Mellman I, Chen DS, Powles T, Turley SJ. The cancer-immunity cycle: Indication, genotype, and immunotype. Immunity 2023;56(10):2188-2205. DOI: 10.1016/j.immuni.2023.09.011.

29. Geraud A, Gougis P, Vozy A, et al. Clinical Pharmacology and Interplay of Immune Checkpoint Agents: A Yin-Yang Balance. Annu Rev Pharmacol Toxicol 2021;61:85-112. DOI: 10.1146/annurev-pharmtox-022820-093805.

30. Wang V, Gauthier M, Decot V, Reppel L, Bensoussan D. Systematic Review on CAR-T Cell Clinical Trials Up to 2022: Academic Center Input. Cancers (Basel) 2023;15(4). DOI: 10.3390/cancers15041003.

31. Wei J, Yang Y, Wang G, Liu M. Current landscape and future directions of bispecific antibodies in cancer immunotherapy. Front Immunol 2022;13:1035276. DOI: 10.3389/fimmu.2022.1035276.

32. Sharma P, Goswami S, Raychaudhuri D, et al. Immune checkpoint therapy-current perspectives and future directions. Cell 2023;186(8):1652-1669. DOI: 10.1016/j.cell.2023.03.006.

33. Chen L, Flies DB. Molecular mechanisms of T cell co-stimulation and co-inhibition. Nat Rev Immunol 2013;13(4):227-42. DOI: 10.1038/nri3405.

34. Nirschl CJ, Drake CG. Molecular pathways: coexpression of immune checkpoint molecules: signaling pathways and implications for cancer immunotherapy. Clin Cancer Res 2013;19(18):4917-24. DOI: 10.1158/1078-0432.CCR-12-1972.

35. Leach DR, Krummel MF, Allison JP. Enhancement of antitumor immunity by CTLA-4 blockade. Science 1996;271(5256):1734-6. DOI: 10.1126/science.271.5256.1734.

36. Tivol EA, Borriello F, Schweitzer AN, Lynch WP, Bluestone JA, Sharpe AH. Loss of CTLA-4 leads to massive lymphoproliferation and fatal multiorgan tissue destruction, revealing a critical negative regulatory role of CTLA-4. Immunity 1995;3(5):541-7. DOI: 10.1016/1074-7613(95)90125-6.

37. Waterhouse P, Penninger JM, Timms E, et al. Lymphoproliferative disorders with early lethality in mice deficient in Ctla-4. Science 1995;270(5238):985-8. DOI: 10.1126/science.270.5238.985.

38. Krummel MF, Allison JP. CD28 and CTLA-4 have opposing effects on the response of T cells to stimulation. J Exp Med 1995;182(2):459-65. DOI: 10.1084/jem.182.2.459.

39. van Elsas A, Hurwitz AA, Allison JP. Combination immunotherapy of B16 melanoma using anti-cytotoxic T lymphocyte-associated antigen 4 (CTLA-4) and granulocyte/macrophage colony-stimulating factor (GM-CSF)-producing vaccines induces

rejection of subcutaneous and metastatic tumors accompanied by autoimmune depigmentation. J Exp Med 1999;190(3):355-66. DOI: 10.1084/jem.190.3.355.

40. Quezada SA, Peggs KS, Curran MA, Allison JP. CTLA4 blockade and GM-CSF combination immunotherapy alters the intratumor balance of effector and regulatory T cells. J Clin Invest 2006;116(7):1935-45. DOI: 10.1172/JCI27745.

41. Hodi FS, Mihm MC, Soiffer RJ, et al. Biologic activity of cytotoxic T lymphocyte-associated antigen 4 antibody blockade in previously vaccinated metastatic melanoma and ovarian carcinoma patients. Proc Natl Acad Sci U S A 2003;100(8):4712-7. DOI: 10.1073/pnas.0830997100.

42. Hodi FS, O'Day SJ, McDermott DF, et al. Improved survival with ipilimumab in patients with metastatic melanoma. N Engl J Med 2010;363(8):711-23. DOI: 10.1056/NEJMoa1003466.

43. Schadendorf D, Hodi FS, Robert C, et al. Pooled Analysis of Long-Term Survival Data From Phase II and Phase III Trials of Ipilimumab in Unresectable or Metastatic Melanoma. J Clin Oncol 2015;33(17):1889-94. DOI: 10.1200/JCO.2014.56.2736.

44. Ishida Y, Agata Y, Shibahara K, Honjo T. Induced expression of PD-1, a novel member of the immunoglobulin gene superfamily, upon programmed cell death. EMBO J 1992;11(11):3887-95. DOI: 10.1002/j.1460-2075.1992.tb05481.x.

45. Terme M, Ullrich E, Aymeric L, et al. IL-18 induces PD-1-dependent immunosuppression in cancer. Cancer Res 2011;71(16):5393-9. DOI: 10.1158/0008-5472.CAN-11-0993.

46. Fanoni D, Tavecchio S, Recalcati S, et al. New monoclonal antibodies against B-cell antigens: possible new strategies for diagnosis of primary cutaneous B-cell lymphomas. Immunol Lett 2011;134(2):157-60. DOI: 10.1016/j.imlet.2010.09.022.

47. Nishimura H, Okazaki T, Tanaka Y, et al. Autoimmune dilated cardiomyopathy in PD-1 receptor-deficient mice. Science 2001;291(5502):319-22. DOI: 10.1126/science.291.5502.319.

48. Pardoll DM. The blockade of immune checkpoints in cancer immunotherapy. Nat Rev Cancer 2012;12(4):252-64. DOI: 10.1038/nrc3239.

49. Stanford SM, Rapini N, Bottini N. Regulation of TCR signalling by tyrosine phosphatases: from immune homeostasis to autoimmunity. Immunology 2012;137(1):1-19. DOI: 10.1111/j.1365-2567.2012.03591.x.

50. Barber DL, Wherry EJ, Masopust D, et al. Restoring function in exhausted CD8 T cells during chronic viral infection. Nature 2006;439(7077):682-7. DOI: 10.1038/nature04444.

51. Wherry EJ, Blattman JN, Murali-Krishna K, van der Most R, Ahmed R. Viral persistence alters CD8 T-cell immunodominance and tissue distribution and results in distinct stages of functional impairment. J Virol 2003;77(8):4911-27. DOI: 10.1128/jvi.77.8.4911-4927.2003.

52. Sfanos KS, Bruno TC, Meeker AK, De Marzo AM, Isaacs WB, Drake CG. Human prostate-infiltrating CD8+ T lymphocytes are oligoclonal and PD-1+. Prostate 2009;69(15):1694-703. DOI: 10.1002/pros.21020.

53. Dong H, Strome SE, Matteson EL, et al. Costimulating aberrant T cell responses by B7-H1 autoantibodies in rheumatoid arthritis. J Clin Invest 2003;111(3):363-70. DOI: 10.1172/JCI16015.

54. Konishi J, Yamazaki K, Azuma M, Kinoshita I, Dosaka-Akita H, Nishimura M. B7-H1 expression on non-small cell lung cancer cells and its relationship with tumor-infiltrating

lymphocytes and their PD-1 expression. Clin Cancer Res 2004;10(15):5094-100. DOI: 10.1158/1078-0432.CCR-04-0428.

55. Dong H, Strome SE, Salomao DR, et al. Tumor-associated B7-H1 promotes T-cell apoptosis: a potential mechanism of immune evasion. Nat Med 2002;8(8):793-800. DOI: 10.1038/nm730.

56. Iwai Y, Terawaki S, Honjo T. PD-1 blockade inhibits hematogenous spread of poorly immunogenic tumor cells by enhanced recruitment of effector T cells. Int Immunol 2005;17(2):133-44. DOI: 10.1093/intimm/dxh194.

57. Hirano F, Kaneko K, Tamura H, et al. Blockade of B7-H1 and PD-1 by monoclonal antibodies potentiates cancer therapeutic immunity. Cancer Res 2005;65(3):1089-96. (https://www.ncbi.nlm.nih.gov/pubmed/15705911).

58. Topalian SL, Hodi FS, Brahmer JR, et al. Safety, activity, and immune correlates of anti-PD-1 antibody in cancer. N Engl J Med 2012;366(26):2443-54. DOI: 10.1056/NEJMoa1200690.

59. Hamid O, Robert C, Daud A, et al. Safety and tumor responses with lambrolizumab (anti-PD-1) in melanoma. N Engl J Med 2013;369(2):134-44. DOI: 10.1056/NEJMoa1305133.

60. Ai L, Chen J, Yan H, et al. Research Status and Outlook of PD-1/PD-L1 Inhibitors for Cancer Therapy. Drug Des Devel Ther 2020;14:3625-3649. DOI: 10.2147/DDDT.S267433.

61. Wei SC, Levine JH, Cogdill AP, et al. Distinct Cellular Mechanisms Underlie Anti-CTLA-4 and Anti-PD-1 Checkpoint Blockade. Cell 2017;170(6):1120-1133 e17. DOI: 10.1016/j.cell.2017.07.024.

62. Das R, Verma R, Sznol M, et al. Combination therapy with anti-CTLA-4 and anti-PD-1 leads to distinct immunologic changes in vivo. J Immunol 2015;194(3):950-9. DOI: 10.4049/jimmunol.1401686.

63. Wolchok JD, Kluger H, Callahan MK, et al. Nivolumab plus ipilimumab in advanced melanoma. N Engl J Med 2013;369(2):122-33. DOI: 10.1056/NEJMoa1302369.

64. Adams S, Othus M, Patel SP, et al. A Multicenter Phase II Trial of Ipilimumab and Nivolumab in Unresectable or Metastatic Metaplastic Breast Cancer: Cohort 36 of Dual Anti-CTLA-4 and Anti-PD-1 Blockade in Rare Tumors (DART, SWOG S1609). Clin Cancer Res 2022;28(2):271-278. DOI: 10.1158/1078-0432.CCR-21-2182.

65. Aggarwal V, Workman CJ, Vignali DAA. LAG-3 as the third checkpoint inhibitor. Nat Immunol 2023;24(9):1415-1422. DOI: 10.1038/s41590-023-01569-z.

66. Lee JB, Ha SJ, Kim HR. Clinical Insights Into Novel Immune Checkpoint Inhibitors. Front Pharmacol 2021;12:681320. DOI: 10.3389/fphar.2021.681320.

67. Selby MJ, Engelhardt JJ, Quigley M, et al. Anti-CTLA-4 antibodies of IgG2a isotype enhance antitumor activity through reduction of intratumoral regulatory T cells. Cancer Immunol Res 2013;1(1):32-42. DOI: 10.1158/2326-6066.CIR-13-0013.

68. Simpson TR, Li F, Montalvo-Ortiz W, et al. Fc-dependent depletion of tumor-infiltrating regulatory T cells co-defines the efficacy of anti-CTLA-4 therapy against melanoma. J Exp Med 2013;210(9):1695-710. DOI: 10.1084/jem.20130579.

69. Chaput N, Lepage P, Coutzac C, et al. Baseline gut microbiota predicts clinical response and colitis in metastatic melanoma patients treated with ipilimumab. Ann Oncol 2017;28(6):1368-1379. DOI: 10.1093/annonc/mdx108.

70. Chen H, Liakou CI, Kamat A, et al. Anti-CTLA-4 therapy results in higher CD4+ICOShi T cell frequency and IFN-gamma levels in both nonmalignant and malignant prostate tissues. Proc Natl Acad Sci U S A 2009;106(8):2729-34. DOI: 10.1073/pnas.0813175106.

71. Liakou CI, Kamat A, Tang DN, et al. CTLA-4 blockade increases IFNgamma-producing CD4+ICOShi cells to shift the ratio of effector to regulatory T cells in cancer patients. Proc Natl Acad Sci U S A 2008;105(39):14987-92. DOI: 10.1073/pnas.0806075105.

72. June CH, Warshauer JT, Bluestone JA. Is autoimmunity the Achilles' heel of cancer immunotherapy? Nat Med 2017;23(5):540-547. DOI: 10.1038/nm.4321.

73. Boutros C, Tarhini A, Routier E, et al. Safety profiles of anti-CTLA-4 and anti-PD-1 antibodies alone and in combination. Nat Rev Clin Oncol 2016;13(8):473-86. DOI: 10.1038/nrclinonc.2016.58.

74. Sznol M, Ferrucci PF, Hogg D, et al. Pooled Analysis Safety Profile of Nivolumab and Ipilimumab Combination Therapy in Patients With Advanced Melanoma. J Clin Oncol 2017;35(34):3815-3822. DOI: 10.1200/JCO.2016.72.1167.

75. Hassel JC, Heinzerling L, Aberle J, et al. Combined immune checkpoint blockade (anti-PD-1/anti-CTLA-4): Evaluation and management of adverse drug reactions. Cancer Treat Rev 2017;57:36-49. DOI: 10.1016/j.ctrv.2017.05.003.

76. Nishimura H, Nose M, Hiai H, Minato N, Honjo T. Development of lupus-like autoimmune diseases by disruption of the PD-1 gene encoding an ITIM motif-carrying immunoreceptor. Immunity 1999;11(2):141-51. DOI: 10.1016/s1074-7613(00)80089-8.

77. Bar N, Costa F, Das R, et al. Differential effects of PD-L1 versus PD-1 blockade on myeloid inflammation in human cancer. JCI Insight 2020;5(12). DOI: 10.1172/jci.insight.129353.

78. Tang SQ, Tang LL, Mao YP, et al. The Pattern of Time to Onset and Resolution of Immune-Related Adverse Events Caused by Immune Checkpoint Inhibitors in Cancer: A Pooled Analysis of 23 Clinical Trials and 8,436 Patients. Cancer Res Treat 2021;53(2):339-354. DOI: 10.4143/crt.2020.790.

79. Nishimura K, Konishi T, Ochi T, et al. CD21(lo) B Cells Could Be a Potential Predictor of Immune-Related Adverse Events in Renal Cell Carcinoma. J Pers Med 2022;12(6). DOI: 10.3390/jpm12060888.

80. Patel AJ, Willsmore ZN, Khan N, et al. Regulatory B cell repertoire defects predispose lung cancer patients to immune-related toxicity following checkpoint blockade. Nat Commun 2022;13(1):3148. DOI: 10.1038/s41467-022-30863-x.

81. Yu Y, Wang S, Su N, et al. Increased Circulating Levels of CRP and IL-6 and Decreased Frequencies of T and B Lymphocyte Subsets Are Associated With Immune-Related Adverse Events During Combination Therapy With PD-1 Inhibitors for Liver Cancer. Front Oncol 2022;12:906824. DOI: 10.3389/fonc.2022.906824.

82. Gonugunta AS, von Itzstein MS, Mu-Mosley H, et al. Humoral and cellular correlates of a novel immune-related adverse event and its treatment. J Immunother Cancer 2021;9(12). DOI: 10.1136/jitc-2021-003585.

83. Das R, Bar N, Ferreira M, et al. Early B cell changes predict autoimmunity following combination immune checkpoint blockade. J Clin Invest 2018;128(2):715-720. DOI: 10.1172/JCI96798.

84. Dhodapkar KM, Duffy A, Dhodapkar MV. Role of B cells in immune-related adverse events following checkpoint blockade. Immunol Rev 2023. DOI: 10.1111/imr.13238.

85. Walunas TL, Bakker CY, Bluestone JA. CTLA-4 ligation blocks CD28-dependent T cell activation. J Exp Med 1996;183(6):2541-50. DOI: 10.1084/jem.183.6.2541.

86. Walunas TL, Lenschow DJ, Bakker CY, et al. CTLA-4 can function as a negative regulator of T cell activation. Immunity 1994;1(5):405-13. DOI: 10.1016/1074-7613(94)90071-x.

87. Nishimura H, Minato N, Nakano T, Honjo T. Immunological studies on PD-1 deficient mice: implication of PD-1 as a negative regulator for B cell responses. Int Immunol 1998;10(10):1563-72. DOI: 10.1093/intimm/10.10.1563.

88. Berner F, Bomze D, Diem S, et al. Association of Checkpoint Inhibitor-Induced Toxic Effects With Shared Cancer and Tissue Antigens in Non-Small Cell Lung Cancer. JAMA Oncol 2019;5(7):1043-1047. DOI: 10.1001/jamaoncol.2019.0402.

89. Johnson DB, Balko JM, Compton ML, et al. Fulminant Myocarditis with Combination Immune Checkpoint Blockade. N Engl J Med 2016;375(18):1749-1755. DOI: 10.1056/NEJMoa1609214.

90. Luoma AM, Suo S, Williams HL, et al. Molecular Pathways of Colon Inflammation Induced by Cancer Immunotherapy. Cell 2020;182(3):655-671 e22. DOI: 10.1016/j.cell.2020.06.001.

91. Reschke R, Shapiro JW, Yu J, et al. Checkpoint Blockade-Induced Dermatitis and Colitis Are Dominated by Tissue-Resident Memory T Cells and Th1/Tc1 Cytokines. Cancer Immunol Res 2022;10(10):1167-1174. DOI: 10.1158/2326-6066.CIR-22-0362.

92. Zou W, Wolchok JD, Chen L. PD-L1 (B7-H1) and PD-1 pathway blockade for cancer therapy: Mechanisms, response biomarkers, and combinations. Sci Transl Med 2016;8(328):328rv4. DOI: 10.1126/scitranslmed.aad7118.

93. Azuma T, Yao S, Zhu G, Flies AS, Flies SJ, Chen L. B7-H1 is a ubiquitous antiapoptotic receptor on cancer cells. Blood 2008;111(7):3635-43. DOI: 10.1182/blood-2007-11-123141.

94. Curiel TJ, Wei S, Dong H, et al. Blockade of B7-H1 improves myeloid dendritic cell-mediated antitumor immunity. Nat Med 2003;9(5):562-7. DOI: 10.1038/nm863.

95. Lin H, Wei S, Hurt EM, et al. Host expression of PD-L1 determines efficacy of PD-L1 pathway blockade-mediated tumor regression. J Clin Invest 2018;128(4):1708. DOI: 10.1172/JCI120803.

96. Tang H, Liang Y, Anders RA, et al. PD-L1 on host cells is essential for PD-L1 blockade-mediated tumor regression. J Clin Invest 2018;128(2):580-588. DOI: 10.1172/JCI96061.

97. Dhodapkar MV. MGUS to myeloma: a mysterious gammopathy of underexplored significance. Blood 2016;128(23):2599-2606. DOI: 10.1182/blood-2016-09-692954.

98. Lesokhin AM, Ansell SM, Armand P, et al. Nivolumab in Patients With Relapsed or Refractory Hematologic Malignancy: Preliminary Results of a Phase Ib Study. J Clin Oncol 2016;34(23):2698-704. DOI: 10.1200/JCO.2015.65.9789.

99. Dhodapkar MV, Krasovsky J, Osman K, Geller MD. Vigorous premalignancy-specific effector T cell response in the bone marrow of patients with monoclonal gammopathy. J Exp Med 2003;198(11):1753-7. DOI: 10.1084/jem.20031030.

100. Spisek R, Kukreja A, Chen LC, et al. Frequent and specific immunity to the embryonal stem cell-associated antigen SOX2 in patients with monoclonal gammopathy. J Exp Med 2007;204(4):831-40. DOI: 10.1084/jem.20062387.

101. Dhodapkar MV, Sexton R, Das R, et al. Prospective analysis of antigen-specific immunity, stem-cell antigens, and immune checkpoints in monoclonal gammopathy. Blood 2015;126(22):2475-8. DOI: 10.1182/blood-2015-03-632919.

102. Paiva B, Azpilikueta A, Puig N, et al. PD-L1/PD-1 presence in the tumor microenvironment and activity of PD-1 blockade in multiple myeloma. Leukemia 2015;29(10):2110-3. DOI: 10.1038/leu.2015.79.

103. Shiravand Y, Khodadadi F, Kashani SMA, et al. Immune Checkpoint Inhibitors in Cancer Therapy. Curr Oncol 2022;29(5):3044-3060. DOI: 10.3390/curroncol29050247.

104. Sade-Feldman M, Yizhak K, Bjorgaard SL, et al. Defining T Cell States Associated with Response to Checkpoint Immunotherapy in Melanoma. Cell 2018;175(4):998-1013 e20. DOI: 10.1016/j.cell.2018.10.038.

105. Schoenberger SP, Toes RE, van der Voort EI, Offringa R, Melief CJ. T-cell help for cytotoxic T lymphocytes is mediated by CD40-CD40L interactions. Nature 1998;393(6684):480-3. DOI: 10.1038/31002.

106. Hartley GP, Chow L, Ammons DT, Wheat WH, Dow SW. Programmed Cell Death Ligand 1 (PD-L1) Signaling Regulates Macrophage Proliferation and Activation. Cancer Immunol Res 2018;6(10):1260-1273. DOI: 10.1158/2326-6066.CIR-17-0537.

107. Herbst RS, Soria JC, Kowanetz M, et al. Predictive correlates of response to the anti-PD-L1 antibody MPDL3280A in cancer patients. Nature 2014;515(7528):563-7. DOI: 10.1038/nature14011.

108. Ghiringhelli F, Apetoh L, Tesniere A, et al. Activation of the NLRP3 inflammasome in dendritic cells induces IL-1beta-dependent adaptive immunity against tumors. Nat Med 2009;15(10):1170-8. DOI: 10.1038/nm.2028.

109. McDermott DF, Huseni MA, Atkins MB, et al. Clinical activity and molecular correlates of response to atezolizumab alone or in combination with bevacizumab versus sunitinib in renal cell carcinoma. Nat Med 2018;24(6):749-757. DOI: 10.1038/s41591-018-0053-3.

110. Lo Russo G, Moro M, Sommariva M, et al. Antibody-Fc/FcR Interaction on Macrophages as a Mechanism for Hyperprogressive Disease in Non-small Cell Lung Cancer Subsequent to PD-1/PD-L1 Blockade. Clin Cancer Res 2019;25(3):989-999. DOI: 10.1158/1078-0432.CCR-18-1390.

111. Kukreja A, Hutchinson A, Dhodapkar K, et al. Enhancement of clonogenicity of human multiple myeloma by dendritic cells. J Exp Med 2006;203(8):1859-65. DOI: 10.1084/jem.20052136.

112. Zheng Y, Cai Z, Wang S, et al. Macrophages are an abundant component of myeloma microenvironment and protect myeloma cells from chemotherapy drug-induced apoptosis. Blood 2009;114(17):3625-8. DOI: 10.1182/blood-2009-05-220285.

113. Bailur JK, McCachren SS, Doxie DB, et al. Early alterations in stem-like/resident T cells, innate and myeloid cells in the bone marrow in preneoplastic gammopathy. JCI Insight 2019;5(11). DOI: 10.1172/jci.insight.127807.

114. Boddupalli CS, Bar N, Kadaveru K, et al. Interlesional diversity of T cell receptors in melanoma with immune checkpoints enriched in tissue-resident memory T cells. JCI Insight 2016;1(21):e88955. DOI: 10.1172/jci.insight.88955.

115. Kini Bailur J, Mehta S, Zhang L, et al. Changes in bone marrow innate lymphoid cell subsets in monoclonal gammopathy: target for IMiD therapy. Blood Adv 2017;1(25):2343-2347. DOI: 10.1182/bloodadvances.2017012732.

116. Satija R, Farrell JA, Gennert D, Schier AF, Regev A. Spatial reconstruction of single-cell gene expression data. Nat Biotechnol 2015;33(5):495-502. DOI: 10.1038/nbt.3192.

117. Huber W, Carey VJ, Gentleman R, et al. Orchestrating high-throughput genomic analysis with Bioconductor. Nat Methods 2015;12(2):115-21. DOI: 10.1038/nmeth.3252.

118. Ritchie ME, Phipson B, Wu D, et al. limma powers differential expression analyses for RNA-sequencing and microarray studies. Nucleic Acids Res 2015;43(7):e47. DOI: 10.1093/nar/gkv007.

119. Lozano AX, Chaudhuri AA, Nene A, et al. T cell characteristics associated with toxicity to immune checkpoint blockade in patients with melanoma. Nat Med 2022;28(2):353-362. DOI: 10.1038/s41591-021-01623-z.

120. Myles A, Sanz I, Cancro MP. T-bet(+) B cells: A common denominator in protective and autoreactive antibody responses? Curr Opin Immunol 2019;57:40-45. DOI: 10.1016/j.coi.2019.01.002.

121. Jenks SA, Cashman KS, Zumaquero E, et al. Distinct Effector B Cells Induced by Unregulated Toll-like Receptor 7 Contribute to Pathogenic Responses in Systemic Lupus Erythematosus. Immunity 2018;49(4):725-739 e6. DOI: 10.1016/j.immuni.2018.08.015.

122. Rubtsova K, Rubtsov AV, Cancro MP, Marrack P. Age-Associated B Cells: A T-bet-Dependent Effector with Roles in Protective and Pathogenic Immunity. J Immunol 2015;195(5):1933-7. DOI: 10.4049/jimmunol.1501209.

123. Claes N, Fraussen J, Vanheusden M, et al. Age-Associated B Cells with Proinflammatory Characteristics Are Expanded in a Proportion of Multiple Sclerosis Patients. J Immunol 2016;197(12):4576-4583. DOI: 10.4049/jimmunol.1502448.

124. Rao DA, Gurish MF, Marshall JL, et al. Pathologically expanded peripheral T helper cell subset drives B cells in rheumatoid arthritis. Nature 2017;542(7639):110-114. DOI: 10.1038/nature20810.

125. Marks KE, Rao DA. T peripheral helper cells in autoimmune diseases. Immunol Rev 2022;307(1):191-202. DOI: 10.1111/imr.13069.

126. Oh SA, Wu DC, Cheung J, et al. PD-L1 expression by dendritic cells is a key regulator of T-cell immunity in cancer. Nat Cancer 2020;1(7):681-691. DOI: 10.1038/s43018-020-0075-x.

127. Garon EB, Rizvi NA, Hui R, et al. Pembrolizumab for the treatment of non-small-cell lung cancer. N Engl J Med 2015;372(21):2018-28. DOI: 10.1056/NEJMoa1501824.

128. Caielli S, Veiga DT, Balasubramanian P, et al. A CD4(+) T cell population expanded in lupus blood provides B cell help through interleukin-10 and succinate. Nat Med 2019;25(1):75-81. DOI: 10.1038/s41591-018-0254-9.

129. Sznol M, Chen L. Antagonist antibodies to PD-1 and B7-H1 (PD-L1) in the treatment of advanced human cancer--response. Clin Cancer Res 2013;19(19):5542. DOI: 10.1158/1078-0432.CCR-13-2234.

130. Blank C, Brown I, Peterson AC, et al. PD-L1/B7H-1 inhibits the effector phase of tumor rejection by T cell receptor (TCR) transgenic CD8+ T cells. Cancer Res 2004;64(3):1140-5. DOI: 10.1158/0008-5472.can-03-3259.

131. Nguyen LT, Ohashi PS. Clinical blockade of PD1 and LAG3--potential mechanisms of action. Nat Rev Immunol 2015;15(1):45-56. DOI: 10.1038/nri3790.

132. Lin H, Wei S, Hurt EM, et al. Host expression of PD-L1 determines efficacy of PD-L1 pathway blockade-mediated tumor regression. J Clin Invest 2018;128(2):805-815. DOI: 10.1172/JCI96113.

133. Brahmer JR, Tykodi SS, Chow LQ, et al. Safety and activity of anti-PD-L1 antibody in patients with advanced cancer. N Engl J Med 2012;366(26):2455-65. DOI: 10.1056/NEJMoa1200694.

134. Reck M, Rodriguez-Abreu D, Robinson AG, et al. Pembrolizumab versus Chemotherapy for PD-L1-Positive Non-Small-Cell Lung Cancer. N Engl J Med 2016;375(19):1823-1833. DOI: 10.1056/NEJMoa1606774.

135. Taube JM, Klein A, Brahmer JR, et al. Association of PD-1, PD-1 ligands, and other features of the tumor immune microenvironment with response to anti-PD-1 therapy. Clin Cancer Res 2014;20(19):5064-74. DOI: 10.1158/1078-0432.CCR-13-3271.

136. Ansell SM, Lesokhin AM, Borrello I, et al. PD-1 blockade with nivolumab in relapsed or refractory Hodgkin's lymphoma. N Engl J Med 2015;372(4):311-9. DOI: 10.1056/NEJMoa1411087.

137. Li H, van der Merwe PA, Sivakumar S. Biomarkers of response to PD-1 pathway blockade. Br J Cancer 2022;126(12):1663-1675. DOI: 10.1038/s41416-022-01743-4.

138. Gabrilovich DI, Nagaraj S. Myeloid-derived suppressor cells as regulators of the immune system. Nat Rev Immunol 2009;9(3):162-74. DOI: 10.1038/nri2506.

139. Lacotte S, Brun S, Muller S, Dumortier H. CXCR3, inflammation, and autoimmune diseases. Ann N Y Acad Sci 2009;1173:310-7. DOI: 10.1111/j.1749-6632.2009.04813.x.

140. Yoshitomi H, Ueno H. Shared and distinct roles of T peripheral helper and T follicular helper cells in human diseases. Cell Mol Immunol 2021;18(3):523-527. DOI: 10.1038/s41423-020-00529-z.

141. Wang S, Wang J, Kumar V, et al. IL-21 drives expansion and plasma cell differentiation of autoreactive CD11c(hi)T-bet(+) B cells in SLE. Nat Commun 2018;9(1):1758. DOI: 10.1038/s41467-018-03750-7.

142. Peng SL, Szabo SJ, Glimcher LH. T-bet regulates IgG class switching and pathogenic autoantibody production. Proc Natl Acad Sci U S A 2002;99(8):5545-50. DOI: 10.1073/pnas.082114899.

143. Rubtsova K, Rubtsov AV, Thurman JM, Mennona JM, Kappler JW, Marrack P. B cells expressing the transcription factor T-bet drive lupus-like autoimmunity. J Clin Invest 2017;127(4):1392-1404. DOI: 10.1172/JCI91250.

144. Rubtsov AV, Rubtsova K, Fischer A, et al. Toll-like receptor 7 (TLR7)-driven accumulation of a novel CD11c(+) B-cell population is important for the development of autoimmunity. Blood 2011;118(5):1305-15. DOI: 10.1182/blood-2011-01-331462.

145. Im SJ, Hashimoto M, Gerner MY, et al. Defining CD8+ T cells that provide the proliferative burst after PD-1 therapy. Nature 2016;537(7620):417-421. DOI: 10.1038/nature19330.

146. Utzschneider DT, Charmoy M, Chennupati V, et al. T Cell Factor 1-Expressing Memory-like CD8(+) T Cells Sustain the Immune Response to Chronic Viral Infections. Immunity 2016;45(2):415-27. DOI: 10.1016/j.immuni.2016.07.021.

147. Kurtulus S, Madi A, Escobar G, et al. Checkpoint Blockade Immunotherapy Induces Dynamic Changes in PD-1(-)CD8(+) Tumor-Infiltrating T Cells. Immunity 2019;50(1):181-194 e6. DOI: 10.1016/j.immuni.2018.11.014.

148. Siddiqui I, Schaeuble K, Chennupati V, et al. Intratumoral Tcf1(+)PD-1(+)CD8(+) T Cells with Stem-like Properties Promote Tumor Control in Response to Vaccination and Checkpoint Blockade Immunotherapy. Immunity 2019;50(1):195-211 e10. DOI: 10.1016/j.immuni.2018.12.021.

149. Jansen CS, Prokhnevska N, Master VA, et al. An intra-tumoral niche maintains and differentiates stem-like CD8 T cells. Nature 2019;576(7787):465-470. DOI: 10.1038/s41586-019-1836-5.

150. Broz ML, Binnewies M, Boldajipour B, et al. Dissecting the tumor myeloid compartment reveals rare activating antigen-presenting cells critical for T cell immunity. Cancer Cell 2014;26(5):638-52. DOI: 10.1016/j.ccell.2014.09.007.

151. Spranger S, Dai D, Horton B, Gajewski TF. Tumor-Residing Batf3 Dendritic Cells Are Required for Effector T Cell Trafficking and Adoptive T Cell Therapy. Cancer Cell 2017;31(5):711-723 e4. DOI: 10.1016/j.ccell.2017.04.003.

152. Salmon H, Idoyaga J, Rahman A, et al. Expansion and Activation of CD103(+) Dendritic Cell Progenitors at the Tumor Site Enhances Tumor Responses to Therapeutic PD-L1 and BRAF Inhibition. Immunity 2016;44(4):924-38. DOI: 10.1016/j.immuni.2016.03.012.

153. Yost KE, Satpathy AT, Wells DK, et al. Clonal replacement of tumor-specific T cells following PD-1 blockade. Nat Med 2019;25(8):1251-1259. DOI: 10.1038/s41591-019-0522-3.

154. Fransen MF, Schoonderwoerd M, Knopf P, et al. Tumor-draining lymph nodes are pivotal in PD-1/PD-L1 checkpoint therapy. JCI Insight 2018;3(23). DOI: 10.1172/jci.insight.124507.

155. Maher VE, Fernandes LL, Weinstock C, et al. Analysis of the Association Between Adverse Events and Outcome in Patients Receiving a Programmed Death Protein 1 or Programmed Death Ligand 1 Antibody. J Clin Oncol 2019;37(30):2730-2737. DOI: 10.1200/JCO.19.00318.

156. Eggermont AMM, Kicinski M, Blank CU, et al. Association Between Immune-Related Adverse Events and Recurrence-Free Survival Among Patients With Stage III Melanoma Randomized to Receive Pembrolizumab or Placebo: A Secondary Analysis of a Randomized Clinical Trial. JAMA Oncol 2020;6(4):519-527. DOI: 10.1001/jamaoncol.2019.5570.

157. Shankar B, Zhang J, Naqash AR, et al. Multisystem Immune-Related Adverse Events Associated With Immune Checkpoint Inhibitors for Treatment of Non-Small Cell Lung Cancer. JAMA Oncol 2020;6(12):1952-1956. DOI: 10.1001/jamaoncol.2020.5012.

158. Suresh K, Naidoo J. Lower Survival in Patients Who Develop Pneumonitis Following Immunotherapy for Lung Cancer. Clin Lung Cancer 2020;21(3):e169-e170. DOI: 10.1016/j.cllc.2019.10.009.

159. Sharma P, Pachynski RK, Narayan V, et al. Nivolumab Plus Ipilimumab for Metastatic Castration-Resistant Prostate Cancer: Preliminary Analysis of Patients in the CheckMate 650 Trial. Cancer Cell 2020;38(4):489-499 e3. DOI: 10.1016/j.ccell.2020.08.007.

160. Morad G, Helmink BA, Sharma P, Wargo JA. Hallmarks of response, resistance, and toxicity to immune checkpoint blockade. Cell 2021;184(21):5309-5337. DOI: 10.1016/j.cell.2021.09.020.

161. Das S, Johnson DB. Immune-related adverse events and anti-tumor efficacy of immune checkpoint inhibitors. J Immunother Cancer 2019;7(1):306. DOI: 10.1186/s40425-019-0805-8.

162. Hasan Ali O, Berner F, Bomze D, et al. Human leukocyte antigen variation is associated with adverse events of checkpoint inhibitors. Eur J Cancer 2019;107:8-14. DOI: 10.1016/j.ejca.2018.11.009.

163. Cappelli LC, Dorak MT, Bettinotti MP, Bingham CO, Shah AA. Association of HLA-DRB1 shared epitope alleles and immune checkpoint inhibitor-induced inflammatory arthritis. Rheumatology (Oxford) 2019;58(3):476-480. DOI: 10.1093/rheumatology/key358.

164. Hoefsmit EP, Rozeman EA, Haanen J, Blank CU. Susceptible loci associated with autoimmune disease as potential biomarkers for checkpoint inhibitor-induced immune-related adverse events. ESMO Open 2019;4(4):e000472. DOI: 10.1136/esmoopen-2018-000472.

165. Dubin K, Callahan MK, Ren B, et al. Intestinal microbiome analyses identify melanoma patients at risk for checkpoint-blockade-induced colitis. Nat Commun 2016;7:10391. DOI: 10.1038/ncomms10391.

166. Routy B, Le Chatelier E, Derosa L, et al. Gut microbiome influences efficacy of PD-1-based immunotherapy against epithelial tumors. Science 2018;359(6371):91-97. DOI: 10.1126/science.aan3706.

167. Conroy M, Naidoo J. Immune-related adverse events and the balancing act of immunotherapy. Nat Commun 2022;13(1):392. DOI: 10.1038/s41467-022-27960-2.

168. Tarhini AA, Zahoor H, Lin Y, et al. Baseline circulating IL-17 predicts toxicity while TGF-beta1 and IL-10 are prognostic of relapse in ipilimumab neoadjuvant therapy of melanoma. J Immunother Cancer 2015;3:39. DOI: 10.1186/s40425-015-0081-1.

169. Valpione S, Pasquali S, Campana LG, et al. Sex and interleukin-6 are prognostic factors for autoimmune toxicity following treatment with anti-CTLA4 blockade. J Transl Med 2018;16(1):94. DOI: 10.1186/s12967-018-1467-x.

170. Lim SY, Lee JH, Gide TN, et al. Circulating Cytokines Predict Immune-Related Toxicity in Melanoma Patients Receiving Anti-PD-1-Based Immunotherapy. Clin Cancer Res 2019;25(5):1557-1563. DOI: 10.1158/1078-0432.CCR-18-2795.

171. Oh DY, Cham J, Zhang L, et al. Immune Toxicities Elicted by CTLA-4 Blockade in Cancer Patients Are Associated with Early Diversification of the T-cell Repertoire. Cancer Res 2017;77(6):1322-1330. DOI: 10.1158/0008-5472.CAN-16-2324.

172. Uzzan M, Martin JC, Mesin L, et al. Ulcerative colitis is characterized by a plasmablast-skewed humoral response associated with disease activity. Nat Med 2022;28(4):766-779. DOI: 10.1038/s41591-022-01680-y.

173. Wei SC, Meijers WC, Axelrod ML, et al. A Genetic Mouse Model Recapitulates Immune Checkpoint Inhibitor-Associated Myocarditis and Supports a Mechanism-Based Therapeutic Intervention. Cancer Discov 2021;11(3):614-625. DOI: 10.1158/2159-8290.CD-20-0856.